Title
Intestinal Immunity to the Commensal Bacterium Akkermansia muciniphila

Author
Ansaldo Gine, Eduardo

Publication Date
2019

Peer reviewed|Thesis/dissertation

Intestinal Immunity to the Commensal Bacterium *Akkermansia muciniphila*

By

Eduardo Ansaldo Gine

A dissertation submitted in partial satisfaction of the

requirements for the degree of

Doctor of Philosophy

in

Molecular and Cell Biology

in the

Graduate Division

of the

University of California, Berkeley

Committee in charge:

Professor Gregory Barton, Chair
Professor Ellen Robey
Professor Sarah Stanley
Professor Michael Shapira

Summer 2019

Abstract

Intestinal Immunity to the Commensal Bacterium *Akkermansia muciniphila*

By

Eduardo Ansaldo Gine

Doctor of Philosophy in Molecular and Cell Biology

University of California, Berkeley

Professor Gregory Barton, Chair

Intestinal immunity plays critical roles in maintaining host health. Despite the abundance of foreign antigens and activated lymphocytes in the intestine, only a few commensal bacteria that induce cognate adaptive immune responses during homeostasis have been identified. In this dissertation, I reveal that *Akkermansia muciniphila*, an intestinal bacterium associated with beneficial effects on host metabolism and cancer immunotherapy, induces cognate T-dependent immunoglobulin G1 (IgG1) and IgA antibody responses and antigen-specific T cell responses during homeostasis. In contrast to the select few examples of previously characterized mucosal responses to commensal bacteria, T cell responses to *A. muciniphila* are limited to T follicular helper cells in the Peyer's patches in a gnotobiotic setting, without appreciable induction of other T helper fates or migration to the lamina propria. However, *A. muciniphila*-specific responses are context-dependent, and adopt other T helper fates in the setting of a conventional microbiota. These findings suggest that contextual signals influence T cell immunity to the microbiota and modulate host immune function during homeostasis. Interestingly, T cells specific to *A. muciniphila* expand dramatically in a novel (but still uncharacterized) genetic mouse model of intestinal inflammation, suggesting that this bacterium may become a major mucosal antigen when homeostasis is disrupted. If so, T cell immunity to *A. muciniphila* may play critical roles during infection and inflammatory bowel diseases.

This dissertation is dedicated to my mother, whose unrealized dream was to become a scientist, and to my father, who always supported me in pursuing my own interests.

Table of Contents

List of Figures

List of abbreviations:

AMPs: antimicrobial peptides
ASF: altered Schaedler flora
ASF+ Akk: ASF + *Akkermansia muciniphila*
BMMs: bone marrow-derived macrophages
FACS: fluorescence-activated cell sorting
IBD: Inflammatory bowel diseases
IEC: intestinal epithelial cell
IFNγ: interferon gamma
IgA: Immunoglobulin A
IgG: Immunoglobulin G
IgM: Immunoglobulin M
IL: interleukin
ILC: innate lymphoid cell
LILP: large intestine lamina propria
MHC: major histocompatibility complex
mLNs: mesenteric lymph nodes
PAMP: pattern-associated molecular pattern
PC: plasma cell
pIgR: polymeric Ig receptor
PPs: Peyer's patches
PRR: pattern-recognition receptor
SFB: segmented filamentous bacteria
SIgA: secretory IgA
SILP: small intestine lamina propria
SPF: specific-pathogen-free
TCR: T cell receptor
TD: T-dependent
T_{FH}: T follicular helper
Th: T helper
TI: T-independent
TLR: toll-like receptor
Treg: regulatory T cell
UC: ulcerative colitis
WT: Wild-type

Acknowledgements

I would like to thank my advisor, Greg Barton, for all his support and mentorship during these years of training. I can confidently say that I wouldn't have become the scientist I am today without his guidance. Careful consideration about choosing the right project and ensuring that you keep in mind the big picture and are asking the right questions will forever be part of my thought process as a scientist.

I would like to thank my parents, Eduardo and Lourdes, for being supportive despite my decision to move abroad and live 6000 miles and a 9h time difference apart. I want to thank them for keeping in touch and always ensuring that I was doing well, for their unconditional love and for their warm welcome when I got to go back and visit.

I would like to thank my sister, Georgina, for putting up with me living so far away, for ensuring that our vacation time at home aligned so that we got to spend time together when I was back, and for her love and support.

I would like to thank Gaby for always being an amazing friend, even when things got tough. Life in Berkeley wouldn't have been the same without you.

I would like to thank Miquel for being a great friend and housemate, for his cheerful demeanor, and for his quick laugh and humor.

I would like to thank Jaime for being a great friend and welcoming me into his home as a new housemate during my last year and a half of graduate school. His willingness to chat and spend downtime together in the house after a long day was very welcome and appreciated.

I would like to thank Julia, Vicenç, Alejandro, Marc, Carmen, Jaime and Miquel for our evenings together at Eureka, playing some guitar or watching a movie. Having a piece of home here was instrumental to my wellbeing.

I would like to thank my classmates, specially Sean, our adopted classmate Katie, Charles, Brian, Elijah and others for our fun game nights, outings and trips.

I would like to thank all the Barton lab members, specially Meghan and April, for all their help, guidance and support. I want to thank Leianna, Krystal and Emily for all their help and hard work on this project.

I would like to thank Natalie and Michael for their hard work on this project during their rotations, as well as Victoria and Kate for their hard work on their rotations.

I would like to thank the other three members of my thesis committee, Ellen Robey, Sarah Stanley and Michael Shapira, for their help and advice.

Finally, I would like to thank my collaborators, James Moon, Ramnik Xavier, Damian Plichta, Eric Brown and Daniel Graham for their contributions to this work.

Chapter 1: Immunity and the microbiota

From model antigens to commensal bacteria

The field of immunology has evolved dramatically from the early days of Élie Metchnikoff and Paul Ehrlich and their conceptualization of "cell-mediated immunity" and "humoral immunity" (*1*). Early focus was devoted to the role of T and B lymphocytes and their limitless capacity to recognize foreign antigen revealed by the discovery of V(D)J recombination. At the time, immune targets were conceived as any epitope not encoded in the host genome, and self vs non-self-discrimination was all the consequence of tolerance mechanisms applied during lymphocyte development. In fact, antigens tended to consist of model, physiologically-irrelevant antigens such as chicken ovalbumin (OVA), with the assumption that immune responses to actual pathogens would follow the same rules unveiled by the study of these contrived epitopes. Of course, the immune system was soon recognized to be more complex than simple targeting of any foreign antigen for elimination via T and B lymphocytes: innate immune recognition of pathogens was required for the induction of immune responses. Recognition of pathogen-associated molecular patterns (PAMPs) by germline-encoded pattern recognition receptors (PRRs) was revealed as an initial, required step for the induction of immune responses (*2*), and thus the concept of immunosurveillance became a major research focus.

Since then, the known breadth and complexity of innate and adaptive immune cell types and effector functions have dramatically expanded. In parallel, it is now clear that immune cells encompass many aspects of tissue and organ physiology other than pathogen recognition and clearance: immune cells participate in cancer surveillance and elimination, tissue repair after infection or sterile injury, tissue remodeling during development and homeostasis, metabolic tuning etc. It appears that immune cells, perhaps due to their ability to circulate, surveil and communicate with other cells, have evolved to be intricately tied to tissue function throughout the body. Immune cells are thus important players in tissue physiology, acting as "rheostats" that promote a homeostatic state that maximizes host fitness.

One particularly interesting example of the role of the immune system in maintaining homeostasis is found at mucosal surfaces. Barrier sites such as the gut, skin, oral cavity and vaginal mucosa are colonized with large amounts of commensal microbes that are acquired early and persist for the lifespan of the host. Commensal microbes provide many beneficial functions to the host. These include colonization resistance against pathogens, which is achieved by occupying niches that pathogens require for their pathogenesis and outcompeting them (*3*–*7*); aid in digestion of dietary fiber, which leads to the secretion of metabolites that are both immunomodulatory and an energy source (*3*, *8*–*10*); and education of the immune system, both locally but also systemically (*3*, *11*, *12*). Furthermore, commensal microbes have been shown to impact many areas of host physiology beyond the tissues that they occupy, such as metabolism, haematopoiesis, brain function, cancer etc (*13*). The immune system plays

critical roles in establishing a homeostatic state at mucosal surfaces that is conducive to all of the aforementioned functions. Immune responses to commensal microbes are still an open area of investigation, and in the work presented in this dissertation I will describe novel types of commensal-specific responses during homeostasis.

Commensal microbes pose a conundrum for the classical view of innate immunity, since all of these microbes are "foreign" and share the ability to stimulate most innate immune receptors with pathogens, yet they don't elicit similar pro-inflammatory immune responses at steady state. Part of this conundrum can be explained by the fact that pathogens tend to engage in certain activities that commensals do not, such as invading systemic tissues, entering the cell cytosol, and carefully manipulating the host to evade immune responses. In this view, discrimination between commensals and pathogens would follow from these additional activities carried by pathogens but not commensal microbes (*14*).

However, I would argue that there are additional layers of regulation to immune responses to commensal microbes than simply the lack of more invasive activities. The important role of the microbiota on many aspects of host physiology, the fact that metazoa have coevolved with microbes since their appearance, and the fact that the acquisition of an adaptive immune system coincides with the acquisition of a complex microbiota, all support the hypothesis that many aspects of the immune system have evolved to mediate symbiotic relationships with the microbiota (*12*). If so, this would predict the existence of specific mechanisms of immune sensing and specific immune functions tailored to interactions with commensal microbes; perhaps independently, or at least parallel to mechanisms for pathogen recognition and clearance. The lack of understanding in this area is exemplified by the obscure etiology of Inflammatory bowel diseases (IBD), which comprise both Crohn's disease and Ulcerative colitis, both complex diseases of the intestine. IBD are characterized by the induction of inappropriate immune responses against the microbiota that lead to immunopathology and tissue dysfunction (*15*), yet the underlying causes and mechanisms are still poorly understood. Thus, study of immune system-commensal interactions is likely to yield important insights into immune and tissue function during homeostasis and disease.

The immune system and the microbiota in the intestine

Many different bacterial communities coexist with mammals. Of those, the most well studied, and also the most abundant, is the intestinal microbiota. The intestine is colonized by very dense and diverse microbial communities, which reach 10^{11} bacteria per gram of contents in the colon (*16*). The intestinal microbiota also comprises other microbes such as fungi, viruses and protozoa, yet intestinal bacterial communities are the most abundant and well-studied. Bacterial load and composition vary from the duodenum, the most proximal intestinal tissue, not including the stomach, through the jejunum, ileum, cecum, proximal colon and distal colon. Furthermore, bacterial species also differ in their localization to the lumen and/or the mucus layer: in the small intestine, a loosely-attached mucus layer is permissive to some degree of bacterial colonization, while also permitting nutrient absorption. In the colon, a dense inner mucus layer is

impenetrable to bacteria and small particles, while the outer mucus layer is less dense and hosts bacterial communities (*17*).

The large bacterial load found in the intestine poses an important risk to the host: bacterial invasion of the underlying tissue or systemic dissemination would have disastrous consequences, leading to intestinal tissue dysfunction and septicemia, respectively. To prevent this, the immune system, alongside the non-hematopoietic intestinal epithelial cell layer, form a mucosal "firewall" that prevents bacterial invasion (*3*, *12*, *18*, *19*). This mucosal barrier is the result of different functions deployed by immune and epithelial cells. First, the mucus layer acts as a first physical barrier to bacterial invasion. Antimicrobial peptides (AMPs) are constitutively secreted by intestinal epithelial cells (IECs), and also by a specialized enterocyte named Paneth cell. AMP production, along with other aspects of barrier function, can also be reinforced by cytokines derived from innate and adaptive immune cells such as IL-22 and IL-17 (*19–21*). Commensal-specific (or "anti-commensal") IgA antibodies are produced by plasma cells in the intestinal lamina propria and are transcytosed through IECs into the intestinal lumen by the polymeric immunoglobulin receptor (pIgR). IgA antibodies in the intestinal lumen contribute to barrier function by binding to commensal bacteria and excluding their targets from deeper invasion into the tissue (*22*). However, other functions of IgA antibodies have been described, such as limiting bacterial motility, modulating bacterial gene expression, facilitating niche occupancy in the mucus layer and mediating antigen uptake (*22–24*). Thus, IgA contributes many different functions to host-microbiota interactions. Finally, phagocytes in the lamina propria, but also the liver (*25*), engulf and process commensal bacteria that manage to breach the intestinal barrier to prevent further dissemination.

Of note, many of these functions deployed at steady state are also important during tissue challenges such as infection, wounding and/or inflammation. They are deployed in parallel to additional measures tailored towards dealing with the specific insult and returning to homeostasis. Depending on the insult, these can include neutrophil and inflammatory monocyte recruitment (*26*, *27*), induction of high affinity IgA antibodies and pro-inflammatory T cell responses towards pathogens (*28*, *29*), induction of intestinal epithelial crypt hyperplasia (*30*), goblet cell hyperplasia (*30*) and others. Immune cells in the intestine lie upstream of all these effector functions: innate and adaptive lymphocytes, dendritic cells, and macrophages integrate signals from epithelial cells and the environment to direct and coordinate immune responses to maintain, or reestablish, homeostasis in the intestine. Much work has been devoted to the study of the role of innate immune effector functions in the intestine (*21*, *31–34*). However, innate sensing and recognition of the microbiota during homeostasis is only now starting to be understood.

The role of the adaptive immune system is clear in response to intestinal pathogens (*28*, *29*). In contrast, much less is known about adaptive immune responses to commensal bacteria, both during homeostasis and disease. Even IgA antibody responses, which were once thought to have a clear adaptive origin, have now been

shown to be largely derived from T-independent B1 innate-like B cells (*22*, *35*, *36*). Thus, how the adaptive immune system responds to commensal bacteria remains largely unexplored. This is of particular importance given the fact that inappropriate T cell responses against commensal antigens are thought to underlie disease pathogenesis in IBD (*15*). Therefore, understanding the regulation of adaptive immune responses against commensals is likely to yield important insights into host-microbiota symbiosis, and could shed light into the mechanisms of this complex set of diseases.

B cell responses to the microbiota in the intestine

IgA antibodies play major roles at many mucosal surfaces throughout the body. IgA has the ability to dimerize and bind the J chain polypeptide, forming secretory IgA (SIgA). SIgA is secreted via interactions with pIgR and transcytosis through epithelial cells (*22*). IgA deficiency is one of the most common human immunodeficiencies (*37*), yet in the absence of IgA, compensatory IgM responses are induced (*22*). IgM has the ability to multimerize into pentamers or hexamers and bind the J-chain, which endows it with the ability to be secreted.

IgA antibodies are secreted into the intestine by plasma cells (PC) present in the lamina propria, and are derived from innate B1 and adaptive B2 B cells (*22*). Commensal-specific IgA antibodies are largely comprised of polyreactive, natural specificities (*36*) that are mostly T-independent (*35*). In contrast, T-dependent antibody responses to the microbiota are restricted to a few species, such as segmented filamentous bacteria (SFB), *Mucispirillum spp., Prevotella spp. and Helicobacter spp.* (*22*, *35*, *38*). There is evidence that some of these commensal bacteria also lead to antigen-specific T cell responses (see below), which suggests that they are more immunostimulatory and engage distinct arms of the mucosal immune system compared to the majority of commensal species.

Due to an apparent lack of IgG antibodies to commensal bacteria, it was initially thought that IgG antibodies did not contribute to intestinal homeostasis (*39*, *40*), and that they were only induced in the context of barrier disruption and systemic dissemination (*39*). However, more recent work from my lab has revealed that mice generate commensal-specific IgG antibody responses during homeostasis (*41*). These antibodies are comprised of the IgG2b and IgG3 isotypes, are T-independent and largely Toll-like Receptor (TLR) 2 and TLR4-dependent. IgG2b and IgG3 antibody responses are broadly reactive against commensal bacteria, similar to IgA responses, and are thought to originate from similar specificities. IgG2b and IgG3 antibodies do not cross into the intestinal lumen like IgA, and can only be detected in the serum of mice, yet they play important roles in the neonatal period. Maternally-derived, commensal-specific antibodies, including IgG2b, IgG3 and IgA, are acquired in the milk and help instruct the developing immune system in the intestine by dampening T cell responses to the microbiota in the pup (*41*). Unsurprisingly, IgG antibody responses are also induced against intestinal pathogens and pathobionts that breach the intestinal barrier and reach systemic sites (*28*, *42*). Finally, IgM^+ and IgG^+ intestinal plasma cells have been detected in humans, and coating of intestinal bacteria by IgM and IgG have also

been detected (*22*, *43*), suggesting that similar responses are at play in humans. Of note, no role for T-dependent IgG antibody responses to the microbiota has been described previously.

T cell responses to the microbiota in the intestine

Mucosal surfaces are home to a large number of activated lymphocytes, including B-cell derived plasma cells; $CD4^+$ and $CD8^+$ $\alpha\beta$ T cells, present largely in the lamina propria; and $\gamma\delta$ T cells and other innate-like T cells such as $CD8\alpha\alpha$ T cells and others, usually present within the epithelial layer. $CD4^+$ T cells differentiate into one of many different fates with different effector functions: T helper 1 (Th1), Th2, Th17, regulatory T cell (Treg) and T follicular helper (T_{FH}) cells (*44*), and each T cell fate expresses a lineage-determining transcription factor. Th1 cells express T-bet and respond to intracellular pathogens by secreting interferon gamma (IFNγ), which activates macrophages and fuels inflammation. Th2 cells express GATA3, are induced in response to extracellular parasites such as helminths (and also allergens), and secrete type-II cytokines such as IL-4, IL-5 and IL-13. These type-II cytokines orchestrate many different functions in tissues such as mucus secretion, eosinophil recruitment, induction of IgE antibodies etc. Th17 cells express RORγt, are induced at mucosal surfaces in response to extracellular bacteria or fungi, and secrete IL-17 and IL-22, which help reinforce barrier function and fuel inflammation. T regulatory cells (Treg cells) express FOXP3, arise in the thymus by agonist selection on self-antigen, or are induced in the periphery in response to innocuous antigens such as food or intestinal bacteria (*45*, *46*). Treg cells have an anti-inflammatory role and act as negative regulators of immune responses through still poorly understood functions, such as secretion of IL-10, sequestration of IL-2 by the high affinity receptor CD25, expression of CTLA-4 etc. T_{FH} cells express Bcl6 and are important for the induction of T-dependent B cell responses: they help activate naïve B cells, localize to germinal centers, provide help to B cells undergoing affinity maturation, and may direct class-switching through cytokine secretion. Other $CD4^+$ T cell fates, such as Th22 cells (IL-22 secreting, Th17-like), Th9 cells (IL-9-secreting, Th2-like), and Tr1 cells (IL-10-secreting, FOXP3-negative) have also been described in particular contexts (*29*, *47*, *48*).

Given the important role of T cells as orchestrators of immune functions, commensal-specific T cell responses are likely to play major roles during both homeostasis and disease in the intestine. However, very little is known about the induction, regulation and function of commensal-specific T cells in both homeostasis and disease. In fact, despite the high abundance of foreign antigens present in the intestine and the large number of antigen-experienced T cells present in the lamina propria and epithelial layer, only a small number of commensal species have been identified that induce cognate T cell responses during homeostasis (*12*). Thus, identification of commensal-specific T cell responses and characterization of their functions and regulation remain important goals in the field.

The number of examples of commensal antigens that induce cognate T cell responses are limited to Segmented filamentous bacteria (SFB), *Helicobacter spp.*, and

a clostridial flagellar antigen, CBir1. Other bacteria have also been shown to induce changes in the intestinal T cell compartment in gnotobiotic settings: namely the induction of Treg cells, both in monocolonization experiments (*49*, *50*) and with bacterial consortia (*46*, *51*, *52*). Human bacteria capable of inducing Th17 cells have also been identified (*53*, *54*). Furthermore, ectopic colonization of oral bacteria in the intestine induces inappropriate Th1 T cell responses which can drive inflammation in susceptible hosts (*55*). Finally, a defined consortium of human microbes has been shown to induce IFNγ-producing CD8$^+$ T cells in the intestine, which influenced responses to cancer immunotherapy (*56*). Importantly, in all these other examples, the T cell antigen specificity wasn't identified: while it is indeed possible that the induced T cells are cognate to the inducing commensals, it is also possible that they are antigen-specific towards other antigens such as bystander commensals, food, or self-antigen. However, many of these studies were carried in monocolonized germ-free mice. The presence of a single commensal is very artificial, and carries many caveats associated with the interpretation of those experiments. Thus, understanding which bacteria induce antigen-specific T cell responses during homeostasis and in the context of a diverse microbiota remains an open question.

SFB was first identified based on its ability to induce Th17 cells in the small intestine lamina propria (SILP) of mice (*57*, *58*). Comparison of genetically identical inbred strains of mice from two different vendors, Jackson laboratories and Taconic Biosciences, revealed that only mice from Taconic harbor Th17 cells in the SILP at steady state. Comparing the microbiota between these mice and performing cohousing and microbiota transfer experiments identified SFB as the microbe responsible for the induction of Th17 cells (*57*, *58*). Further work revealed that intestinal Th17 cells are indeed specific for SFB antigens (*59*, *60*), and that adhesion to epithelial cells by SFB is necessary for the induction of Th17 cells (*54*). While the molecular nature of the signals required for the induction of Th17 cells by SFB still remain elusive, one surprising observation was that intestinal dendritic cells are largely dispensable for the induction of Th17 cells towards SFB, yet CX3CR1$^+$ monocyte-derived intestinal macrophages are required (*61*). Production of IL-17A by Th17 cells is induced by Serum amyloid A 1 and 2 derived from epithelial cells in the ileum, where SFB is located. SAA production is in turn induced by ILC3-derived IL-22. Thus, proinflammatory cytokine secretion by commensal-specific Th17 cells is locally regulated by cues derived from multiple cell types in the intestine.

Colonic T regulatory cells are induced by the presence of the microbiota (*51*, *62*), while Treg cells in the small intestine are induced by dietary antigens (*45*). Colonic T reg cells are largely derived from naïve peripheral T cells, not from thymic-derived Tregs (*62*, *63*), suggesting that they are specific for foreign antigens. Regarding the signals required for their generation, short chain fatty acids (SCFAs) lead to the induction of Treg cells in the colon (*8–10*). Clostridium species can make SCFA and were initially identified as inducers of colonic Treg cells in germ-free colonization experiments (*51*, *52*), yet other bacteria and consortia are also able to induce colonic Treg cells in gnotobiotic settings (*46*, *49*, *50*). Surprisingly, in the context of a complex

microbiota, at least a fraction of colonic Treg cells are antigen-specific for *Helicobacter spp.*, which is considered a pathobiont (*64*, *65*). Interestingly, a big fraction of colonic Treg cells, and most of the *Helicobacter*-specific ones, coexpress the lineage-determining transcription factors FOXP3 and RORγt. In IL-10-deficient mice, which lack a critical anti-inflammatory cytokine and develop *Helicobacter*-dependent colitis (*66*), *Helicobacter*-specific T cells develop into pathogenic Th17 cells instead of RORγt$^+$ Treg cells (*65*). Thus, commensal-specific T cell responses need also be examined in the context of a diverse microbiota to avoid caveats associated with monocolonized settings.

Finally, Cbir1 is an antigen derived from a clostridial flagellin that was first identified in patients with Crohn's disease (*67*). Later work revealed that CBir1-specific T cells remain naïve in Wild-type (WT) mice, yet they are activated in mice that lack IgA antibodies (*68*). Furthermore, CBir1-specific T cells also become activated in WT mice in the context of acute gastrointestinal infection or chemically-induced intestinal inflammation, and adopt CD4$^+$ T cell fates that parallel those induced by the respective insult (*69*). This body of work reveals that one fate of commensal-specific T cells during homeostasis is ignorance, or the lack of a response, and that these antigens only lead to cognate responses in situations where homeostasis is disturbed. Indeed, given the paucity of commensal-specific adaptive B and T cell responses that have been identified, it is possible that this is the fate of the majority of commensal antigens, and is a general mechanism that prevents inappropriate reactivity to innocuous antigens and helps maintain homeostasis.

T cell responses to commensal bacteria have been hypothesized to provide bystander protection against infection (*70*): disruption of the intestinal barrier caused by an enteric pathogen would lead to concomitant antigen sampling from commensal species. Consequently, preexisting commensal-specific T cells could respond to this influx of commensal antigens and promote effector functions that are also protective against the pathogen. In parallel, T cell responses to commensals are known to underlie the etiology of IBD, so dysregulation of existing commensal-specific T cell responses would pose a large risk to the host.

During intestinal infection or inflammation, novel commensal-specific T cell responses are induced (CBir1), but homeostatic T cell responses can also adopt different fates, such as for *Helicobacter spp.* in IL-10 deficient mice (*65*). Given the scarcity of examples of commensal-specific responses, it is unclear if one of these two scenarios is representative of most commensal-specific responses during disruption of homeostasis. Bacteria that are able to induce responses at steady state are more immunostimulatory, and may thus be able to dominate responses during inflammation. However, some of the most abundant bacteria in the intestine such as Clostridia or Bacteroides species appear to be largely ignored by the adaptive immune system during homeostasis, but could provide major antigens during barrier disruption due to their abundance. I would also hypothesize that the composition of the microbiota,

genetic makeup and environmental conditions in the gut are also likely to play important roles in determining which bacteria are sensed during homeostasis and disease.

In conclusion, intestinal adaptive B and T cell responses to commensal bacteria are likely to play important roles during homeostasis and disease, yet very few examples of commensal-specific responses have been described and little is known about the signals required for their induction, their regulation, and their functions. Therefore, for my dissertation work I decided to explore antigen-specific adaptive immune responses against commensal bacteria. In particular, I decided to explore T-dependent IgG responses and utilize them to identify immunostimulatory commensal bacteria that induce T cell responses during homeostasis.

Chapter 2: Commensal bacteria induce T-dependent IgG antibody responses during homeostasis

Many materials in this Chapter have been adapted or reproduced from my publication (*71*): Ansaldo et al. "*Akkermansia muciniphila* induces intestinal adaptive immune responses during homeostasis", *Science*, 364, 1179-1184 (2019). Reprinted with permission from AAAS.

Background:

The discovery of T-independent (TI) commensal-specific IgG antibodies and their similar ontogeny and specificity as anti-commensal TI IgA suggested to me that a T-dependent (TD) IgG counterpart to commensal-specific TD IgA may also exist. IgG antibodies are divided into different isotypes: IgG1, IgG2c, IgG2b and IgG3; which can be differentiated based on their constant region. The discovery of a commensal-specific IgG isotype that is entirely T-dependent would provide me with an avenue to easily identify commensal bacteria that induce cognate adaptive immune responses during homeostasis. The rationale is that any bacteria that induces T-dependent IgG antibodies is also likely to induce cognate T cell responses, given the requirement for T cells. IgA can't easily be used for the same purpose given that both TI and TD IgA specificities coexist within animals. Thus, identifying IgA-bound commensal bacteria is insufficient to directly identify bacteria that induce T cell responses, since one cannot easily distinguish between TI and TD coating. Even when comparing T cell-deficient mice (*Tcrb*$^{-/-}$) to WT mice to detect TD coating, this analysis will only reveal commensal species that rely strongly on the induction of TD specificities for their coating, and may fail to reveal bacteria that can be coated with both TI and TD specificities (*35*, *38*). Therefore, existing analysis of T-dependent IgA binding to commensal bacteria are likely to miss important targets of adaptive immune responses.

Commensal-specific antibodies have been implicated in many aspects of host-microbiota symbiosis. Maternally-transmitted antibodies help dampen intestinal T cell responses to commensal bacteria in the neonatal period (*41*), and also contribute to neonatal intestinal immune development by transferring microbial molecules to the pup in utero, increasing innate lymphoid cell 3 (ILC3) and mononuclear cell numbers in the intestine (*72*). Furthermore, systemic commensal-specific antibodies have been shown to protect against gut-derived septicemia during intestinal barrier disruption (*42*, *73*, *74*). However, pathogenic roles for commensal-specific antibodies have also been described: increased commensal-specific IgG is a hallmark of patients with Ulcerative colitis (UC), where IgG antibodies contribute to disease in genetically susceptible people and mice through activation of IgG receptors (FcγR) on intestinal macrophages (*75*). Thus, just like with commensal-specific T cell responses, it appears that antibody responses to commensal bacteria underlie both mutualistic and pathogenic aspects of host-microbiota symbiosis.

T-independent anti-commensal antibody responses are comprised of low-affinity polyreactive specificities (*36*). Given their ability to recognize broad fractions of commensals, TI antibodies are likely to contribute to some of the important roles outlined above. High-affinity TD IgA antibodies are only induced against select members of the microbiota (*35*, *38*), and TD IgG anti-commensal antibodies haven't been previously described before this work. However, I would argue that due to their high affinity, and their highly selective specificities, these are likely to play important roles in the functions outlined above, as well as new roles. Indeed, AID-dependent, SFB-specific IgA antibodies, which are T-dependent (*35*), have been shown to be important to contain SFB in the mucosa and prevent inflammation (*76*). Thus, delineating which commensal species induce high affinity T-dependent antibody responses is likely to unveil important host-commensal interactions.

In summary, I hypothesized that a T-dependent arm of the commensal-specific IgG antibody response exists. To test this hypothesis, I decided to explore commensal-specific responses of all IgG isotypes and compare T cell deficient and T cell sufficient mice. Identification of an IgG isotype that is entirely T-dependent would allow me to identify commensal bacteria that induce cognate T cell responses and are likely to play important roles during homeostasis and disease.

Results:

To examine commensal-specific T-dependent IgG antibody responses, I utilized a previously-described method to detect serum IgG specificities capable of binding to the intestinal bacterial microbiota (*41*). I collected paired mouse serum (containing antibodies) and feces (containing intestinal microbes), and stained preparations of fecal bacteria with serum antibodies. I then used secondary antibodies against specific mouse IgG isotypes, IgG1, IgG2c, IgG3 and IgG2b, to probe binding to the microbiota by performing flow cytometry (Figure 2.1A). Flow cytometry is a single-cell assay that reads out fluorescence on multiple, predetermined channels for each individual cell, and allows for analysis of large number of events per second, up to 10,000/s. Sybr-green I and side scatter allowed for the discrimination of bacteria from small food particles. Biotinylated secondary antibodies specific for IgG isotypes and fluorophore-conjugated streptavidin allowed for the detection of IgG-bound bacteria. Finally, B-cell deficient mouse sera (*Ighm*$^{-/-}$) served as a negative control that lacks all antibodies in the serum.

I compared serum binding to commensal bacteria in WT and T cell-deficient (*Tcrb*$^{-/-}$) mice to determine whether T-dependent IgG antibody responses against commensals are induced at homeostasis. Surprisingly, this analysis revealed that mice mount a microbiota-reactive IgG1 antibody response that is entirely dependent on T cells (Figure 2.1A, B), while anti-commensal IgG2b, IgG3 and IgA are induced in a T-independent manner as previously reported (Figure 2.2A) (*35*, *41*, *77*). Importantly, *Ighm*$^{-/-}$ serum has only minimal binding to the fecal microbiota. The small amount of remaining staining with the *Ighm*$^{-/-}$ serum is likely due to nonspecific binding of the streptavidin-PE-Cy7 secondary fluorophore used in the assay, since it is still present when the secondary IgG-specific biotinylated antibody is omitted from the assay (Data not shown). The fraction of commensals bound by T-dependent IgG1 was approximately 10% (Figure 2.1B), far less than the percentage recognized by IgG2b, IgG3 and IgA (Figure 2.2A). This relatively small percentage suggested that mice produce IgG1 that recognizes only a subset of microbes in the intestine, in contrast to the polyreactive T-independent antibodies that bind diverse bacteria (*36*, *41*).

The microbiota composition of mice from different sources or even different lines of mice housed in the same facility can vary significantly (*13*, *58*), and mouse genetic background and microbiota composition have been linked to differences in the anti-commensal IgA response (*78*, *79*). Cohoused littermate mice are critical controls in phenotypes affected by the microbiome, as they allow for the discrimination between genetic and microbiome contributions to a given phenotype (*13*). Thus, to rule out the possibility that the different phenotypes observed in WT and *Tcrb*$^{-/-}$ mice were due to different microbiota composition, and not due to the lack of T cells in *Tcrb*$^{-/-}$ mice, I analyzed T cell-sufficient (*Tcrb*$^{+/-}$) and T cell-deficient (*Tcrb*$^{-/-}$) cohoused littermates and again observed an anti-commensal IgG1 response only in T cell-sufficient mice (Figure 2.2B). Moreover, analysis of mice from multiple vendors and of different genetic backgrounds revealed that this IgG1 response is a general feature of healthy mice (Figure 2.1C).

To identify the commensal species targeted by serum IgG1 antibodies, I adapted a previously-described assay that identified fecal bacteria bound by IgA, IgA-Seq (*35*, *38*). In this assay, I stained fecal bacteria with serum from corresponding mice and secondary antibodies for IgG1 as described above, and then performed fluorescence activated cell sorting (FACS) to isolate IgG1-bound bacteria and IgG1-negative bacteria. Importantly, this assay differs from IgA-Seq in that it uses serum to provide antibody binding to the bacteria, and thus probes systemic antibody specificities. Then, I performed 16S rDNA (ribosomal DNA) sequencing on the resulting fractions. 16S rDNA sequencing amplifies a small hypervariable region within the 16S ribosomal RNA gene from bacteria, such as region V4, and then performs next-generation sequencing on the PCR product library. After paired-end sequence alignment and filtering, the resulting 250bp reads are then clustered to OTUs (operational taxonomic units) with clusters of 97% DNA sequence identity. This step allows to reduce noise from sequencing errors, and bins together strains of the same species with very similar 16S sequences.

I sorted IgG1-bound and unbound populations from fecal samples stained with sera from corresponding mice (Figure 2.3A, B) and performed 16S rDNA sequencing on the resulting fractions (IgG1-Seq). Two Operational Taxonomic Units (OTUs) were significantly enriched in the IgG1-positive fractions compared to the IgG1-negative fractions (Figure 2.1D and Figure 2.3C, D). These OTUs correspond to the *Akkermansia* genus (OTU2) and the Bacteroides S24-7 family (OTU63). Bacteroides S24-7 consists of an uncultured and poorly characterized family of mouse intestinal microbes (*80*, *81*). *Akkermansia* is a genus of intestinal commensals in the Verrucomicrobia phylum that until recently only contained one member, *Akkermansia muciniphila* (*82*, *83*) . Performing IgG1-Seq on other cohorts of mice also identified *Akkermansia muciniphila* and Bacteroides S24-7 as targets of IgG1 antibodies (Figure 2.4A). Importantly, only specific OTUs assigned to the Bacteroides S24-7 family were recognized by IgG1, while many others remained in the left part of the volcano plot in Figure 2.1D and Figures 2.4A and B. Given the lack of characterization of this bacterial family, it is likely that only individual genera or species within Bacteroides S24-7 induce IgG1 responses, while many others do not.

At least one cohort had a different major target pertaining to the *Faecalibacullum* genus, and targeting of *Akkermansia* and Bacteroides S24-7 was still present, but weaker (Figure 2.4B). Importantly, the same *Faecalibacullum* OTU was clearly IgG1-negative in a parallel cohort of mice (Figure 2.4A), suggesting that it may not be a common target of IgG1 antibodies across mice with different bacterial communities.

Discussion:

Commensal-specific TD antibodies were previously thought to be restricted to IgA responses specific for a small subset of commensal species (*22*). My work reveals that such TD antibodies also include IgG antibodies, in particular IgG1. While T-independent IgG isotypes (IgG2b and IgG3) are broadly reactive against a large fraction of the microbiota (*41*), IgG1 responses are much more restricted to a small number of commensal bacteria. These bacteria include *Akkermansia* and specific members of the Bacteroides S24-7 family, but can also include additional bacteria in certain cohorts.

IgG1-targeted bacteria may share certain features, such as proximity to the intestinal epithelium, which may increase their potential to cause disease during barrier disruption. Thus, preemptive induction of high affinity systemic antibodies against them could help protect in the event of barrier disruption and systemic access of these bacteria. Indeed, systemic antibodies specific for commensal bacteria have been reported to protect against gut-derived septicemia (*42*, *74*), although a role for microbiota-specific TD IgG specificities wasn't explored. Furthermore, *Akkermansia muciniphila* can promote disease in certain immunodeficient settings (*84*), which supports the hypothesis that IgG1-targeted bacteria are immunostimulatory and may contribute to disease pathogenesis in the context of immune dysregulation or systemic access. TD commensal-specific IgG1 responses are likely to contribute to other functions in addition to protection against systemic dissemination. IgG antibodies are transmitted in utero and in the milk, and they help instruct the neonatal immune system and protect against enteric pathogens (*41*, *72*, *85*), while also driving intestinal disease in genetically susceptible settings (*75*). Commensal-specific IgG1 antibodies are likely to contribute to these effects. In fact, I would argue that given their specificity and affinity, IgG1 antibodies could play dominant or non-redundant roles in the aforementioned functions.

Finally, bacteria that induce T-dependent IgG1 antibody responses are likely to induce cognate T cell responses during homeostasis. Given the scarcity of examples of commensal-specific T cell responses and the important roles that T cells play during homeostasis and disease in the gut (*12*), identifying T cell-inducing commensal bacteria gives me an opportunity to gain important insights in this understudied area.

Methods:

Animals:

Mice were housed under specific-pathogen-free (SPF) or gnotobiotic conditions at UC Berkeley. Mice in Figure 2.1C were analyzed upon arrival from the indicated vendors. For SPF experiments, adult (8-16 weeks of age, male and female) C57BL/6J mice were used as wild-type mice. Congenic C57BL/6J.SJL (B6.SJL-*Ptprc*^{a} *Pepc*^{b}/BoyJ) mice were also included as wild-type mice for one of the repeats in Figure 2.1D. Mice in Figure 2.1D comprised two consecutive litters (two cohorts of littermate mice) born to the same breeding cage. All experiments were performed in accordance with the Animal Care and Use Committee guidelines at the University of California Berkeley.

Microbiota/bacterial flow cytometry and sorting:

Microbiota flow cytometry was performed as previously described (*41*). Briefly, fresh fecal pellets and blood were collected from individual mice. Blood was centrifuged at 13,000×*g* for 15 min twice to collect serum. Fecal pellets were homogenized in 1mL phosphate-buffered saline (PBS) and filtered through a 40-μm filter, centrifuged at 10,000×*g* for 3 min and washed in PBS. Optical density (OD) was measured and an OD 1=10^9 bacteria/mL approximation was used for all samples.

Fecal samples were stained overnight at 2.5x10^7 bacteria/mL in 50μL of bacterial staining buffer (BSB) (1%BSA in PBS + 0.025%NaN) with serum added at 1:50 final dilution factor (unless otherwise noted) in a V-bottom 96-well plate. For microbiota flow cytometry, feces and sera originated from the same mouse, except when otherwise noted. Samples were washed with 150 μL of BSB, pelleted (3,220×*g* 5 min 4ºC) and resuspended in BSB with secondary antibodies. Biotinylated secondary antibodies were used at 1:200: anti-mouse IgG1 A85-1 (BD Pharmigen), anti-mouse IgG2a 5.7 (BD Pharmigen), anti-mouse IgG3 R40-82 (BD Pharmigen), and polyclonal anti-mouse IgA (1040-08 Southern Biotech). After washing and pelleting, samples were resuspended in BSB + Streptavidin-PE-Cy7 (SA-PE-Cy7) (Invitrogen) at 1:200. Samples were washed with BSB and resuspended in 200 μL BSB with Sybr-green I nucleic acid stain (Invitrogen) at 1:10,000. Samples were analyzed on a BD LSR Fortessa or a BD LSR Fortessa X-20.

For sorting of IgG1-bound commensals, 4x10^6 bacteria (assuming OD 1=10^9 bacteria/mL) were stained overnight in 4 mL with 80 μL of serum (1:50 dilution) in BSB. After pelleting (10,000×*g* 3 min 4ºC) samples were washed in BSB, pelleted and resuspended in 1 mL BSB with secondary anti-mouse IgG1-biotin for 30min at 4C. BSB was added to wash, samples were pelleted and resuspended in 1 mL BSB with SA-PE-Cy7 for 25 min at 4ºC, pelleted, washed with BSB, pelleted and resuspended in 3 mL BSB (with SYBR Green 1:10,000). Samples were sorted into IgG1$^+$ and IgG1$^-$ fractions on a BD FACSAria Fusion sorter. 1x10^6 IgG1$^+$ and 2x10^6 IgG1$^-$ events were collected, and input and sorted fractions were pelleted, resuspended in 100 μL of PBS and frozen at -80ºC prior to sample processing.

16S rDNA sequencing and analysis:

Sample processing and 16S rDNA sequencing were performed at the Alkek Center for Metagenomics and Microbiome Research at Baylor College of Medicine. Sample processing was performed with a DNeasy PowerSoil kit (QIAGEN). V4 16S rDNA sequencing was conducted on a MiSeq (Illumina) with 2×250 paired-end reads.

Sequence processing was performed using Mothur 1.39.5 according to the MiSeq SOP protocol (*86*), using the 128 release of the SILVA ribosomal RNA database (*87*). Operational taxonomic units (OTUs) were clustered to 97% identity. Rare OTUs with two sequences or fewer, OTUs that were not present in at least 25% of the samples and OTUs that were less than 0.01% of total sequences were removed. Paired ratio Student's *t*-tests (Paired Student's *t*-test on log-transformed data) were calculated using scipy.stats in Python 3.7, and Benjamini, Krieger and Yekutieli's two-stage false discovery rate (FDR) approach was used to correct for multiple comparisons, with an FDR (Q) of 0.01, using statsmodels.stats in Python 3.7.

Quantification and statistical analysis:

Statistical tests were performed as indicated on the figure legends with Prism 8 software (Graphpad Prism). Statistical analysis of 16S rDNA sequencing data was performed as indicated above.

Figures:

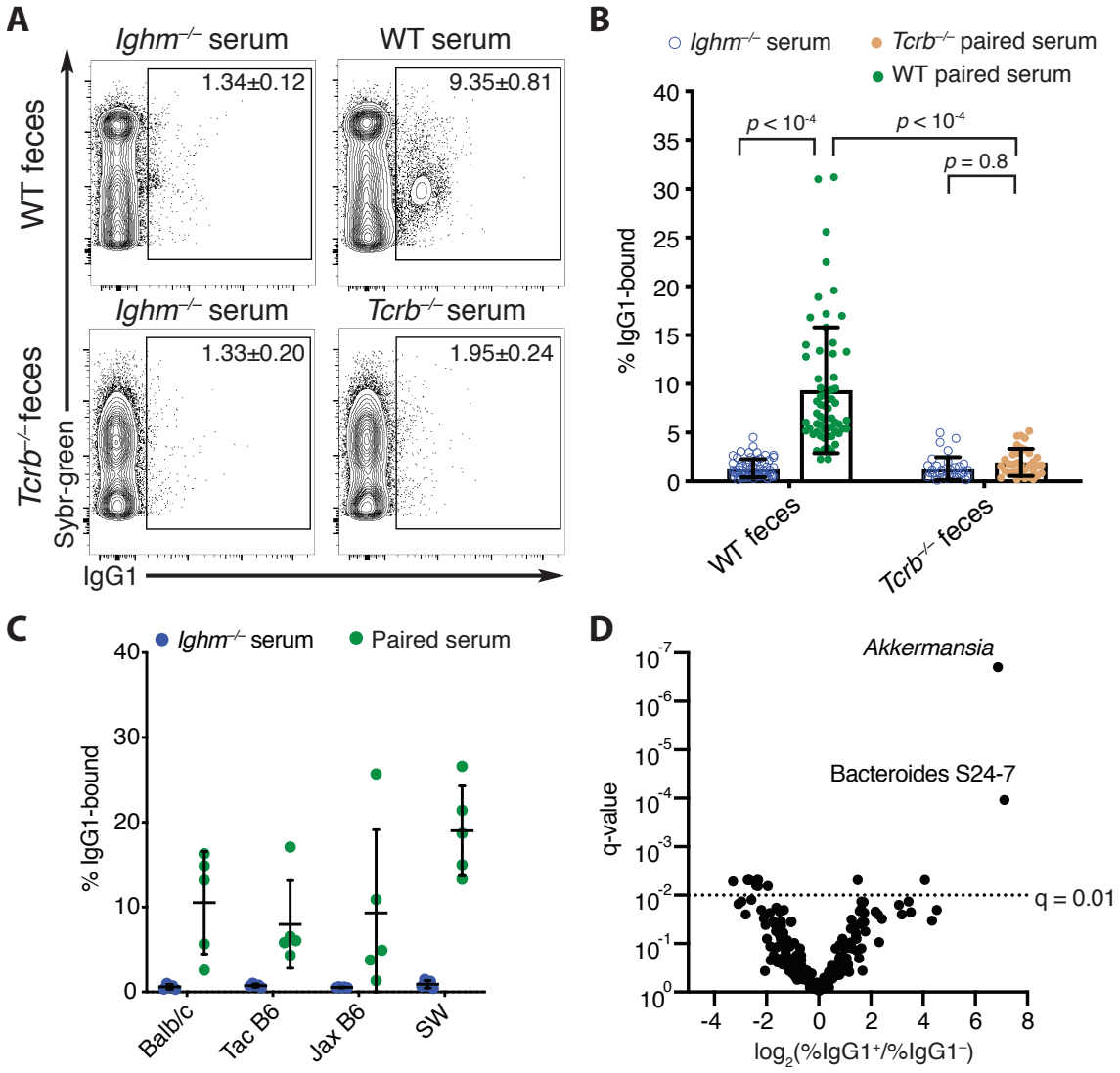

Figure 2.1. Mice generate anti-commensal IgG1 antibodies during homeostasis
(**A**) Representative IgG1 flow cytometric analysis of fecal microbiota with sera from WT and T cell-deficient (*Tcrb*$^{-/-}$) mice. Feces and sera originated from the same mouse (paired serum), except when using antibody-deficient (*Ighm*$^{-/-}$) serum as a negative staining control. SYBR-green labels a fraction of the microbiota, ensuring that SYBR^{hi} events are bacteria, whereas some of the SYBR^{lo} events are also commensals that are less permeable to the dye (*41*).
(**B**) IgG1 microbiota flow cytometric analysis, compiled from eight independent experiments. All mice were housed at UC Berkeley. WT n=63, *Tcrb*$^{-/-}$ n=35 in total.
(**C**) IgG1 microbiota flow cytometric analysis with paired feces and sera from mice of the indicated genetic backgrounds and vivaria. Balb/c from Jackson Laboratories. Jax B6 and Tac B6: C57BL/6 from Jackson Laboratories or Taconic Biosciences, respectively.

SW: Swiss Webster from Taconic Biosciences. n=5 mice per group. Data are representative of two independent experiments.
(**D**) Results from sorting and 16S rDNA sequencing of IgG1-bound and unbound fractions (n=12 mice). Graph depicts the average log2 ratio of abundances between both fractions for each individual OTU and the corresponding q-value. Data are representative of two independent experiments.
Each symbol represents a mouse (B, C) or an OTU (D). Error bars represent mean ± SD. Gates on flow cytometry plots show mean±SEM. *p*-values were calculated by a Kruskal–Wallis test followed by Dunn's multiple comparisons (B) or by Paired ratio Student's *t*-test followed by Benjamini, Krieger and Yekutieli's two-stage false discovery rate (FDR) to correct for multiple comparisons, with an FDR (Q) of 0.01 (D).

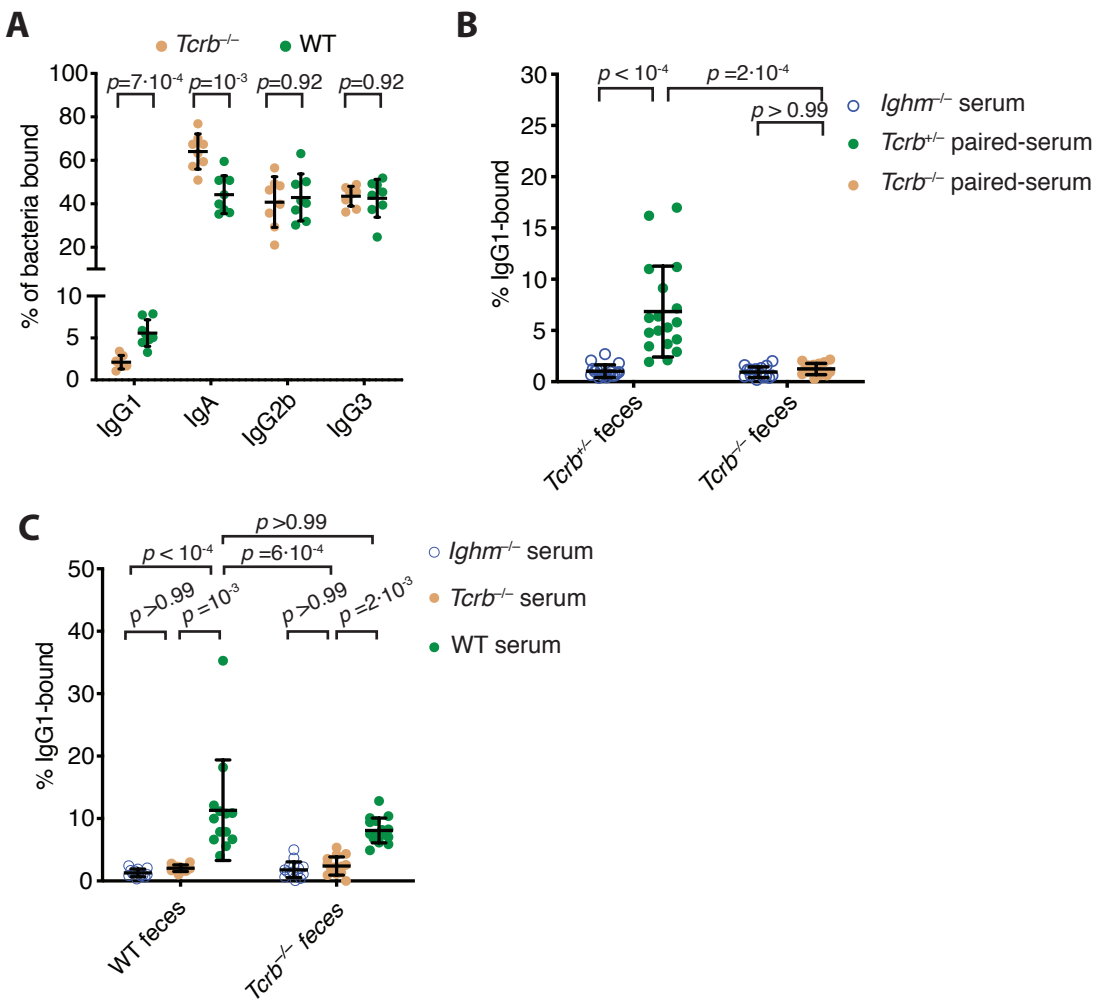

Figure 2.2. Anti-commensal IgG1 antibodies, but not other isotypes, are T cell-dependent

(**A**) Microbiota flow cytometric analysis of WT and T cell deficient (*Tcrb*$^{-/-}$) mice comparing different antibody isotypes. Data are representative of two independent experiments. WT n=8, *Tcrb*$^{-/-}$ n=8.

(**B**) IgG1 microbiota flow cytometric analysis of *Tcrb*$^{+/-}$ and *Tcrb*$^{-/-}$ littermate mice that were kept cohoused upon weaning. Data are compiled from four independent experiments. *Tcrb*$^{+/-}$ n=18, *Tcrb*$^{-/-}$ n=16 in total.

(**C**) IgG1 microbiota flow cytometric analysis of WT and *Tcrb*$^{-/-}$ mice. WT and *Tcrb*$^{-/-}$ feces were stained with paired sera, and sera from *Tcrb*$^{-/-}$ and WT mice, respectively, to show the presence of IgG1-inducing bacteria in the *Tcrb*$^{-/-}$ microbiota. n=13 WT mice, n=15 *Tcrb*$^{-/-}$ mice. Data are representative of three independent experiments.

Each symbol represents a mouse, error bars represent mean ± SD. *p*-values were calculated by Multiple *t*-tests with Holm–Sidak correction (A) or a Kruskal–Wallis test followed by Dunn's multiple comparisons (B and C).

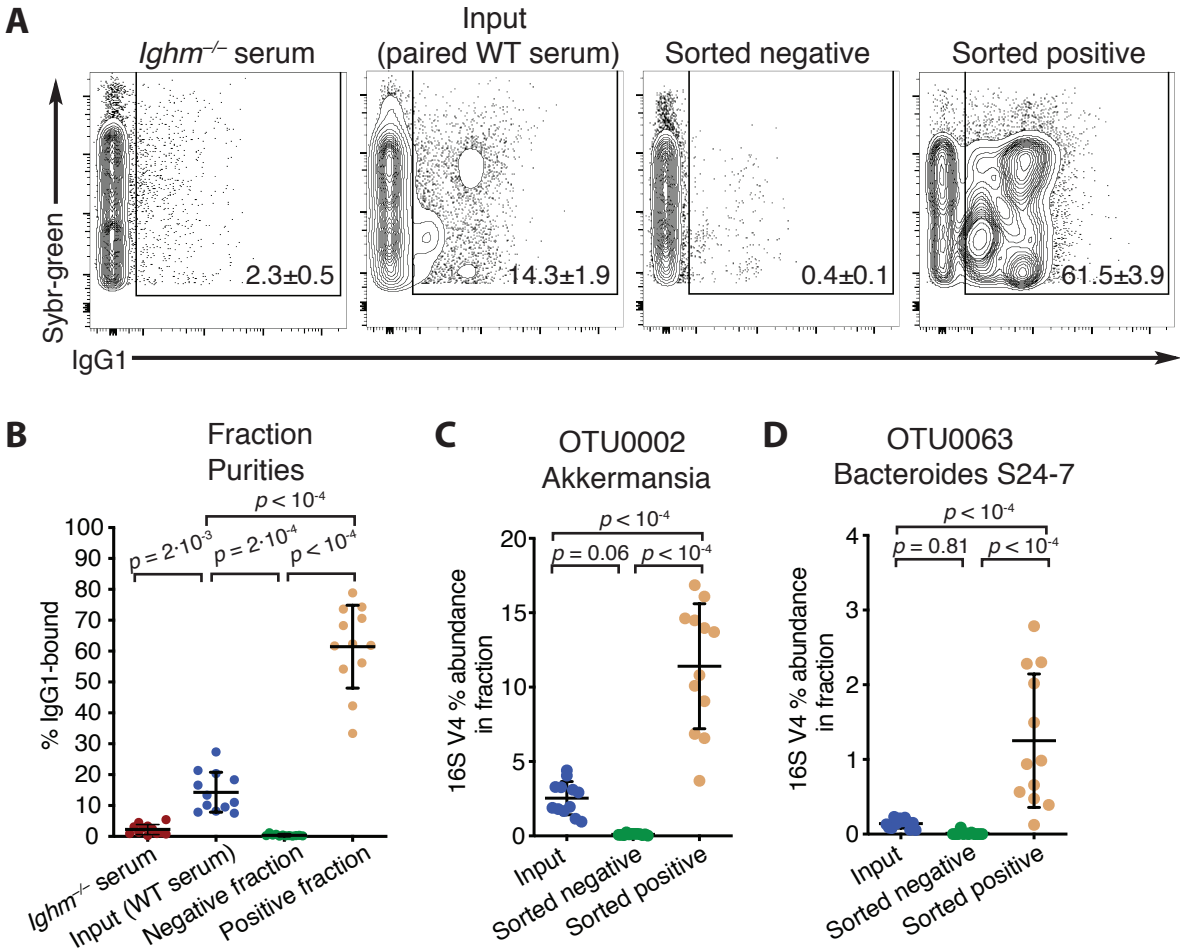

Figure 2.3. Supporting data for sorting and 16S rDNA sequencing of IgG1-bound and unbound bacteria

(**A**) Representative IgG1 microbiota flow cytometric analysis pre- and post-flow cytometric sorting.

(**B**) Frequencies of IgG1-bound bacteria in the indicated fractions, n=12 mice.

(**C**) 16S rDNA sequencing abundances in the three fractions for OTU0002 *Akkermansia*. n=12 mice.

(**D**) 16S rDNA sequencing abundances in the three fractions for OTU0063 Bacteroides S24-7, n=12 mice.

All data are representative of two independent experiments. Each symbol represents a mouse, error bars represent mean ± SD. Gates on flow cytometry plots show mean±SEM. *p*-values were calculated with a one-way ANOVA followed by Tukey's corrected multiple comparisons.

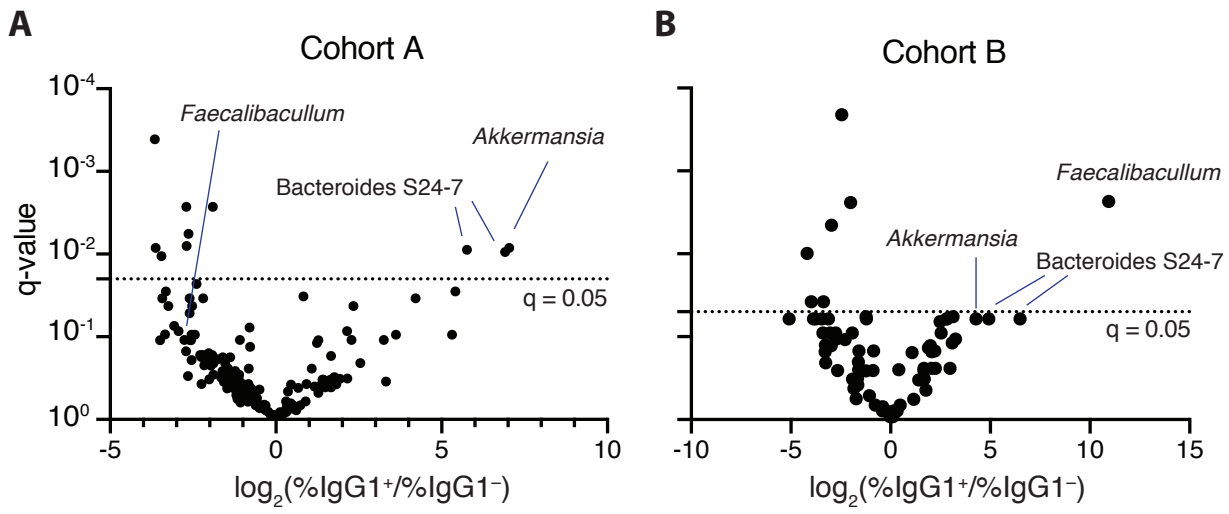

Figure 2.4. Additional IgG1-Seq experiments confirm targeting of *Akkermansia* and Bacteroides S24-7

(**A** and **B**) Results from sorting and 16S rDNA sequencing of IgG1-bound and unbound fractions. n=6 mice (A) or 7 mice (B). Graph depict the average log2 ratio of abundances between both fractions for each individual OTU and the corresponding q-value. Data are representative of two independent experiments.

Each symbol represents an OTU. *p*-values were calculated by Paired ratio Student's *t*-tests followed by Benjamini, Krieger and Yekutieli's two-stage false discovery rate (FDR) to correct for multiple comparisons, with an FDR (Q) of 0.05.

Chapter 3: *A. muciniphila* induces cognate IgG1 antibody responses in conventional and gnotobiotic mice

Many materials in this Chapter have been adapted or reproduced from my publication (*71*): Ansaldo et al. "*Akkermansia muciniphila* induces intestinal adaptive immune responses during homeostasis", *Science*, 364, 1179-1184 (2019). Reprinted with permission from AAAS.

Background:

Of the two major targets of IgG1 antibodies that I identified, only *Akkermansia* was amenable to further study: Bacteroides S24-7 contains many different uncharacterized taxa (*80*), all of which were uncultured at the time of this work. A few members of the S24-7 family have been cultured recently, but this family contains at least 685 species detected by sequencing, including the type strain *Muribacullum intestinalis* (*88*, *89*). This bacterial family has been renamed to *Muribaculaceae* after its first cultured member. Because my IgG1-Seq analysis identified many Bacteroides S24-7 taxa that were not targeted by IgG1 antibodies (Figure 2.1D), isolating and culturing the IgG1-targeted OTU may still remain challenging today.

In contrast, *Akkermansia* is a culturable genus of intestinal commensals in the Verrucomicrobia phylum that until recently only contained one species, *Akkermansia muciniphila* (*82*). A second species of *Akkermansia*, *Akkermansia glycanyiphila*, was recently isolated from pythons (*83*). *A. muciniphila* was first isolated from human feces based on its ability to utilize mucin as a sole carbon and nitrogen source (*82*), which also serves as selective media to culture and obtain *A. muciniphila* isolates. *A. muciniphila* is an abundant member of the human intestinal microbiota (*90*). The genome of *A. muciniphila* has been sequenced, and probing full 16S rDNA sequences from human individuals (*91*), as well as more recent sequencing and culturing efforts (unpublished communications), have revealed that different *Akkermansia* species and strains exist in humans.

After its initial characterization, subsequent studies revealed that *A. muciniphila* exerts diverse effects on the host: First, it was shown that *A. muciniphila* has protective effects in diet-induced obesity (*92*), and also appears to underlie the protective effects of interferon gamma (IFN γ) deficiency on glucose metabolism (*93*). Further studies explored outer membrane proteins in *Akkermansia* (*94*), and focused on an individual protein that appears to be sufficient to improve metabolism in diabetic mice (*95*). A proof-of-concept clinical trial has been conducted with positive results utilizing daily oral *A. muciniphila* supplementation to improve type-II diabetes in humans (*96*). Recent studies have also shown that *A. muciniphila* and its metabolites may influence Amyotrophic Lateral Sclerosis (*97*).

Akkermansia muciniphila has also been shown to localize and bloom in wound beds in the intestine during wound healing (*98*). Here, *A. muciniphila* takes advantage of oxygen depletion and Muc3 secretion at the wound bed to rapidly expand at this site, and then enhances enterocyte proliferation and migration in a FPR1/NOX-1-dependent manner, which contributes to wound healing. Furthermore, *A. muciniphila* colonization is increased in a ketogenic diet, which in turn confers protection against seizures in mouse models of epilepsy (*99*). Finally, *A .muciniphila* abundance has been associated with improved responses to anti-PD-1 cancer immunotherapy (*100*). In this study, patients with evidence of systemic type-I T cell responses to *A. muciniphila* responded better than patients without such responses. *A. muciniphila*-mediated improvements in anti-PD-1 cancer immunotherapy were recapitulated in mouse models, although the mechanism of protection was not elucidated.

The mechanisms by which *A. muciniphila* mediates these diverse effects remain poorly understood, as little is known about host sensing of this bacterium. However, these observations show that *A. muciniphila* is playing active roles in modulating host physiology, and many of these effects appeared to involve immune components, suggesting that this commensal species interacts closely with the immune system. Based on my observations that *A. muciniphila* induces TD IgG1 responses, and based on its reported effects on host physiology, I hypothesized that understanding homeostatic immune responses to this commensal bacterium could reveal novel aspects of immune system-microbiota interactions and shed light into the mechanisms of the aforementioned physiological effects. Therefore, I sought to characterize the immune response to *A. muciniphila*.

Results:

In order to validate the results obtained by IgG1-Seq, first I isolated *A. muciniphila* from mice the colony by plating feces on selective media that contains mucin as the only carbon and nitrogen source (*82*). This yielded an *A. muciniphila* isolate with a 16S rDNA gene identical to the type strain ATCC BAA-835 first isolated from humans (*82*). I then used bacterial flow cytometric analysis to confirm the presence of *A. muciniphila*-specific IgG1 antibodies in the sera of mice that harbored *A. muciniphila* at steady state (Figure 3.1A), thus validating that *A. muciniphila* is a target of serum IgG1 antibodies.

IgA antibodies consist predominantly of natural, polyreactive specificities (*101*). Thus, binding to any given commensal bacterium by IgA is not dependent on previous encounter with that specific species. Anti-commensal IgG2b and IgG3 are also comprised of broadly-reactive specificities (*41*), as they probably share a similar ontogeny to IgA responses. IgG1 antibody responses to *A. muciniphila* could consist of pre-existing natural polyreactive specificities or antigen-specific responses. Given the T-dependent nature of the anti-commensal IgG1 response, I hypothesized that *A. muciniphila*-specific IgG1 antibodies would be comprised of specific, high affinity responses, which would predict that previous colonization with *A. muciniphila* would be required for the induction of the cognate IgG1 response. To test this hypothesis, I identified C57BL/6 mice lacking *A. muciniphila* in their microbiota (Figure 3.1B) from a specific room in Jackson laboratories (a mouse vendor). Comparing IgG1 antibody responses between *A. muciniphila*-negative and *A. muciniphila*-positive mice confirmed that the induction of *A. muciniphila*-specific serum IgG1 responses required colonization with *A. muciniphila,* as well as T cells (Figure 3.1A-C and Figure 3.2A). *A. muciniphila*-positive mice also mounted serum *A. muciniphila*-specific TD IgA responses (Figure 3.2B). Moreover, de novo colonization of *A. muciniphila*-negative mice by oral gavage was sufficient to induce *A. muciniphila*-specific IgG1 antibodies (Figure 3.1D-F and Figure 3.2C). Thus, IgG1 responses to *A. muciniphila* are not derived from pre-existing cross-reactive specificities. Rather, mice mount an antigen-specific TD IgG1 antibody response upon *A. muciniphila* colonization.

Gnotobiotic mice are generated by colonizing germ-free mice with specific bacteria, and are then maintained and bred in a gnotobiotic isolator. Microbial communities tend to be very stable in gnotobiotic mice once they have achieved equilibrium, and the axenic conditions of gnotobiotic isolators prevent contamination with additional environmental microbes. This reductionist approach allows investigators to carefully control microbiota composition and test the role of individual variables, such as the addition of a single species, without additional changes in microbiota composition that are hard to avoid in specific-pathogen-free (SPF, or conventional) mice.

I noted that titers of serum IgG1 responses against *A. muciniphila* were variable across *A. muciniphila*-positive mice. A small number of mice lacked *A. muciniphila*-specific IgG1 altogether, despite similar colonization (Figure 3.1B, C and Figure 3.2A). One explanation for this variability is that variation within intestinal microbial

communities may alter the response to *A. muciniphila*. Indeed, previous studies have shown that intestinal infection or inflammation can lead to altered bystander responses against commensal microbes (*69*). To overcome such complications, I established a defined gnotobiotic system to examine whether direct engagement of the mucosal immune system by *A. muciniphila* underlies the TD IgG1 response. I introduced *A. muciniphila* into gnotobiotic C57BL/6 mice colonized with altered Schaedler flora (ASF) (*102*) to generate two mouse colonies with identical microbiota, except for the presence of *A. muciniphila* in the ASF+Akk colony. The altered Schaedler flora is a consortium of eight mouse intestinal microbes, including six obligate anaerobes. The ASF recapitulates many of the features of a conventional microbiota, such as the induction of colonic Treg cells and intestinal IgA (*46*), and thus avoids many of the caveats associated with germ-free mice, including their underdeveloped immune systems.

A. muciniphila colonized ASF+Akk mice to high levels and was vertically transmitted (Figure 3.1G, and Figure 3.2D). In order to study homeostatic responses and avoid potential caveats associated with oral gavage of bacteria, I restricted all of my analyses to descendants of ASF+Akk mice that acquired *A. muciniphila* via vertical transmission. Mice colonized with the ASF+Akk flora, but not the ASF flora alone, mounted IgG1 responses specific for *A. muciniphila* which, in contrast to conventional mice, had very consistent titers between mice (Figure 3.1H, I). Importantly, I also observed very robust serum IgA binding to *A. muciniphila* in ASF+Akk mice. Interestingly, ASF mice showed a small amount of IgA binding, perhaps resulting from polyreactive T-independent IgA specificities present in the serum. Thus, *A. muciniphila* directly engages the immune system to induce TD IgG1 and IgA.

Discussion:

The work described in this chapter reveals that *A. muciniphila* is both necessary and sufficient to induce cognate IgG1 antibodies in mice. In contrast to polyreactive specificities characteristic of T-independent isotypes (*101*), IgG1 antibodies to *A. muciniphila* require previous colonization with this commensal. Antibody titers to *A. muciniphila* were rather variable in conventional (SPF) mice, suggesting that complex interactions with other commensal microbes or environmental variables that differ between mice in my colony are at play.

Mucosal infection or inflammation (*69*), as well as barrier disruption (*39*) have been shown to induce ectopic adaptive immune responses to commensal microbes. Thus, it was formally possible that *A. muciniphila* was being targeted by systemic TD antibodies as a direct consequence of ongoing (and variable) infection or inflammation in my mouse colony, and not due to direct engagement of the immune system by *A. muciniphila* at homeostasis. De novo colonization of *A. muciniphila*-free mice is sufficient to induce a response, which partially addresses this concern. Finally, gnotobiotic ASF+Akk mice, which are not exposed to pathogens from the environment, induce very robust and consistent antibody responses to *A. muciniphila*, which definitively shows that *Akkermanisa* is actively engaging the intestinal immune system at homeostasis.

Interestingly, *A. muciniphila* also induced high titers of specific IgA antibodies both in SPF and gnotobiotic conditions, which were partially T-dependent, suggesting a broader immune response to this commensal bacterium. The dependency on T cells, as well as the robust binding observed argue that IgG1 and IgA responses to *A. muciniphila* are comprised of high-affinity antibodies. This is in contrast to the majority of the commensal microbiota, which is only targeted by T-independent low-affinity IgA (*22*). Only a few commensal species are targeted by T-dependent IgA (*35*, *38*), including now *A. muciniphila*.

Given that systemic antibodies have been implicated in protection against gut-derived septicemia (*42*, *73*, *74*), high affinity antibodies against select immunostimulatory members of the commensal microbiota may provide enhanced protection against systemic dissemination of these specific bacteria during barrier disruption. These bacteria appear to all colonize niches close to the intestinal epithelium: SFB attaches to epithelial cells in the terminal ileum, and *A. muciniphila* and *Mucispirillum spp*. both reside in the intestinal mucus layer. Colonization of these niches may be interpreted by the immune system as having increased potential to invasion and dissemination, and thus the induction of high affinity local (IgA) and systemic (IgG) antibodies may be a preemptive strategy to deal with the possibility of dissemination. In support of this hypothesis, high levels of *A. muciniphila* can drive inflammatory disease in immunodeficient settings (*84*).

In contrast, commensal-specific antibodies are increased during inflammatory bowel disease (*75*, *103*), and commensal flagellin appears to be an immunodominant

epitope for antibodies and T cells in patients with IBD (*104*). Furthermore, polymorphisms in a receptor for IgG antibodies, FcγRIIA, are implicated in ulcerative colitis, where IgG antibodies can drive Th17 immunity and disease (*75*). Thus, pre-existing high affinity antibodies to the commensal microbiota, such as for *A. muciniphila*, may be detrimental in genetically susceptible people.

Finally, commensal-specific antibodies have been implicated in neonatal (*41*), as well as in utero education of the immune system (*72*). High affinity TD antibody responses to select immunostimulatory commensals may help educate the early immune system and prevent dysregulated responses against these immunostimulatory bacteria that could otherwise drive intestinal disease.

Methods:

Animals:

Mice were housed under specific-pathogen-free (SPF) or gnotobiotic conditions at UC Berkeley. For SPF experiments, adult (8-16 weeks of age, male and female) C57BL/6J mice were used as wild-type mice. All experiments were performed in accordance with the Animal Care and Use Committee guidelines at the University of California Berkeley. For gnotobiotic experiments, gnotobiotic C57BL/6NTac mice colonized with altered Schaedler's flora were obtained from Taconic Biosciences and imported into the gnotobiotic facility at the University of California Berkeley. ASF and ASF+Akk mouse colonies were maintained in separate flexible film isolators (Class Biologically Clean). ASF+Akk mice were generated from C57BL/6NTac ASF mice by two oral gavages of 10^9 cfu of *Akkermansia muciniphila* (colony isolate) 2 days apart. Colonization with *A. muciniphila* was tested by 16S *A. muciniphila* fecal qPCR and absence of contaminants was routinely tested by bacterial plating and fecal 16S rDNA sequencing. For experiments including ASF+Akk mice, I analyzed progeny (or progeny of progeny) of *A. muciniphila*-gavaged mice.

A. muciniphila-positive and *A. muciniphila*-negative C57BL/6J mouse colonies were kept and bred under SPF conditions. *A. muciniphila*-positive mice were already present in my colony at the University of California Berkeley. *A. muciniphila*-negative mice were initially obtained from Jackson Laboratories, room RB08 (for experiments in Figures 3.1 and 3.2). I also determined that a 3-week course of tetracycline hydrochloride in the drinking water (3 g/L tetracycline hydrochloride, 1% sucrose, pH=7, changed every 3 days) was sufficient to clear mice of *A. muciniphila*.

Isolation and culture of *A. muciniphila*:

A. muciniphia was isolated from mice in my SPF colony by plating mouse feces on selective media. Briefly, serial dilutions of homogenized fecal samples in PBS were plated on mucin plates in an anaerobic chamber (COY). Mucin plate composition: 0.4 g/L KH_2PO_4, 0.53 g/L Na_2HPO_4, 0.3 g/L NH_4Cl, 0.3 g/L NaCl, 0.1 g/L $MgCL_2{\cdot}6H_2O$, 0.15 g/L $CaCl_2{\cdot}2H_2O$, 4 g/L $NaHCO_3$, 0.5 g/L L-Cys·HCl·H_2O, 2.5 g/L Type III hog gastric mucin (Sigma), 3mL/L trace mineral solution (ATCC), 0.75 mg/L resazurin, pH=6.5, 7.5 g/L agar, autoclaved for 15 min. The full 16S rRNA gene of the obtained isolate was amplified using universal 16S primers (27F and 1492R), sequenced, and revealed to be identical to the 16S rRNA gene for the type strain *A. muciniphila* ATCC BAA-835.

Liquid cultures of *A. muciniphila* for oral gavage were grown in brain heart infusion (BHI) + 2.5g/L Type-III hog gastric mucin and 0.5g/L L-Cys·HCl·H_2O in an anaerobic chamber (COY). 36-48-h cultures were harvested, centrifuged at 10,000×*g* for 3 min and resuspended in anaerobic PBS (PBS + L-Cys·HCl·H_2O, pH=7).

Fecal *A. muciniphila* 16S qPCR:

DNA was isolated from fecal samples using the QIAamp DNA Stool Minikit or QIAamp Fast DNA Stool Minikit (Qiagen) according to manufacturer's instructions. Homogenization was performed on a Mini Beadbeater (BioSpec products) for 2 min. Quantitative PCR was performed on a StepOnePlus thermocycler (Applied Biosystems) with SsoAdvanced universal SYBR green supermix (Bio-RAD). The 16S gene from *A. muciniphila* was PCR-amplified using 16S primers 27F (5′-AGAGTTTGATCMTGGCTCAG-3′) and AmucR-V1 (5′- CCTTGCGGTTGGCTTCAGAT -3′), cloned into a pCR-BluntII TOPO vector (Invitrogen), and then linearized with the restriction enzyme BamHI. This linearized vector was used to generate standard curves for qPCR (included on each qPCR plate). Primers were synthesized by Integrated DNA Technologies. One of two different pairs of *A. muciniphila*-specific primers were used (with same results):

A.muciniphila-F V1: 5′-CAGCACGTGAAGGTGGGGAC-3′.

A.muciniphila-R V1: 5′-CCTTGCGGTTGGCTTCAGAT-3′.

A.muciniphila-F V2: 5′-AGTATCGAAAGATTAAAGCAGCAATGC-3′.

A.muciniphila-R V2: 5′-TCTTGTGGTACTATCTTTTTAATTTGCT-3′.

Fecal DNA samples were diluted to a range with a proportional relationship between dilution and C_T value (usually 1:40) and the resulting C_T value was used to calculate the concentration of *A. muciniphila* 16S gene copies using the standard curve. The amount of recovered 16S gene copies was normalized to the input fecal material (weight), and after applying the appropriate dilution factors, a factor of 3 copies/genome was used to calculate genome equivalents per gram of feces (based on the genome sequence for ATCC BAA-835 *A. muciniphila* strain).

Bacterial flow cytometry:

A 36-48-h culture of *A. muciniphila* was grown in brain heart infusion (BHI) + 2.5g/L Type-III hog gastric mucin (Sigma) and 0.5g/L L-Cys·HCl·H_2O in an anaerobic chamber (COY). Bacterial cultures were stained overnight at $2.5x10^7$ bacteria/mL in 50μL of bacterial staining buffer (BSB) (1%BSA in PBS + 0.025%NaN) with serum added at 1:50 final dilution factor (unless otherwise noted) in a V-bottom 96-well plate. Samples were washed with 150 μL of BSB, pelleted (3,220×*g* 5 min 4ºC) and resuspended in BSB with secondary antibodies. Biotinylated secondary antibodies were used at 1:200: anti-mouse IgG1 A85-1 (BD Pharmigen), and polyclonal anti-mouse IgA (1040-08 Southern Biotech). After washing and pelleting, samples were resuspended in BSB + Streptavidin-PE-Cy7 (SA-PE-Cy7) (Invitrogen) at 1:200. Samples were washed with BSB and resuspended in 200 μL BSB with Sybr-green I nucleic acid stain (Invitrogen) at 1:10,000. Samples were analyzed on a BD LSR Fortessa or a BD LSR Fortessa X-20.

Figures:

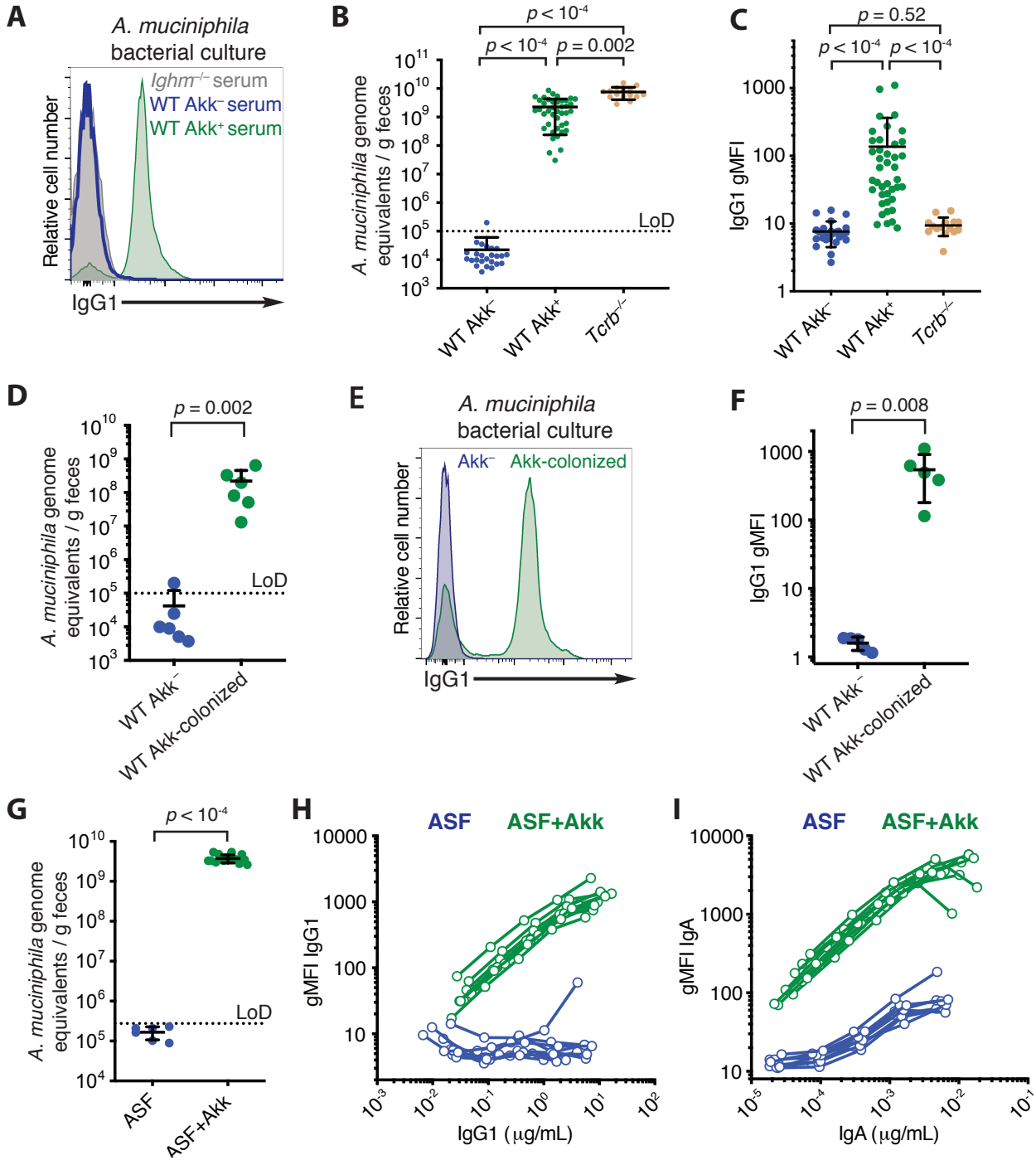

Figure 3.1 *Akkermansia muciniphila* is necessary and sufficient to induce cognate *A. muciniphila*-specific IgG1 antibody responses

(**A**) Representative IgG1 bacterial flow cytometric analysis of *A. muciniphila* incubated with the indicated mouse sera. Applies to results shown in C.

(**B**) Quantification of *A. muciniphila* colonization by fecal 16S qPCR for mice in (C).
(**C**) *A. muciniphila* IgG1 bacterial flow cytometric analysis for mice of the indicated genotypes and indicated *A. muciniphila* colonization status. WT Akk^{-} n=25, WT Akk^{+} n=41, *Tcrb*$^{-/-}$ n=15. gMFI: geometric mean fluorescence intensity. Data are compiled from seven independent experiments.
(**D**) Quantification of *A. muciniphila* colonization by fecal 16S qPCR before (WT Akk^{-}) and 5 weeks after (WT Akk-colonized) a single *A. muciniphila* oral gavage of 10^9 cfu. n=6 mice. Applies to results shown in F. Data are representative of three independent experiments.
(**E, F**) Representative plot (E) and quantification (F) of *A. muciniphila* IgG1 bacterial flow cytometric analysis using sera from mice before (Akk^{-}) and 5 weeks after colonization (Akk-colonized). n=5 mice. Data are representative of three independent experiments.
(**G**) Quantification of *A. muciniphila* colonization by fecal 16S qPCR. n=6 ASF, n=16 ASF+Akk mice. Data are representative of two independent experiments.
(**H** and **I**) *A. muciniphila* bacterial flow cytometric analysis with serial dilution of serum in ASF and ASF+Akk mice. Each line represents one mouse. The *x*-axis denotes total serum IgG1 (H) or serum IgA (I) concentration in the assay. n=9 mice per group. Data are representative of two independent experiments.
LoD: limit of detection. Each symbol represents a mouse, error bars represent mean ± SD. *p*-values were calculated with a Kruskal–Wallis test followed by Dunn's multiple comparisons (B, C) or a Mann–Whitney test (D, F, G).

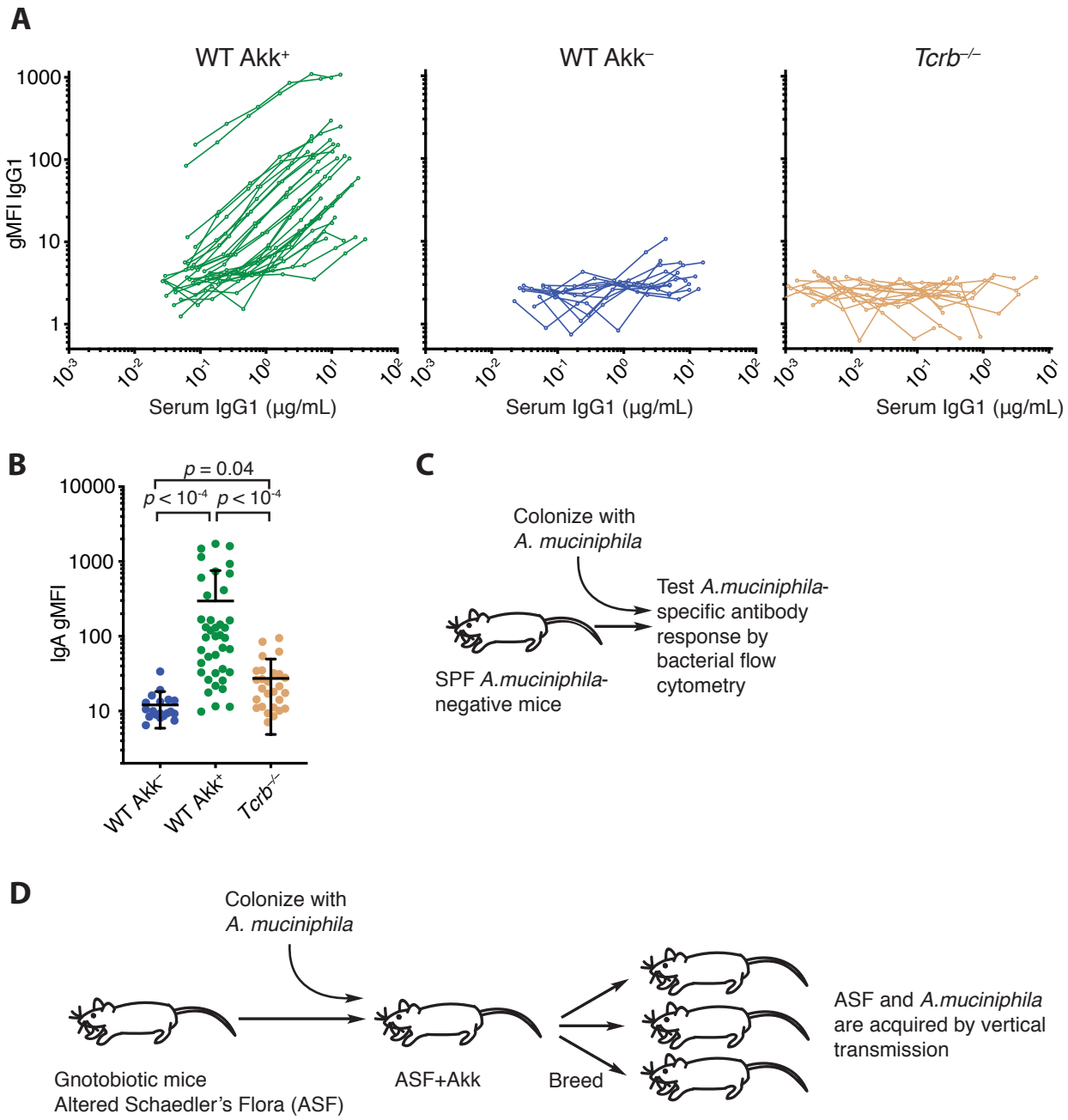

Figure 3.2 *A. muciniphila* induces antigen-specific IgG1 and IgA antibody responses in SPF and gnotobiotic mice

(**A**) *A. muciniphila* IgG1 bacterial flow cytometric analysis with serial dilution of serum from WT Akk^{+} (n=30 mice), WT Akk^{-} (n=12 mice), and *Tcrb*$^{-/-}$ (n=16 mice). Each line represents one mouse. The *x*-axis denotes total serum IgG1 in the assay. Data are representative of two independent experiments.

(**B**) *A. muciniphila* bacterial flow cytometric analysis for serum IgA antibodies. WT Akk^{-} n=19, WT Akk^{+} n=40, *Tcrb*$^{-/-}$ n=27. gMFI: geometric mean fluorescence intensity. Data are compiled from two independent experiments. Each symbol represents a mouse,

error bars represent mean ± SD. *p*-values were calculated with a Kruskal–Wallis test followed by Dunn's multiple comparisons.
(**C**) Experimental design for *de novo* colonization with *A. muciniphila*. Applies to results shown in Fig. 2 D-F.
(**D**) Schematic of the generation of the gnotobiotic ASF + *A.muciniphila* mouse line (ASF+Akk).

Chapter 4: *A. muciniphila* induces antigen-specific T cell responses during homeostasis

Many materials in this Chapter have been adapted or reproduced from my publication (*71*): Ansaldo et al. "*Akkermansia muciniphila* induces intestinal adaptive immune responses during homeostasis", *Science*, 364, 1179-1184 (2019). Reprinted with permission from AAAS.

Background:

Despite the large abundance of antigen-experienced T cells in the intestine, very few examples of commensal-specific T cell responses have been identified (*12*). Given their roles as orchestrators of immune responses, $CD4^+$ T cells specific for commensal antigens are likely to play important roles during homeostasis and disease. Indeed, inappropriate T cell responsiveness to the microbiota are considered to be a hallmark of IBD (*15*), and unrestrained T cell responses have been observed in many models of colitis in mice (*65*, *66*, *105*, *106*). Furthermore, commensal-specific T cell responses have been hypothesized to help protect against bystander infections (*70*). Finally, the role of such T cell responses during homeostasis still remains poorly understood. In the case of SFB, it appears that small intestine Th17 responses help limit the burden of SFB in the intestine and prevent dysbiosis (*107*). Furthermore, *Helicobacter*-specific $ROR\gamma t^+$ Treg cells help mediate tolerance against this pathobiont (*65*). However, outside of these two examples and the case of CBir-specific T cells, which remain naïve at homeostasis but become activated during infection (*68*, *69*), no other examples of commensal-specific T cells have been identified. Thus, identification of novel commensal antigens that induce cognate T cell responses during homeostasis would help shed light on the breath and role of T cell responses to the microbiota.

The results obtained in Chapters 2 and 3 show that T cells are required for the induction of *A. muciniphila*-specific IgG1 and IgA. The role for T cells in this response, coupled with the presence of antigen-specific, high-affinity antibodies, argues that cognate T cell responses to *Akkermansia* are induced, which would in turn provide T cell help for the induction of classical, TD B cell responses. Thus, I hypothesized that *A. muciniphila*-specific T cell responses exist in mice, which are providing T cell help and orchestrating effector responses to *A. muciniphila*.

Characterization of T cell responses to *A. muciniphila* may also shed light into the mechanisms by which this commensal bacterium exerts effects on host metabolism (*92*, *93*) and cancer immunotherapy (*100*). It is now clear, based on multiple studies, that the microbiota influences the outcome of PD-1 cancer immunotherapy in mice and humans (*56*, *100*, *108*, *109*), although the mechanisms are still poorly understood. The effects of *A. muciniphila* on PD-1 cancer immunotherapy in cancer patients correlated with $IFN\gamma$ production by peripheral $CD4^+$ T cells upon restimulation with *A. muciniphila* antigens. Interestingly, $IFN\gamma$ also appears to be involved in the influence of *Akkermansia*

on glucose tolerance and metabolism by limiting *A. muciniphila* colonization, although a role for T cells wasn't explored (*93*).

In this chapter, I decided to explore CD4 T cell responses to *A. muciniphila* during homeostasis by generating TCR transgenic mice and peptide:MHCII tetramers and characterizing homeostatic T cell responses in gnotobiotic ASF+Akk mice and SPF mice.

Results:

I hypothesized that *A. muciniphila*-specific T cells must exist in intestinal tissues of colonized mice at frequencies higher than the precursor frequency. In order to identify *A. muciniphila*-specific T cell receptors (Figure 4.1A), I expanded T cell lines from intestinal tissues (mesenteric lymph nodes and Peyer's patches) of *A. muciniphila*-positive SPF mice by repeated stimulation with *A. muciniphila*-loaded splenocytes. Importantly, T cell lines only expanded from *A. muciniphila*-positive mice (Figure 4.2A); and the few T cell lines that expaned from *A. muciniphila*-negative mice were not responding to *Akkermansia* antigens (Figure 4.2B). From these *Akkermansia*-specific lines I generated T cell hybridomas by fusion with BWZ.36 cells, which enable screening for TCR engagement by a colorimetric assay (*110*, *111*). I identified multiple T cell hybridomas that responded to *A. muciniphila* antigens but not *E. coli* antigens (Figure 4.1C). I identified the antigens recognized by two of these hybridomas (124-2 and 168-H10) by screening an *A. muciniphila* genomic expression library for clones that stimulated each T cell hybridoma (Figure 4.1B and D). The 124-2 hybridoma recognized Amuc_RS03735, an outer membrane autotransporter domain-containing protein. Further peptide fine-mapping and use of *in silico* epitope prediction tools identified the precise I-A^b binding sequence recognized by 124-2 cells as YIGSGAILS (Figure 4.2C). The 168-H10 hybridoma recognized a peptide derived from Amuc_RS07575 (GAPDH).

To facilitate tracking of the T cell response to *A. muciniphila* I generated *A. muciniphila*-specific TCR transgenic mice (Amuc124), using the TCRα and TCRβ chains from the 124-2 T cell hybridoma (Figure 4.1A and D). As expected for an MHCII-restricted TCR transgenic mouse, T cell development in Amuc124 mice was heavily skewed toward $CD4^+$ T cells, and the skewing was even more dramatic in Amuc124 mice on the *Rag1*$^{-/-}$ background (Figure 4.3A). Amuc124 T cells proliferated when stimulated *in vitro* with *A. muciniphila*-loaded splenocytes but not *E. coli*-loaded splenocytes (Figure 4.3B). Importantly, I maintained Amuc124 mice free of *A. muciniphila* colonization for all subsequent experiments.

Next, I sought to track the T cell response to *A. muciniphila* by performing low frequency adoptive transfers of naïve congenically-marked Amuc124 T cells into ASF and ASF+Akk mice (Figure 4.4A). *A. muciniphila*-specific T cells expanded in ASF+Akk mice but were undetectable in ASF mice, indicating that *A. muciniphila* antigens are presented under homeostatic conditions (Figure 4.B and C). Interestingly, Amuc124 T cells localized to the Peyer's patches (PPs) sand mesenteric lymph nodes (mLNs), but few cells were found in the small intestine or large intestine lamina propria (SILP or LILP) (Figure 4.4B). The majority of transferred T cells expressed PD-1, Bcl6 and CXCR5, which are markers for T follicular helper cells (T_{FH}) (Figure 4.4D-G), with a small percentage adopting Treg markers (FOXP3). The small amount of T cells detectable in the lamina propria were also skewed towards T_{FH} cells, most likely indicating that secondary or tertiary lymphoid tissues were not completely excluded from these preparations (Figure 4.4G). Surprisingly, I did not detect a significant number of transferred T cells that expressed markers for T_H1, T_H2 or T_H17 markers (T-bet, GATA3,

or RORγt, respectively) (Figure 4.4G). The fact that I did not observe any T cells in ASF mice, which lack *A. muciniphila*, proves that the responses observed in ASF+Akk mice are antigen-specific. However, TCR transgenic mice on a Rag-sufficient background exhibit incomplete allelic exclusion and some amount of endogenous rearrangement of T cell receptors, particularly in the alpha chain (*106*, *112*). Thus, I crossed the Amuc124 TCR transgenic mice onto a *Rag1*$^{-/-}$ background, which prevents rearrangements of the endogenous TCR locus and ensures that all T cells express the transgenic T cell receptor. Comparing T cell transfers with Amuc124 T cells on a *Rag1*$^{+/+}$ or a *Rag1*$^{-/-}$ background yielded similar results (Figure 4.5), which confirms that the response observed in ASF+Akk mice is antigen-specific.

To eliminate the possibility that these surprising results were due to caveats associated with T cell transfers, I also examined the endogenous T cell response to *A. muciniphila*. First, I generated I-A^{b} tetramers loaded with the peptide TLYIGSGAILS from the outer membrane protein Amuc_RS03735 (Am3735-1) and confirmed that these tetramers bound Amuc124 TCR transgenic T cells (Figure 4.2D). Endogenous, tetramer-positive, *A. muciniphila*-specific T cells were identified in the PPs of ASF+Akk but not ASF mice (Figure 4.6A, and B), consistent with the results obtained with Amuc124 T cells after adoptive transfer. Moreover, the endogenous *A. muciniphila*-specific T cells identified by tetramer staining also expressed T_{FH} cell markers (Figure 4.6C and D). An independent tetramer with a different *Akkermansia* epitope from Amuc_RS03740 (Am3740-1) predicted in silico yielded very similar results (Figure 4.6B-D). Finally, I probed all gut-associated lymphoid tissue (LILP, PPs, and SILP) and mLNs with both tetramers. *A. muciniphila*-specific T cells were detected in the PPs but not in the lamina propria (Figure 4.6E), which confirmed results obtained with Amuc124 T cell transfers. Thus, *A. muciniphila* induces antigen-specific T cell responses in the intestine that manifest primarily as T_{FH} cells in the Peyer's patches.

Finally, I returned to SPF mice, where I had observed greater variability in the *A. muciniphila* IgG1 response, and used my newly developed tools to characterize the T cell response to *A. muciniphila* in the context of a conventional microbiota. Similar to my findings for the ASF system, transferred Amuc124 T cells expanded and localized to the PPs in *A. muciniphila*-positive mice but were undetectable in *A. muciniphila*-negative mice (Figure 4.7A and B, and Figure 4.8A). The majority of transferred T cells in the Peyer's patches also adopted T_{FH} cell markers (Figure 4.7C and Figure 4.8B) Therefore, *A. muciniphila* also induces a T_{FH} cell response in the context of a complex microbiota. However, unlike the ASF+Akk system, greater numbers of transferred T cells were detected in the intestinal LP of *A. muciniphila*-positive mice (Figure 4.7B), some of which adopted markers consistent with pro-inflammatory T cell fates (Figure 4.6D and E, and Figure 4.8C-E). Consistent with the variable *A. muciniphila*-specific IgG1 titers observed in SPF mice (Figure 3.1C), some cohorts of SPF Akk^{+} mice lacked detectable T cell activation and proliferation after transfer, despite the presence of *A. muciniphila* (Data not shown). Thus, T cell responses to *A. muciniphila* appear to be context-dependent, resulting in the induction of other CD4 T effector fates in addition to T_{FH} cells in certain conditions. Interestingly, and in contrast to what has been described

for segmented filamentous bacteria (SFB) and *Helicobacter* spp. (*59*, *64*, *65*), T cell responses to *A. muciniphila* in SPF mice were mixed between different $CD4^+$ T cell fates (Figure 4.8E).

Discussion:

Very few commensal antigens have been identified to date that lead to antigen-specific T cell responses in the gut during homeostasis. SFB and *Helicobacter* spp. both elicit very defined responses. SFB induce RORγt$^+$ T_H17 cells both in conventional and mono-colonized mice (*59*), whereas *Helicobacter* spp. induce RORγt$^+$ FOXP3$^+$ Treg cells in the large intestine lamina propria (*64*, *65*). T_{FH} cells comprised a small proportion of SFB and *Helicobacter*-specific T cells, but these were in the context of T_H17 cell - or Treg cell-dominated responses, respectively (*65*). T_{FH} cells in the intestine have been suggested to differentiate from either T_H17 cells or Treg cells (*68*, *113*, *114*). By contrast, the ASF+Akk system produced commensal-specific T cell responses dominated by the induction of T_{FH} cells, with very few Treg, T_H1, T_H2, or T_H17 cells. Thus, commensal-specific T_{FH} responses can occur in the absence of a primary CD4$^+$ T cell response of a different fate and may differentiate from naïve commensal-specific T cells in the mesenteric lymph nodes or Peyer's patches. Consequently, *A. muciniphila* appears to engage the mucosal immune system in a manner distinct from previously described T cell-activating commensal bacteria. This commensal-specific T_{FH} response appears in conjunction with robust anti-commensal TD IgG1 and IgA.

Surprisingly, in the context of a conventional microbiota, and in addition to the induction of T_{FH} cells, *A. muciniphila* can induce CD4$^+$ T cells of other fates that home to the lamina propria. Together, these results support the hypothesis that T cell responses against commensals can be context-dependent, not just in the setting of acute gastrointestinal infection or inflammation (*69*), but also during homeostasis. Interactions with certain microbes may change the localization or function of *A. muciniphila*, or signals provided by other microbes may shape the immune response against this commensal bacterium.

Prior work has established that *A. muciniphila* mediates effects on host metabolism (*92*, *93*) and can influence the efficacy of anti-PD-1-based immunotherapy against cancer (*100*). The mechanisms for these effects remain poorly understood, but both appear to be immune-mediated and correlated with type 1 immunity. In particular, responses to anti-PD-1-based immunotherapy in humans were correlated with interferon gamma production by peripheral T cells incubated with *A. muciniphila* antigens in vitro (*100*). Interestingly, not all patients generated type 1 responses against *A. muciniphila*. My results provide a potential explanation for this varied response, and suggest that differential skewing of *A. muciniphila*-specific T cell responses in individuals due to differences in microbiota composition, or other environmental signals, may have profound systemic effects. Defining the mechanisms by which these commensal-specific T cell responses can be skewed towards different fates is an important goal with clear clinical implications.

Methods:

Animals:

Mice were housed under specific-pathogen-free (SPF) or gnotobiotic conditions at UC Berkeley. For SPF experiments, adult (8-16 weeks of age, male and female) C57BL/6J mice were used as wild-type mice. All experiments were performed in accordance with the Animal Care and Use Committee guidelines at the University of California Berkeley. For gnotobiotic experiments, gnotobiotic C57BL/6NTac mice colonized with altered Schaedler's flora were obtained from Taconic Biosciences and imported into the gnotobiotic facility at the University of California Berkeley. ASF and ASF+Akk mouse colonies were maintained in separate flexible film isolators (Class Biologically Clean). ASF+Akk mice were generated from C57BL/6NTac ASF mice by two oral gavages of 10^9 cfu of *Akkermansia muciniphila* (colony isolate) 2 days apart. Colonization with *A. muciniphila* was tested by 16S *A. muciniphila* fecal qPCR and absence of contaminants was routinely tested by bacterial plating and fecal 16S rDNA sequencing. For experiments including ASF+Akk mice, I analyzed progeny (or progeny of progeny) of *A. muciniphila*-gavaged mice. I used littermate mice for SPF Akk-positive T cell transfers in Figures 4.7 and 4.8, except for one of the repeats (Figure 4.8E Experiment 2), which consisted of two groups of littermate mice.

A. muciniphila-positive and *A. muciniphila*-negative C57BL/6J mouse colonies were kept and bred under SPF conditions. *A. muciniphila*-positive mice were already present in the mouse colony at the University of California Berkeley. For these experiments, I determined that a 3-week course of tetracycline hydrochloride in the drinking water (3 g/L tetracycline hydrochloride, 1% sucrose, pH=7, changed every 3 days) was sufficient to clear mice of *A. muciniphila*. I analyzed progeny (or progeny of progeny) of tetracycline-treated mice for SPF experiments in this chapter.

For adoptive T cell transfers into ASF and ASF+Akk mice, animals were removed from gnotobiotic isolators and transferred into sterilized cages within a biosafety cabinet. Mice were anesthetized by the isoflurane drop jar method and T cells were transferred by retro-orbital injection. Mice were then housed for 12 days in sterilized cages on a ventilated rack within the barrier facility at the University of California, Berkeley, without further manipulation. Absence of contaminating microbes was tested by plating on different media at the time of euthanasia.

Isolation and culture of *A. muciniphila:* See previous chapter

Fecal *A. muciniphila* 16S qPCR: See previous chapter

Cell and tissue culture conditions:

T cell lines were generated from mesenteric lymph nodes and Peyer's patches of SPF mice 2-3 weeks after oral gavage of 10^9 cfu (*A. muciniphila*-colonized). CD4 T cells were isolated using magnetic separation with CD4 beads (L3T4, Miltenyi Biotec) and incubated with irradiated splenocytes that had been loaded with *A.*

muciniphila (MOI = 50), which was prepared from a 36-48-h culture by resuspending at OD=1 and heat-killing at 95ºC for 30 min. T cells were incubated in RPMI-10: RPMI + 10% (v/v) fetal bovine serum (FBS) supplemented with L-glutamine, penicillin-streptomycin, sodium pyruvate and HEPES (pH=7.2) (Invitrogen). Recombinant IL-2 (10 U/mL) was added to the second and subsequent rounds of stimulation. T cell lines were stimulated every 7 days, with removal of dead cells on Ficoll separation media (MP Biomedicals).

T cell hybridomas were generated by fusion of the myeloma cell line BWZ.36 with the generated T cell lines as previously described (*110*, *115*). T cell hybridomas were cultured in RPMI-10 and stimulated with splenocytes loaded with the indicated antigens. Anti-CD3 (145-2C11) and anti-CD28 (37.51) were used at 2 μg/mL as a positive control. Overnight *E. coli* (DH5α) or 36-48-h *A. muciniphila* cultures were harvested, resuspended at OD 1 in PBS and heat-killed at 95ºC for 30 min before being added to splenocytes at the indicated ratios (MOI). After overnight incubation, β-galactosidase activity (the reporter of TCR stimulation in BWZ.36 cells) was measured in a bulk assay or on a single cell basis as previously described (*110*). For bulk assays, cells on a 96-well plate were washed with PBS and resuspended in CPRG buffer (0.125% (v/v) NP-40, 9mM $MgCl_2$, 0.15mM chlorophenol red-β-D-galactopyranoside (CPRG) in PBS) and incubated at 37C for 4 h. Absorbance at 595nm was measured with 635nm as a reference. Single cell β-galactosidase activity was measured in the screen described in figure S4C. For single cell assays, cells were washed in PBS, fixed in 2% (v/v) formaldehyde 0.2% (v/v) glutaraldehyde solution, washed in PBS and overlaid with X-gal staining solution (2 mM $MgCl_2$, 5 mM $K_4Fe(CN)_6$, 5 mM $K_3Fe(CN)_6$ and 1 mg/mL X-gal (5-bromo-4-chloro-3-indolyl-β-D-galactopyranoside) in PBS). After an overnight incubation at 37ºC, blue cells were quantified using light microscopy.

For stimulation of primary Amuc124 TCR transgenic T cells, CD4 T cells were isolated by magnetic separation with CD4 beads (L3T4, Miltenyi Biotec) and labeled with carboxyfluorescein succinidyl ester (CFSE) (Invitrogen) according to manufacturer's instructions. CFSE-labeled T cells were incubated with antigen-loaded splenocytes in the presence of 20 U/mL recombinant IL-2. Three days later samples were stained for flow cytometry and proliferation was measured on a BD LSR Fortessa or LSR Fortessa X-20.

Identification of hybridoma-stimulating peptides:

T cell hybridomas 124-2 and 168-H10-1 were used to screen a genomic expression library (from *A. muciniphila*) as previously described (*111*). Briefly, a partial digest of *A. muciniphila* genomic DNA using Sau3A1 was cloned into the IPTG-inducible expression vector pGEX-4T3 and electroporated into DH10B T1R *E. coli* ElectroMax electrocompetent cells (ThermoFisher) to generate a library. Pools of 30 clones were screened for their ability to stimulate individual T cell hybridomas by the single cell β-galactosidase assay as described above. Individual stimulatory clones were isolated from stimulatory pools and their inserts were sequenced and mapped to the published *A. muciniphila* genome sequence (*91*). The stimulatory region was narrowed down by

cloning smaller fragments into the pGEX-4T3 vector. Candidate epitopes were identified using both in-house and online peptide-MHCII binding prediction tools (*116*, *117*). Candidate peptides were ordered from Genscript and tested for their ability to stimulate the 124-2 T cell hybridoma.

Cell isolation:

Cells from mesenteric lymph nodes, Peyer's patches (including cecal patch), spleen and thymus were isolated by mechanical dissociation on a 70-μm filter. Cells from small intestine lamina propria (after removal of Peyer's patches) and large intestine lamina propria (cecum and colon, after removal of cecal patch) were cut longitudinally after removing excess adipose tissue, washed in PBS and incubated at 37ºC for 20 min with stirring in Hank's balanced salt solution (HBSS) with 1 mM DTT, 10% (v/v) FBS, penicillin–streptomycin and HEPES. Intestines were then incubated at 37ºC for 25 min with stirring in HBSS with 1.3 mM EDTA, penicillin–streptomycin and HEPES, with further dissociation of epithelial cells in 10 mL PBS by shaking. Tissues were digested in RPMI with collagenase VIII (1 mg/mL, Sigma), DNaseI (5 μg/mL, Sigma), penicillin–streptomycin and HEPES for 45 min, and lymphocytes were collected at the interface of a 44%/67% Percoll gradient (GE Healthcare).

Generation of Amuc124 TCR transgenic mice:

124-2 T cell hybridoma paired TCRα and TCRβ sequence usage was identified by nested RT-PCR as previously described (*118*). Rearranged VDJ regions were amplified from genomic DNA from the 124-2 hybridoma using the following primers: 124F: 5′-GATCTCAGTCCTCAGTGAAGAGG-3′, 124R: 5′-CCCTGTACATTGCAGGAATATCC-3′

(plus restriction enzyme target sequences) and cloned into the pTα and pTβ cassettes (*119*). TCR transgenic mice were generated at the Cancer Research Laboratory Gene targeting facility at the University of California Berkeley by microinjection of linearized plasmids into C57BL/6J one-cell embryos. Positive pups were genotyped by PCR and maintained free of *A. muciniphila* colonization.

T cell adoptive transfers:

Peripheral lymph nodes and spleen of *A. muciniphila*-negative Amuc124 TCR transgenic Thy1.1 mice were dissociated mechanically on a 70-μm filter. Naïve CD4 T cells ($CD3^+$ $CD4^+$ $CD62L^+$ $CD44^{lo}$) were sorted on a BD FACSAria Fusion cell sorter and 10,000 cells were transferred by retro-orbital injection into C57BL/6 recipient mice (Thy1.2). Recipient mice were analyzed 12 days post adoptive T cell transfer.

Flow cytometry and sorting:

Cells were isolated as described above and stained in a 96-well U-bottom plate. Dead cells were excluded with a fixable Near-IR or Aqua live/dead dye (Life technologies) in PBS. Surface staining was performed in PBS with 2% FBS (v/v), 1 mM

EDTA and 0.1% NaN_3 for 30 min at 4ºC, or for 1 h at room temperature (RT) when staining for CXCR5 (no NaN_3). Staining with tetramers was performed for 30' at 37C in the presence of 50 nM Dasatinib (Sigma), followed by an additional 30' at RT. Anti-CXCR5 antibodies were included in this tetramer staining step, and the rest of surface staining was performed in a subsequent step for 30' at 4˚C. Intracellular transcription factor staining (eBioscience buffer set, ThermoFisher) was performed by fixation for 1 h at RT and staining for 40 min at RT. Samples were analyzed on a BD LSR Fortessa or a BD LSR Fortessa X-20. The list of antibodies used can be found in Table S1.

Computational prediction and validation of the Am3740-1 epitope:

Utilizing BOTA, a previously described computational algorithm for predicting microbial epitopes from genomic data (*120*), the top 10 epitopes most likely to be immune-dominant from the strain *Akkermansia muciniphila ATCC BAA-835* were predicted. Next, Xavier, R. and colleagues analyzed which of these epitopes were specific to *A. muciniphila* by using BLAST on all known public databases with published bacterial genomes. Three of the ten epitopes were predicted to be from proteins restricted to *A. muciniphila* genomes only, and these 3 peptides were synthesized for further validation of MHCII binding and activity. Peptides from the three predicted epitopes were re-suspended in DMSO and screened for production of cytokines by pulsing murine splenocytes with each peptide for 18 h at 37°C as described previously (*120*). Cytokine production was measured by cytometric bead array (Flex Set; BD Biosciences) for IFN-γ (cat no. 558296), IL-17A (cat no. 560283), and IL-10 (cat no. 558300), and the LIFESSNALGLGR peptide was selected for tetramer production.

Generation of I-A^b tetramers:

The Am3735-1 and Am3740-1 I-A^b tetramers were constructed by previously described methods (*121*). The peptide sequences used to generate tetramers were the following: TLYIGSGAILS (Am3735-1) or LIFESSNALGLGR (Am3740-1), consisting of the 9-mer MHCII-binding cores of the epitope plus 2 additional N-terminal residues, and also 2 additional C-terminal residues for Am3740-1. In brief, these peptide sequences were encoded as covalent fusions to soluble heterodimeric I-A^b molecules stably expressed in *Drosophila* S2 cells. Purified biotinylated peptide:MHCII complexes were then tetramerized with PE or APC fluorochrome-conjugated streptavidin (Prozyme).

Quantification and statistical analysis:

Statistical tests were performed as indicated on the figure legends with Prism 8 software (Graphpad Prism).

Table S1: Antibody list

Target	Fluorophores	Clone	Dilution	Concentration	Company
CD3	BV421, PerCP-Cy5.5	145-2C11	1/200	1 µg/mL	BD Horizon
CD4	BV785, APC	GK1.5	1/200	1 µg/mL	Biolegend
CD44	BV711, FITC	IM7	1/400	0.5 µg/mL	Biolegend
Thy1.1	BUV395, BV650	OX7	1/400	0.5 µg/mL	BD optibuild
PD-1	PE-Cy7	J43	1/200	1 µg/mL	invitrogen
FOXP3	Alexa Fluor (AF) 488	FJK-16s	1/250	2 µg/mL	eBioscience
CXCR5	AF 647, BV650	L138D7	1/100	2 µg/mL	Biolegend
RORγt	PE	AFKJS-9	1/100	2 µg/mL	invitrogen
T-bet	PE-Cy7	4B10	1/200	0.5 µg/mL	Biolegend
GATA3	AF 647	L50-823	1/20	NA	BD Pharmigen
Bcl6	PE	K112-91	1/50	NA	BD Horizon
CD62L	PE	MEL-14	1/200	1 µg/mL	Tonbo
CD8	eFluor 450	53-6.7	1/400	0.5 µg/mL	eBioscience
Fc Block	NA	2.4G2	1/200	2.5 µg/mL	UCSF
TCRb	APC	H57-597	1/100	2 µg/mL	TONBO
B220	FITC, PercP-Cy5.5	RA2-6B2	1/200	1 µg/mL	Biolegend
CD11c	FITC	N418	1/200	2.5 µg/mL	eBioscience
CD11b	FITC	M1/70	1/200	2.5 µg/mL	Biolegend
Near-Ir L/D	NA	NA	1/1000	NA	Invitrogen
Aqua L/D	NA	NA	1/1000	NA	Invitrogen
IgG1	biotinylated	A85-1	1/200	2.5 µg/mL	BD Pharmigen
IgG2b	biotinylated	R12-3	1/200	2.5 µg/mL	BD Pharmigen
IgG2a	biotinylated	5.7	1/200	2.5 µg/mL	BD Pharmigen
IgG3	biotinylated	R40-82	1/200	2.5 µg/mL	BD Pharmigen
IgA	biotinylated	Polyclonal (1040-08)	1/200	2.5 µg/mL	Southern Biotech
SA-PE-Cy7	PE-Cy7	NA	1/200	1 µg/mL	eBioscience

Figures:

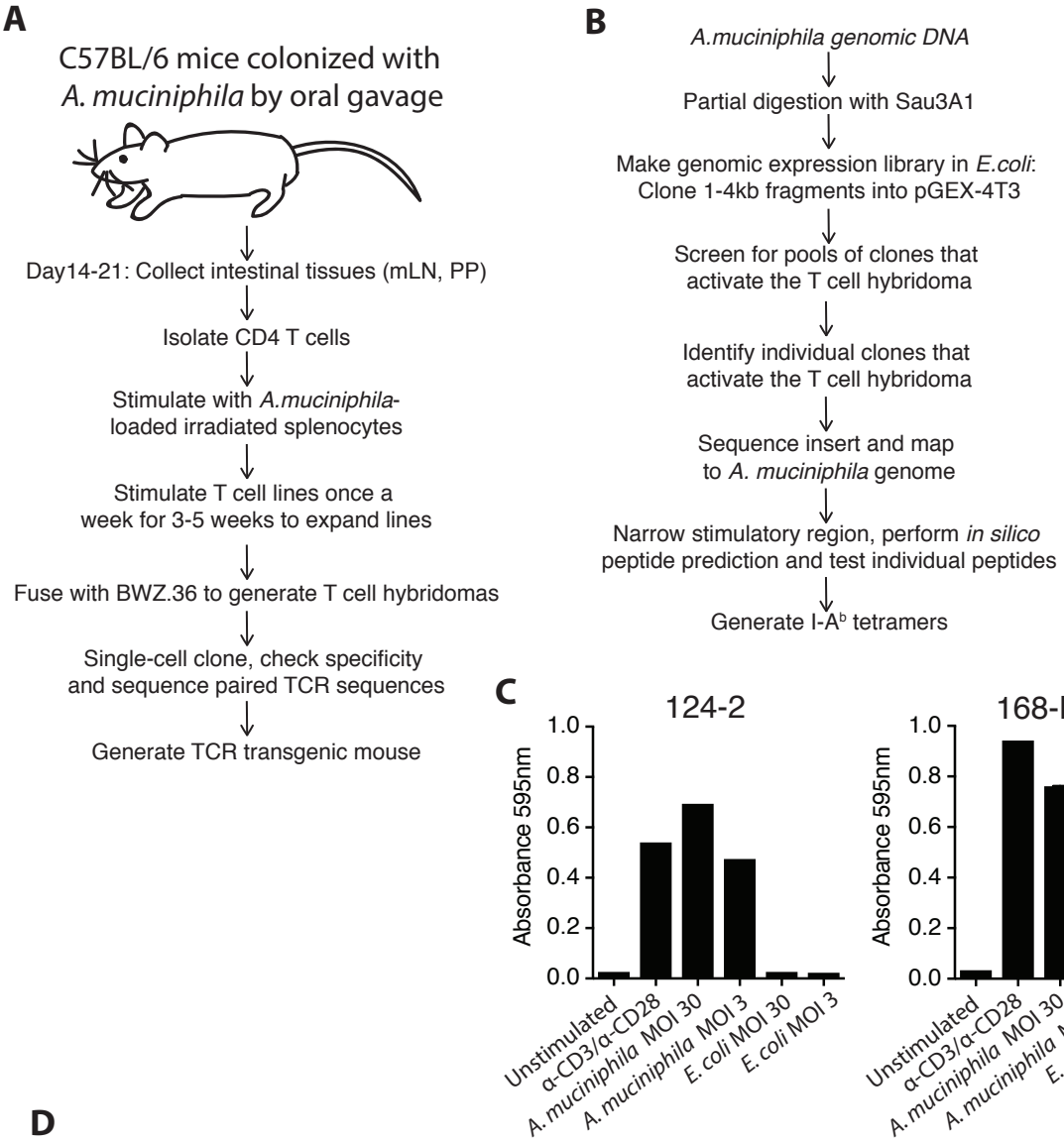

D

Hybridoma	TCRVβ usage	CDR3 (Vβ) sequence	TCRVα usage	CDR3 (Vα) sequence	*A. muciniphila* antigen	*A. muciniphila epitope*
124-2	TRBV20*01 (Vβ15), TRBJ1-1*01, TRVD1*01	CGAGGTSNTEVFF	TRAV7D-3*01, TRAJ57*01	CAVNQGGSAKLIF	Amuc_RS03735 Outer membrane autotransporter barrel-domain containing protein.	TLYIGSGAILSGN
168-H10-1	TRBV31*01 (Vβ14), TRBJ1-1*01, TRBD1*01	CAWSPTGRDTEVFF	TRAV6D-6*02, TRAVJ15*01	CALGVYQGGRALIF	Amuc_RS07575: GAPDH	N.D.

Figure 4.1. Generation of *A. muciniphila*-specific hybridomas, TCR transgenic mice, and I-A^b tetramers
(**A**) Diagram summarizing the generation of *A. muciniphila*-specific T cell lines from *A. muciniphila*-colonized mouse intestinal tissues, generation of T cell hybridomas and TCR transgenic mice.
(**B**) Stimulation of T cell hybridomas with splenocytes loaded with the indicated antigens. Data are representative of >3 independent experiments.
(**C**) Diagram summarizing the identification of *A. muciniphila* antigens recognized by individual T cell hybridomas via screening of an expression library of *A. muciniphila* genomic DNA.
(**D**) Summary table of TCR gene usage, CDR3 sequence and antigen specificity for the indicated *A. muciniphila*-specific T cell hybridomas.
(**E**) Stimulation of *A. muciniphila*-specific T cell hybridoma 124-2 with an identified peptide from the protein RS03735. A serial dilution of peptide was used to test for specificity.
(**F**) Staining of Amuc124 *Rag1*$^{-/-}$ TCR transgenic T cells with Am3735-1 tetramer. Data are representative of two independent experiments.

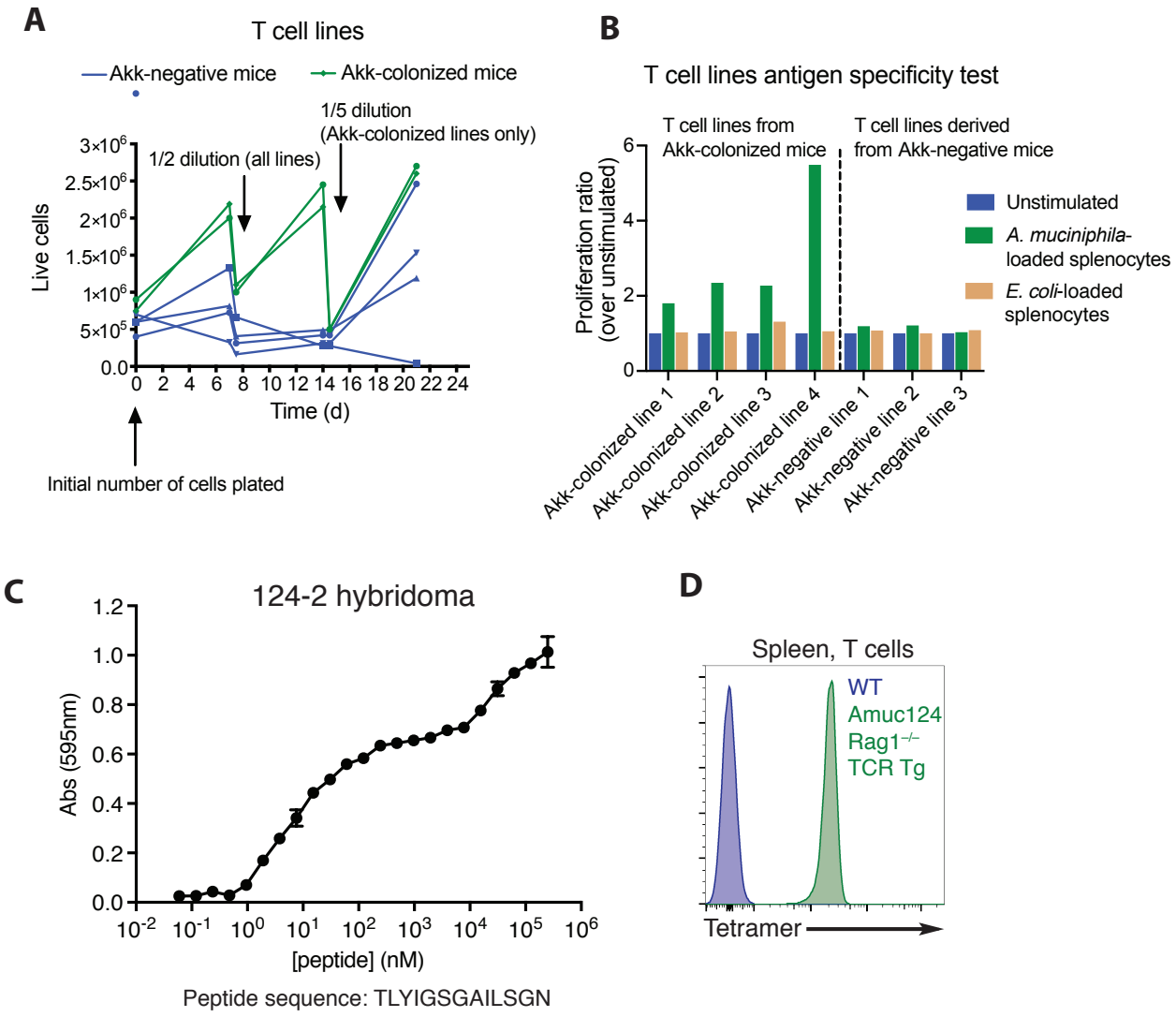

Figure 4.2. Generation of *A. muciniphila*-specific I-A^b tetramers and validation of T cell lines

(**A**) Cell numbers for 6 of the T cell lines: 2 T cell lines derived from intestinal tissues (mLN and PP) of *A. muciniphila*-colonized mice 14-21 days post oral gavage (Akk-colonized), and 4 T cell lines derived from intestinal tissues of *A. muciniphila*-negative mice (Akk-negative). All T cell lines were diluted ½ after seven days and Akk-colonized T cell lines were diluted 1/5 on day 14. All T cell lines were stimulated with *A. muciniphila*-loaded irradiated splenocytes on day 0. At the end of each week live cells were collected on a Ficoll gradient and stimulated with *A. muciniphila*-loaded irradiated splenocytes for another week.

(**B**) Proliferation ratios of seven T cell lines. T cell lines were labeled with CFSE and incubated for three days with irradiated splenocytes loaded with different antigens or nothing (unstimulated). T cells that proliferate dilute their CFSE and thus have lower CFSE gMFI. Thus, the proliferation ratio for each antigen was calculated as the inverse

of the gMFI ratio over unstimulated. The hybridoma 124 (and Amuc124 TCR transgenic mice) were derived from Akk-colonized line 4.
(**C**) Stimulation of *A. muciniphila*-specific T cell hybridoma 124-2 with an identified peptide from the protein RS03735. A serial dilution of peptide was used to test for specificity.
(**D**) Staining of Amuc124 *Rag1*$^{-/-}$ TCR transgenic T cells with Am3735-1 tetramer. Data are representative of two independent experiments.

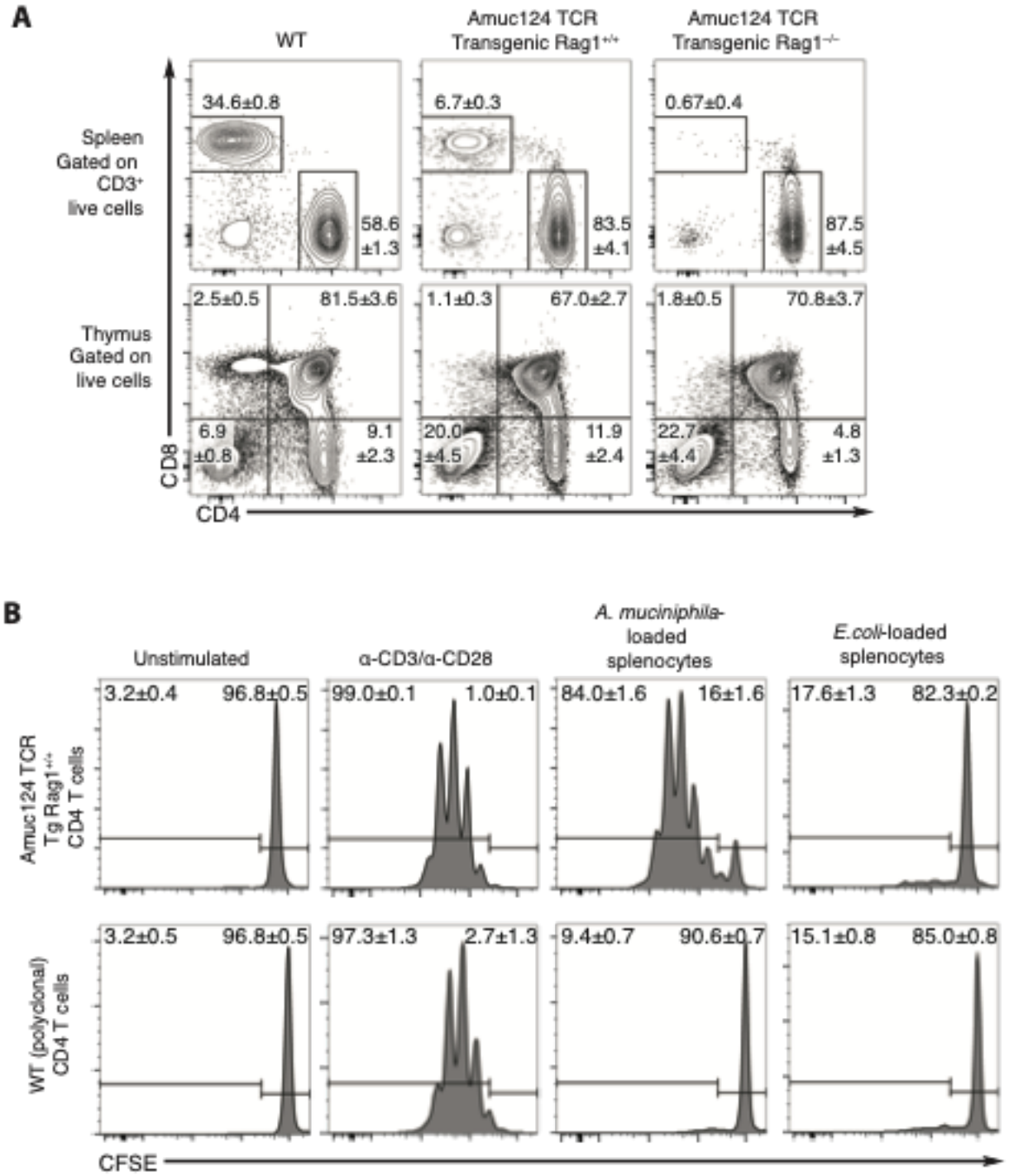

Figure 4.3 Characterization of Amuc124 TCR Transgenic mice

(**A**) Representative flow cytometric analysis of spleen and thymus for the indicated mice. n=3 mice per group.

(**B**) Amuc124 *Rag1*$^{+/+}$ TCR transgenic T cells were labeled with the proliferation dye CFSE and stimulated with the indicated antigens for 3 days. Proliferation was measured by flow cytometry. Data are representative of two independent experiments. Gates on flow cytometry plots show mean±SEM

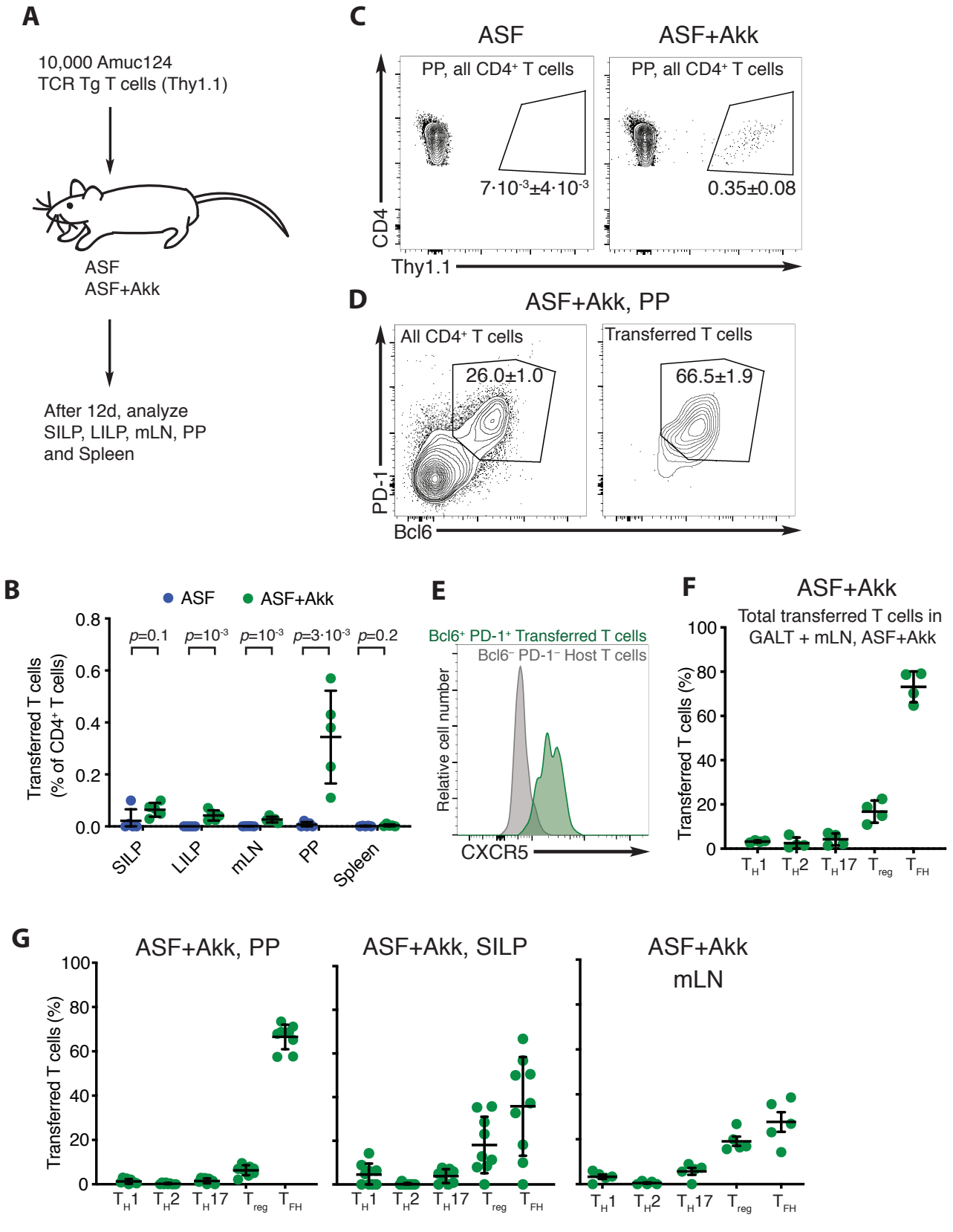
A
10,000 Amuc124
TCR Tg T cells (Thy1.1)
ASF
ASF+Akk
After 12d, analyze
SILP, LILP, mLN, PP
and Spleen
C
ASF
ASF+Akk
PP, all CD4+ T cells
PP, all CD4+ T cells
7·10-3±4·10-3
0.35±0.08
CD4
Thy1.1
D
ASF+Akk, PP
All CD4+ T cells
Transferred T cells
26.0±1.0
66.5±1.9
PD-1
Bcl6
B
ASF
ASF+Akk
p=0.1
p=10-3
p=10-3
p=3·10-3
p=0.2
Transferred T cells
(% of CD4+ T cells)
SILP
LILP
mLN
PP
Spleen
E
Bcl6+ PD-1+ Transferred T cells
Bcl6- PD-1- Host T cells
Relative cell number
CXCR5
F
ASF+Akk
Total transferred T cells in
GALT + mLN, ASF+Akk
Transferred T cells (%)
TH1
TH2
TH17
Treg
TFH
G
ASF+Akk, PP
ASF+Akk, SILP
ASF+Akk
mLN
Transferred T cells (%)

Figure 4.4. *A. muciniphila* induces antigen-specific T follicular helper cell responses during homeostasis

(**A**) Experimental design of Amuc124 TCR transgenic T cell adoptive transfers. Ten thousand naïve ($CD44^{lo}$ $CD62L^{+}$ $CD3^{+}$ $CD4^{+}$) Amuc124 TCR Transgenic T cells expressing the congenic marker Thy1.1 were transferred for all adoptive transfers.
(**B**) Frequencies of transferred T cells in intestinal tissues of ASF and ASF+Akk mice. n=5 mice per group, data are representative of six independent experiments.
(**C**) Representative flow cytometric analysis depicting transferred T cells ($Thy1.1^{+}$) as percentage of all $CD4^{+}$ T cells in the Peyer's patches of ASF and ASF+Akk mice 12 days after low-frequency adoptive transfer of Amuc124 TCR transgenic T cells. Quantified in (B).
(**D** and **E**) Representative flow cytometric analysis of expression of T follicular helper markers (PD-1, Bcl6, and CXCR5) by endogenous and transferred T cells in the Peyer's patches of ASF+Akk mice.
(**F**) Total transferred T cell percentages expressing T_H1 (T-bet^{+} $FOXP3^{-}$), T_H2 ($GATA3^{+}$ $FOXP3^{-}$), T_H17 ($ROR\gamma t^{+}$ $FOXP3^{-}$), T_{reg} ($FOXP3^{+}$) or T_{FH} ($Bcl6^{+}$ $PD\text{-}1^{+}$) markers in gut-associated lymphoid tissue (SILP, LILP and PP) and mesenteric lymph nodes (mLN) in ASF+Akk mice 12 days post Amuc124 TCR transgenic adoptive transfer. Numbers for each CD4 T cell fate were analyzed separately for each tissue and then combined together for this analysis. n=4 mice, data are representative of six independent experiments.
(**G**) Expression of T_H1 (T-bet^{+} $FOXP3^{-}$), T_H2 ($GATA3^{+}$ $FOXP3^{-}$), T_H17 ($ROR\gamma t^{+}$ $FOXP3^{-}$), T_{reg} ($FOXP3^{+}$) or T_{FH} ($Bcl6^{+}$ $PD\text{-}1^{+}$) markers by transferred T cells in intestinal tissues of ASF+Akk mice. Data are representative of six independent experiments.
Each symbol represents a mouse, error bars represent mean ± SD. Gates on flow cytometry plots show mean±SEM. *p*-values were calculated with unpaired Student's *t*-tests (B).

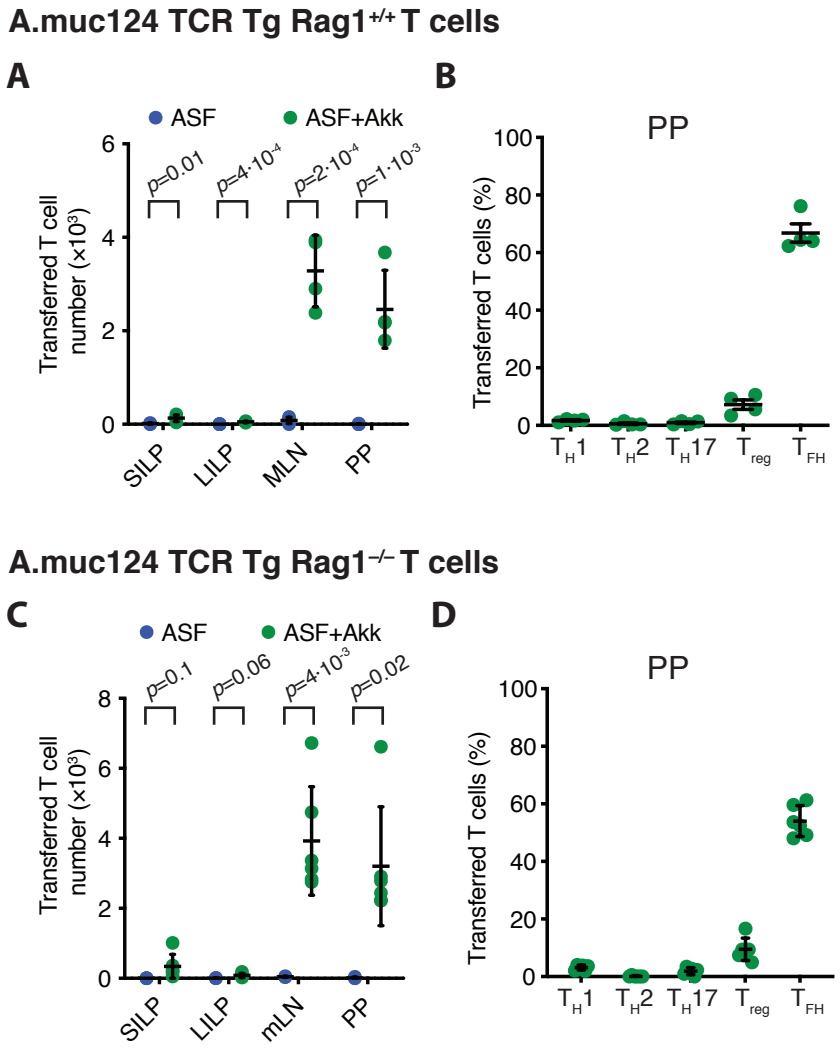

Figure 4.5. Amuc124 TCR transgenic *Rag1*$^{+/+}$ and *Rag1*$^{-/-}$ cells expand similarly in ASF+Akk mice

(**A** and **C**) Numbers of transferred T cells in intestinal tissues of ASF and ASF+Akk mice post adoptive transfer of Amuc124 TCR transgenic *Rag1*$^{+/+}$ cells (A) or Amuc124 TCR transgenic *Rag1*$^{-/-}$ cells (C). n=4 (A) or n=5 (C) mice per group. Data are representative of three independent experiments.

(**B** and **D**) Expression of T_H1 (T-bet$^+$ FOXP3$^-$), T_H2 (GATA3$^+$ FOXP3$^-$), T_H17 (RORγt$^+$ FOXP3$^-$), T_{reg} (FOXP3$^+$) or T_{FH} (Bcl6$^+$ PD-1$^+$) markers by transferred T cells in the Peyer's patches of ASF+Akk mice post adoptive transfer of Amuc124 TCR transgenic *Rag1*$^{+/+}$ cells (B) or Amuc124 TCR transgenic *Rag1*$^{-/-}$ cells (D). n=4 (B) or n=5 (D) mice per group. Data are representative of three independent experiments.

Each symbol represents a mouse, error bars represent mean ± SD. *p*-values were calculated with unpaired Student's *t*-tests.

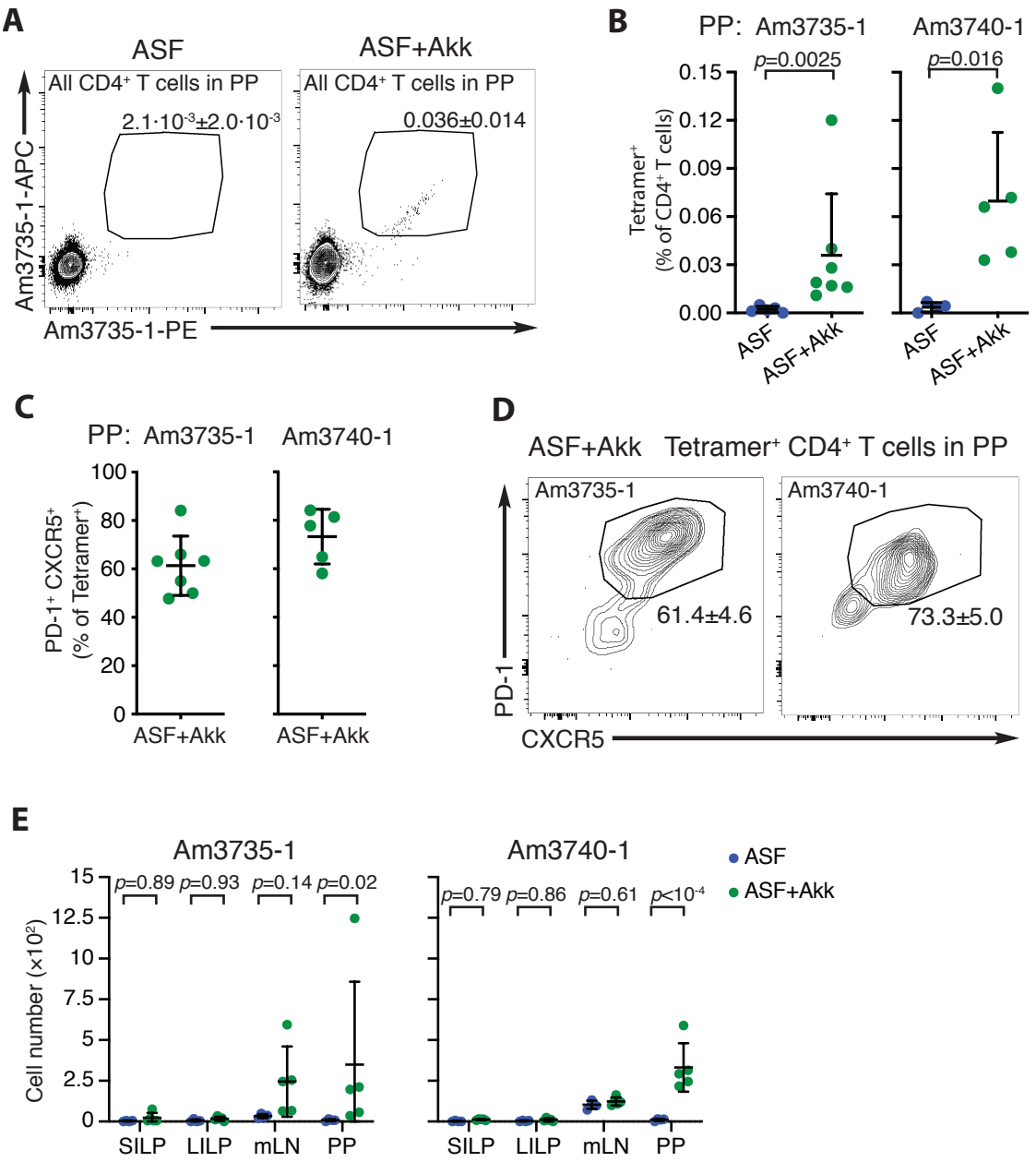

Figure 4.6. Endogenous *A. muciniphila*-specific T cells localize to the Peyer's patches and adopt T_{FH} markers.

(**A**) Representative Am3735-1 tetramer flow cytometric analysis of Peyer's patches from ASF and ASF+Akk mice.

(**B**) Frequencies of Am3735-1 or Am3740-1 tetramer$^+$ endogenous T cells in ASF and ASF+Akk mice as a percentage of total CD4$^+$ T cells. n=4 ASF, n=5-7 ASF+Akk mice. Data are representative of three (Am3740-1) or six (Am3735-1) independent experiments.

(**C**) Frequencies of Am3735-1 or Am3740-1 tetramer$^+$ cells expressing T_{FH} markers (PD-1 and CXCR5, as shown in (D)) in the PPs of ASF+Akk mice. n=5-7 mice, data are representative of three (Am3740-1) or six (Am3735-1) independent experiments.

(**D**) Representative flow cytometric analysis of expression of T_{FH} markers (PD-1 and CXCR5) by endogenous Am3735-1 or Am3740-1 tetramer$^+$ cells.
(**E**) Numbers of Am3735-1 and Am3740-1 tetramer$^+$ cells in all intestinal tissues in ASF and ASF+Akk mice. n=4 ASF, n=5 ASF+Akk mice. Data are representative of two (Am3740-1) or three (Am3740-1) independent experiments.
Each symbol represents a mouse, error bars represent mean ± SD. Gates on flow cytometry plots show mean±SEM. *p*-values were calculated with unpaired Student's *t*-tests (E), or a Mann–Whitney test (B).

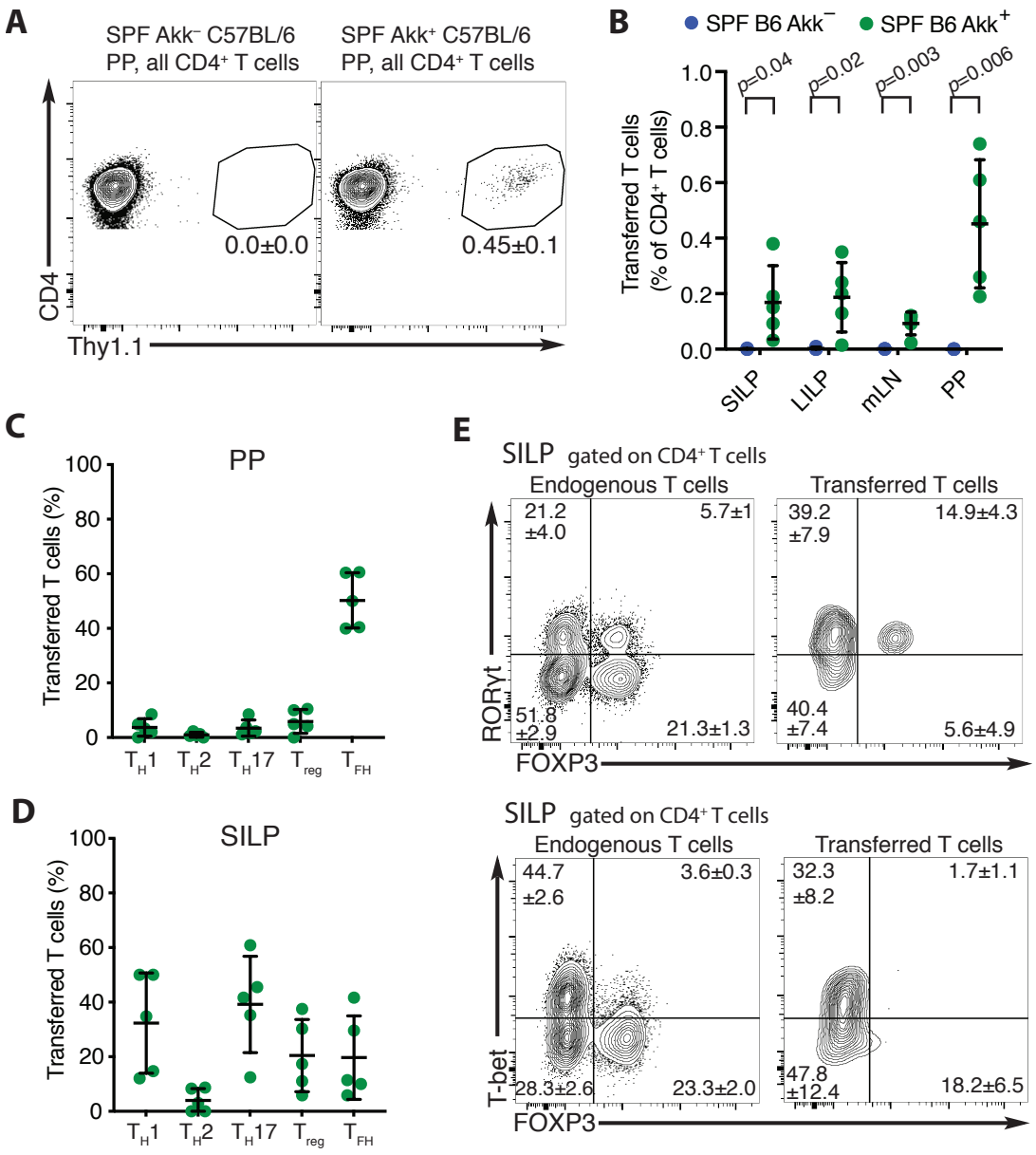

Figure 4.7. *A. muciniphila*-specific T cells adopt other fates in the context of a complex microbiota

(**A**) Representative flow cytometric analysis depicting transferred Amuc124 T cells (Thy1.1⁺) as percentage of all CD4⁺ T cells in the Peyer's patches of SPF Akk⁻ and SPF Akk⁺ mice.

(**B**) Frequencies of transferred T cells as percentage of all CD4⁺ T cells in intestinal tissues of conventional specific pathogen-free (SPF) *A. muciniphila*⁻ (n=4) and SPF *A. muciniphila*⁺ (n=5) mice. Data are representative of three independent experiments.

(**C** and **D**) Expression of T_H1 (T-bet⁺ FOXP3⁻), T_H2 (GATA3⁺ FOXP3⁻), T_H17 (RORγt⁺ FOXP3⁻), T_{reg} (FOXP3⁺) or T_{FH} (Bcl6⁺ PD-1⁺) markers by transferred T cells in the Peyer's patches (C) or small intestine lamina propria (D) of SPF *A. muciniphila*⁺ mice. n=5 mice, data are representative of three independent experiments.

(**E**) Representative flow cytometric analysis of expression of T_H1 and T_H17 markers by endogenous total $CD4^+$ T cells and *A. muciniphila*-specific (transferred) T cells in the SILP of SPF *A. muciniphila*$^+$ mice.
Each symbol represents a mouse, error bars represent mean ± SD. Gates on flow cytometry plots show mean±SEM. *p*-values were calculated with unpaired Student's *t*-tests (B).

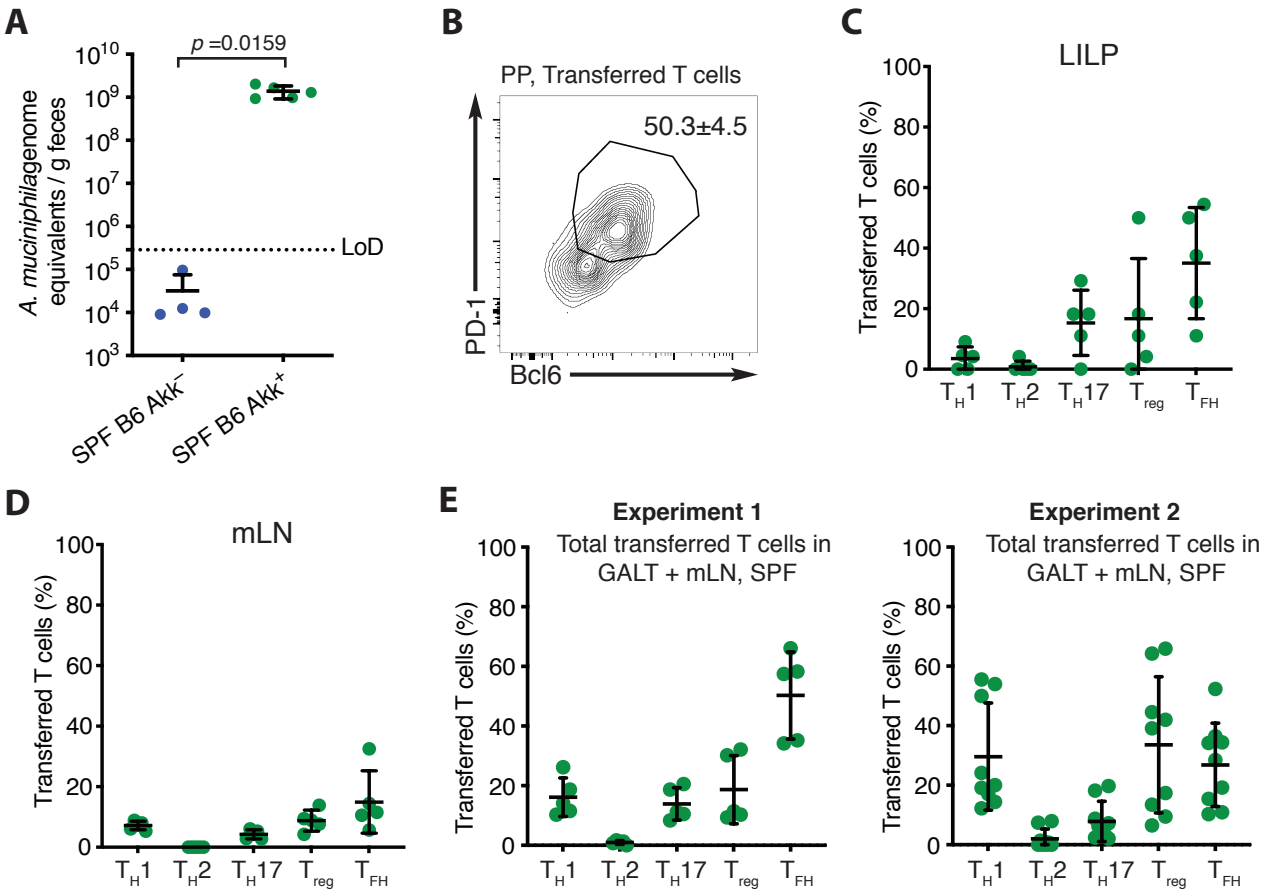

Figure 4.8. *A. muciniphila*-specific T cells adopt T_{FH} but also T_H1 and T_H17 markers in SPF Akk⁺ mice

(**A**) Quantification of *A. muciniphila* colonization by fecal 16S qPCR for SPF Akk⁻ (n=4) and SPF Akk⁺ mice (n=5). Applies to experiments in Fig. 4 and this figure. Data are representative of three independent experiments.

(**B**) Representative plot of T_{FH} marker expression (Bcl6 and PD-1) by transferred T cells in the Peyer's patches of SPF Akk⁺ mice.

(**C** and **D**) Expression of T_H1 (T-bet⁺ FOXP3⁻), T_H2 (GATA3⁺ FOXP3⁻), T_H17 (RORγt⁺ FOXP3⁻), T_{reg} (FOXP3⁺) or T_{FH} (Bcl6⁺ PD-1⁺) markers by transferred T cells in the LILP (C) or mLN (D) of SPF Akk⁺ mice. Data are representative of three independent experiments.

(**E**) Total transferred T cell percentages expressing T_H1 (T-bet⁺ FOXP3⁻), T_H2 (GATA3⁺ FOXP3⁻), T_H17 (RORγt⁺ FOXP3⁻), T_{reg} (FOXP3⁺) or T_{FH} (Bcl6⁺ PD-1⁺) markers in gut-associated lymphoid tissue (SILP, LILP and PP) and mesenteric lymph nodes (mLN) of two independent experiments in SPF Akk⁻ and SPF Akk⁺ mice. Numbers for each CD4 T cell fate were analyzed separately for each tissue and then combined for these plots. Each symbol represents a mouse, error bars represent mean ± SD. Gates on flow cytometry plots show mean±SEM. *p*-values were calculated with a Mann–Whitney test (A).

Chapter 5: Description of a novel mouse line that induces ectopic responses to the microbiota

Part of the work presented in this chapter was performed with the help of Shaina Carroll.

Background:

Conditions of intestinal infection or inflammation are known to induce proinflammatory T cell fates against commensal antigens that are ignored during homeostasis (*69*), and immune dysregulation caused by lack of the anti-inflammatory cytokine IL-10 leads to proinflammatory responses to *Helicobacter* spp., which drive colitis in IL-10 deficient mice (*65*, *66*, *122*). In addition, T cell responses to the microbiota could provide bystander protection against pathogen infection, but can also pose a pathogenic risk if they become dysregulated (*70*).

Prior to this work, there were no examples of homeostatic T cell responses to intestinal commensal antigens that changed based on contextual signals in wild-type mice. The varying T cell fates I observed to *A. muciniphila* in SPF mice (Chapter 4) suggest that responses to commensal bacteria can be context-dependent, which doesn't appear to be the case for SFB or *Helicobacter* spp. (*59*, *65*). Only CBir1 induces different kinds of responses in different inflammatory contexts, but this occurs in the absence of a steady state response, since this antigen does not induce T cell responses during homeostasis (*68*, *69*). Thus, I became very interested in understanding what signals can change the response to *A. muciniphila* and lead to pro-inflammatory T cell fates (Th1, Th17). Elucidating these signals would not only help understand overall host-microbiota interactions during inflammation and the subsequent return to homeostasis, but may also shed light into some of the specific mechanisms that *A. muciniphila* engages to mediate its protection in metabolic disease and PD-1 cancer immunotherapy (*92*, *93*, *100*). Of particular interest is the fact that Type-I $CD4^+$ T cell responses to *A. muciniphila* correlated with improved responsiveness to PD-1 therapy.

One could envision attempting to modulate the response to *A. muciniphila* in mice modeling what would occur in humans: through intestinal infection and inflammation. Preliminary results suggested that the response to *A. muciniphila* may change under DSS-induced colitis (Data not shown), but I haven't performed those experiments enough times and will not discuss them here. During my studies exploring T cell responses to *A. muciniphila* in SPF mice, I encountered a very striking phenotype in a specific mouse line, which quickly became the focus of my work, and I will describe my current findings in this chapter.

Results:

During my experiments in SPF mice in Chapter 4, I encountered a very surprising result in a specific mouse line: C57BL/6 (B6) and SJL are two inbred mouse strains used in research. B6 mice are widely used in the field of immunology, and many genetic tools, mouse knockouts, reporters of gene expression etc exist in this genetic background. The SJL mouse strain carries a distinct allele of the gene CD45, among many other genes. The polymorphism in CD45 between the two alleles does not impact function, but creates different epitopes that are recognized by two different monoclonal antibodies (*123*). The CD45 allele of B6 mice is named CD45.2 (or Ly5.2), and the CD45 allele of SJL mice, is named CD45.1 (or Ly5.1). The CD45.1 allele from SJL mice has been backcrossed onto the B6 background, thus generating C57BL/6.SJL (or B6.SJL) mice. B6.SJL mice are isogenic to B6 mice except for carrying the CD45 locus from SJL mice (or "congenic"), although additional polymorphisms can occur (*124*, *125*). B6.SJL mice are widely used as congenics in models of adoptive cell transfers, transplantation, bone marrow chimeras etc as a method to track cell origin via CD45.1 and CD45.2. A major assumption in these transfer experiments is that the donor (B6 or B6.SJL) and recipient cells (B6.SJL or B6, respectively) share the same genetic background.

With the goal of characterizing the T cell response to *A. muciniphila* in conventional mice, I performed Amuc124 TCR transgenic adoptive transfers into SPF C57BL/6 mice (Figure 4.7 and 4.8) and also B6.SJL mice, since both of these strains are considered to be wild-type and isogenic except for the CD45 locus. However, performing low frequency Amuc124 T cell adoptive transfers into B6.SJL mice revealed very exuberant T cell responses compared to B6 controls. *A. muciniphila*-specific T cells expanded dramatically in B6.SJL mice, homed preferentially to the SILP and adopted Th17 markers, but also homed to the PP and LILP (Figure 5.1A and B). For the purpose of this work, I renamed B6.SJL mice housed in the Barton lab at UC Berkeley from early 2010s until 2019 as B6.SJL*. Amuc124 T cells reached extremely high frequencies (% of $CD4^+$ T cells) in B6.SJL* mice, particularly in the small intestine (Figure 5.1A and B). These frequencies are orders of magnitude larger than the frequencies observed in the ASF+Akk and B6 SPF mice, or the frequencies observed for SFB or *Helicobacter*-specific T cells with similar experimental design (*59*, *65*), evidencing the large degree of expansion of Amuc124 T cells in B6.SJL* mice.

Two non-mutually exclusive hypothesis exist to explain these surprising results: First, differences in microbiota composition, such as the presence of an ongoing infection in the B6.SJL* mice, could account for this exuberant response. Second, the phenotype has a genetic basis: B6.SJL* mice may harbor a polymorphism or mutation in an immunoregulatory gene that leads to this response. Transferred T cells have a B6 genetic background and don't present the same phenotype in other strains of mice. Consequently, if genetic, this phenotype would occur in a Amuc124 T cell-extrinsic manner.

Initially, I favored the first hypothesis. *A. muciniphila* has been shown to bloom in mucosal wound beds in the intestine in a manner dependent on the induction of hypoxia and MUC3 (*98*). I hypothesize that *A. muciniphila* may become a major mucosal antigen during events that lead to intestinal infection, wounding or inflammation. This would be mediated through an increase in *A. muciniphila* colonization on the inflamed/wounded/infected epithelium due to its production of hypoxic conditions and upregulation of Muc3 mucin. Subsequent sampling in situ by immune cells would lead to potent induction of T cell responses to this epithelium-associated bacterium in the context of inflammation.

If the phenotype that I observed is due to microbiota composition, this would predict that this phenotype would be transferrable to B6 mice. To test this, I performed cohousing experiments in which I cohoused *A. muciniphila*-positive B6 and B6.SJL* mice from the moment of weaning until the age of 10-12 weeks, and then performed Amuc124 T cell adoptive transfers. These experiments, however, failed to transfer the phenotype to B6 mice, while B6.SJL* mice that were cohoused with B6 mice maintained the same exuberant T cell responses post transfer (Figure 5.2C). The percentage of transferred T cells expressing Th17, Th1 and T_{FH} markers was similar between the groups, but B6.SJL* mice had higher percentage of Th17 in the SILP and a substantial increase in the magnitude of the response (Figure 5.2C and D).

During the course of experiments, I realized that B6.SJL* mice presented increased amounts of endogenous polyclonal T-bet^{+} FOXP3^{-} CD4^{+} T cells (which are markers of Th1 cells) in intestinal but also systemic secondary lymphoid organs (Figure 5.3A and B). Importantly, this phenotype was observed even when adoptive transfers of Amuc124 T cells were not performed (Figure 5.2B). Analysis of previous experiments involving Amuc124 T cell adoptive transfers into B6 and B6.SJL* mice revealed the same increase in polyclonal Th1 cells when looking at the non-TCR transgenic endogenous population in the spleen and mLNs (Figure 5.2C). However, this phenotype appears to be incompletely penetrant (Figure 5.2C), despite the fact that all these mice were cohoused littermates. This incomplete penetrance is also true for the Amuc124 T cell adoptive transfers (Figure 5.1B), and correlates with the exuberant Amuc124 T cell activation (Data not shown). While I lack the numbers and experiments to support this claim, it appears that this phenotype is more prevalent as the mice age, which is also a hallmark of other mouse models of colitis (*126*). Furthermore, I have observed that B6.SJL* mice present with frequent rectal prolapse and enlarged mesenteric lymph nodes, both signs of intestinal inflammation and disease, although I haven't quantified this rigorously yet (Data not shown).

To further test the transferability of this phenotype, I performed fecal microbiota transplants into germ-free mice. I collected intestinal contents from *A. muciniphila*-positive B6 or B6.SJL* mice and immediately performed oral gavages into adult germ-free mice that were subsequently housed under SPF conditions. I selected B6.SJL* mice with signs of intestinal inflammation for this fecal transplant. After 30 days, but also after 60 days in a second cohort, I performed Amuc124 T cell adoptive transfers and

also analyzed the endogenous CD4+ T cell compartment (Figure 5.3A). Ex-germ-free (ExGF) mice that received B6.SJL* microbiota induced similar responses to *A. muciniphila* upon T cell adoptive transfer compared to mice that received B6 microbiota (Figure 5.3B). The expansion of transferred T cells was similar to the results observed in SPF *A. muciniphila*-positive B6 mice (Figure 4.7). In addition, the endogenous CD4+ T cell compartment between these two groups was almost identical, with no signs of an increase in Th1 cells in the mice that received B6.SJL* microbiota (Figure 5.3C). In conclusion, these data show that neither of the two phenotypes observed in B6.SJL* mice, the exuberant expansion of Amuc124 transferred T cells or the aberrant endogenous Th1 responses, can be readily transferred by microbiota transplantation.

These results argue against the hypothesis that the phenotype observed in B6.SJL* mice is due to a distinct microbiota, and point to a for a genetic underpinning instead. To see if this was a general feature of all B6.SJL mice, I obtained new B6.SJL mice from Jackson laboratories, and preliminary observations suggest that "fresh" B6.SJL/J mice don't present the same phenotypes (Data not shown). Thus, I predict that the B6.SJL* mouse line has acquired a de novo spontaneous mutation that has been fixed in the mouse colony in the Barton lab at UC Berkeley due to repeated sibling inbreeding. Inbreeding is the standard practice to maintain mouse lines and keep track of genotypes, such as the absence of a particular gene that has been knocked out or, in this case, the presence of the congenic marker CD45.1. However, inbreeding carries the risk of acquiring new polymorphisms compared to the C57BL/6 strain, which can reach fixation in the colony after many generations.

Aberrant Th1 responses, intestinal inflammation, enlarged mLNs and rectal prolapse are all the major phenotypes present in the IL-10-deficient mouse model of colitis (*66*, *105*, *127*), which depends on the presence of *Helicobacter spp.* to trigger disease. B6.SJL* mice exhibit all these same phenotypes, and *Helicobacter spp.* are present in the mouse colony at UC Berkeley (Data not shown). Thus, I decided to test the IL-10 pathway in B6.SJL* mice before embarking on more complicated genetic analyses, such as crosses and genome sequencing approaches. I generated Bone-marrow derived macrophages (BMMs) from B6 and B6.SJL* mice, and tested their ability to respond to and produce interleukin 10 (IL-10). B6.SJL* BMMs responded similarly to B6 BMMs as measured by STAT3 phosphorylation (Y705) upon stimulation with recombinant IL-10 (Figure 5.4A and B). Importantly, LPS and PamC3SK4, TLR2 and TLR4 ligands respectively, were able to induce IL-10 protein production by both B6 and B6.SJL* BMMs (Figure 5.4C). Taken together, these data show that the IL-10 pathway is likely intact in B6.SJL* mice.

In order to establish the genetic basis of this phenotype, I decided to perform genetic analysis of B6.SJL* mice. I intercrossed B6.SJL* mice with B6 mice to generate F1 progeny (F1: first generation). Even if genetic, there could be contributions from the microbiota to this phenotype. For example, IL-10 deficient mice develop colitis that depends on the presence of *Helicobacter* spp. (*66*). The microbiota is thought to be acquired from the mothers, so I set up crosses with a B6.SJL* dam and a B6 sire, but

also crosses with a B6 dam and a B6.SJL* sire. I removed the sires from the cages before or soon after birth of the pups, to ensure that I was able to trace the microbiota back to a B6 or a B6.SJL* dam. An autosomal recessive form of inheritance would predict that none of the F1 mice would present with this phenotype. An X-linked autosomal recessive mutation would predict that only F1 males born to B6.SJL* dams would exhibit this phenotype. Given the incomplete penetrance of this phenotype in B6.SJL* mice, interpretations about numbers or percentages of mice with a given phenotype become more complicated. Thus, in the X-linked recessive scenario, only some of the F1 males born to B6.SJL* dams would present the phenotype. Dominant forms of inheritance would predict that the phenotype would be present in the F1 generation with similar prevalence as in B6.SJL* mice. Of course, this could be complicated by the fact that the microbiota could be a contributor. Consequently, I included F1 mice born to different dams as described above, and carried these separate lines of F1 mice into the second generation after sibling inbreeding F1 mice.

Comparing 4 month-old F1 mice to age-matched B6 and B6.SJL* controls revealed that none of the 20 F1 mice analyzed so far presented this phenotype (Figure 5.5A). Interestingly, analysis of Th1 cells in the blood may be sufficient to detect this phenotype, although the sensitivity was lower than in the spleen or mLNs (Figure 5.5B). Performing adoptive transfers and analysis of intestinal tissues is not feasible for such large numbers of mice, so I restricted my readouts to the abundance endogenous Th1 cells. These results are so far consistent with an autosomal recessive form of inheritance.

Discussion:

The phenotype observed in B6.SJL* mice is likely to be due to a mutation in a gene that impacts immune regulation in the intestine, and perhaps also systemic sites. This mutation can impact T cell responses to the microbiota in a T cell-extrinsic manner, given my results with adoptive transfers of *A. muciniphila*-specific T cells. The exuberant expansion of Amuc124 transferred T cells in B6.SJL* mice suggests that *A. muciniphila* becomes a major mucosal antigen in this particular context. While I still don't know the mechanisms behind this phenotype, these striking observations would support the hypothesis that *A. muciniphila* is a major target of intestinal immune responses during inflammation. This effect could be mediated by its ability to take advantage of host-mediated effector functions, such as neutrophil-induced epithelial hypoxia and production of Muc3 by epithelial cells (*98*). If so, understanding the role of responses to *A. muciniphila* in contexts of inflammation and/or immune dysregulation could shed light into the pathogenesis of IBD.

Importantly, the observed T cell expansion in B6.SJL* mice occurs upon adoptive transfer. It remains possible that endogenous responses to *A. muciniphila* and other commensals don't mirror these striking results. The large accumulation of transferred T cells likely result from the mutation in an immunoregulatory gene, since the same effect is not observed in B6 mice. However, the slightly larger precursor frequency of transferred T cells, as well as the "acute" nature of a T cell transfer may constitute artifacts that contribute to this striking expansion observed at the 12-day timepoint. Thus, it will be important to analyze the endogenous *A. muciniphila*-specific T cell populations in these mice.

The hypothesis that this phenotype is a result of different microbiota composition between B6 and B6.SJL* mice is not supported by the data: neither cohousing or fecal microbiota transplant were able to transfer the phenotype. Thus, I designed experiments to establish a genetic basis. The results from the F1 cohort suggest that an autosomal-recessive mutation is responsible. I have established crosses between F1 mice, keeping the two F1 mouse lines separate (B6 or B6.SJL* dam), and will analyze F2 progeny once they reach the appropriate age where the phenotype is prevalent enough to detect. An autosomal recessive mode of inheritance would predict that 25% of the F2 progeny would present this phenotype. An X-linked recessive mode of inheritance is not supported by my F1 data (see above).

B6 and B6.SJL mice have been diverging for more than 55 generations at Jackson laboratories, plus an additional 10-20 generations at UC Berkeley since they were obtained in the lab. Before arriving at Jackson labs, SJL mice were backcrossed to B6 mice for 22 generations to generate the congenic B6.SJL strain. Thus, there may be additional polymorphisms between B6 and B6.SJL* mice that are unrelated to the causative mutation for this phenotype. Once I have identified F2 mice that present with increased Th1 cells and thus presumably carry the mutation, I will perform whole genome sequencing of >5 mice. Bulk segregate analysis (*128*) will allow me to identify the causative mutations from other segregating polymorphisms in B6.SJL* mice: any

polymorphism that is fixed in every single F2 mouse that presents this phenotype is a likely candidate for the causative mutation, while any irrelevant polymorphisms between B6 and B6.SJL* mice will segregate randomly in my F2 crosses, and their chance of being homozygous in every single F2 mouse that presents this phenotype will be very small. For this analysis, higher number of sequenced mice will increase my statistical power to identify the causative mutation.

Methods:

Animals:

Mice were housed under specific-pathogen-free (SPF) or gnotobiotic conditions at UC Berkeley. Mice were analyzed between 2.5 and 4.5 months of age. 4 months of age was selected as a minimum age to analyze F1 and F2 mice (Figure 5.5). C57BL/6J mice were used as wild-type mice. B6.SJL* mice consist of congenic C57BL/6J.SJL (B6.SJL-*Ptprc*^{a} *Pepc*^{b}/BoyJ) mice housed at UC Berkeley for several years (at least since early 2010s).

For experiments with Ex Germ-free mice, germ-free mice were removed from their isolators and gavaged with 0.2mL NaHCO3 5-10% w/v to neutralize stomach acid . Intestinal contents from B6 or B6.SJL* mice were collected in PBS, homogenized mechanically, filtered through a 40um filter and 0.3mL were gavaged into germ-free mice. Germ-free mice were subsequently housed under SPF conditions at UC Berkeley.

Cell isolation:

Cells from mesenteric lymph nodes, Peyer's patches (including cecal patch), spleen and thymus were isolated by mechanical dissociation on a 70-μm filter. Cells from small intestine lamina propria (after removal of Peyer's patches) and large intestine lamina propria (cecum and colon, after removal of cecal patch) were cut longitudinally after removing excess adipose tissue, washed in PBS and incubated at 37ºC for 20 min with stirring in Hank's balanced salt solution (HBSS) with 1 mM DTT, 10% (v/v) FBS, penicillin–streptomycin and HEPES. Intestines were then incubated at 37ºC for 25 min with stirring in HBSS with 1.3 mM EDTA, penicillin–streptomycin and HEPES, with further dissociation of epithelial cells in 10 mL PBS by shaking. Tissues were digested in RPMI with collagenase VIII (1 mg/mL, Sigma), DNaseI (5 μg/mL, Sigma), penicillin–streptomycin and HEPES for 45 min, and lymphocytes were collected at the interface of a 44%/67% Percoll gradient (GE Healthcare).

Cells from the blood were collected into 500uL PBS with heparin, washed in PBS and resuspended in ACK red blood cell lysis buffer. After two rounds of ACK lysis, cells were resuspended in PBS.

T cell adoptive transfers:

Peripheral lymph nodes and spleen of *A. muciniphila*-negative Amuc124 TCR transgenic Thy1.1 mice were dissociated mechanically on a 70-μm filter. Naïve CD4 T cells ($CD3^{+}$ $CD4^{+}$ $CD62L^{+}$ $CD44^{lo}$) were sorted on a BD FACSAria Fusion cell sorter and 10,000 cells were transferred by retro-orbital injection into recipient mice (Thy1.2). Recipient mice were analyzed 12 days post adoptive T cell transfer.

Flow cytometry and sorting:

Cells were isolated as described above and stained in a 96-well U-bottom plate. Dead cells were excluded with a fixable Near-IR or Aqua live/dead dye (Life technologies) in PBS. Surface staining was performed in PBS with 2% FBS (v/v), 1 mM EDTA and 0.1% NaN_3 for 30 min at 4ºC, or for 1 h at room temperature (RT) when staining for CXCR5 (no NaN_3). Staining with tetramers was performed for 30' at 37C in the presence of 50 nM Dasatinib (Sigma), followed by an additional 30' at RT. Anti-CXCR5 antibodies were included in this tetramer staining step, and the rest of surface staining was performed in a subsequent step for 30' at 4˚C. Intracellular transcription factor staining (eBioscience buffer set, ThermoFisher) was performed by fixation for 1 h at RT and staining for 40 min at RT. Samples were analyzed on a BD LSR Fortessa or a BD LSR Fortessa X-20. The list of antibodies used can be found in Table S1.

Stimulation of Bone marrow-derived macrophages (BMMs):

Femur and tibias from B6 or B6.SJL* mice were harvested, washed in ethanol and smashed with mortar and pestle in RPMI-5 (RPMI with 5% v/v Fetal bovine serum, L-glutamine, HEPES and penicillin/streptomycin (Invitrogen)). Bone marrow samples were treated with ACK buffer to lyse red blood cells, and plated on 15cm non-tissue culture-treated plates in RPMI-10 with M-CSF. At Day 3 the media was changed, and at day 7 cells were scraped with cold PBS and replated in RPMI-10 onto 96-well plates with 100,000 cells/well and left overnight in the 37C incubator. The next day, cells were stimulated with recombinant mouse IL-10 (Tonbo), Lipopolysaccharide (Invitrogen) or PamC3SK4 (Invitrogen).

Measurement of cytokine production by stimulated BMMs:

IL-10 cytokine production was measured in the supernatants with a Cytometric Bead Array (BD 552364) according to manufacturer's instructions.

Detection of STAT3 Y705 phosphorylation by flow cytometry:

BMMs were stimulated with recombinant mouse IL-10 (Tonbo) for 10-15 minutes in RPMI-10 at 37C. PFA was added at 1.6% final concentration to immediately fix the samples, and samples were incubated at room temperature for 10-15 minutes. Samples were pelleted, resuspended in ice-cold methanol and incubated overnight at -20C. Samples were washed and resuspended in FACS buffer with Fc Block and pSTAT3-Y705 antibody (clone 13A3).

Quantification and statistical analysis:

Statistical tests were performed as indicated on the figure legends with Prism 8 software (Graphpad Prism).

Figures:

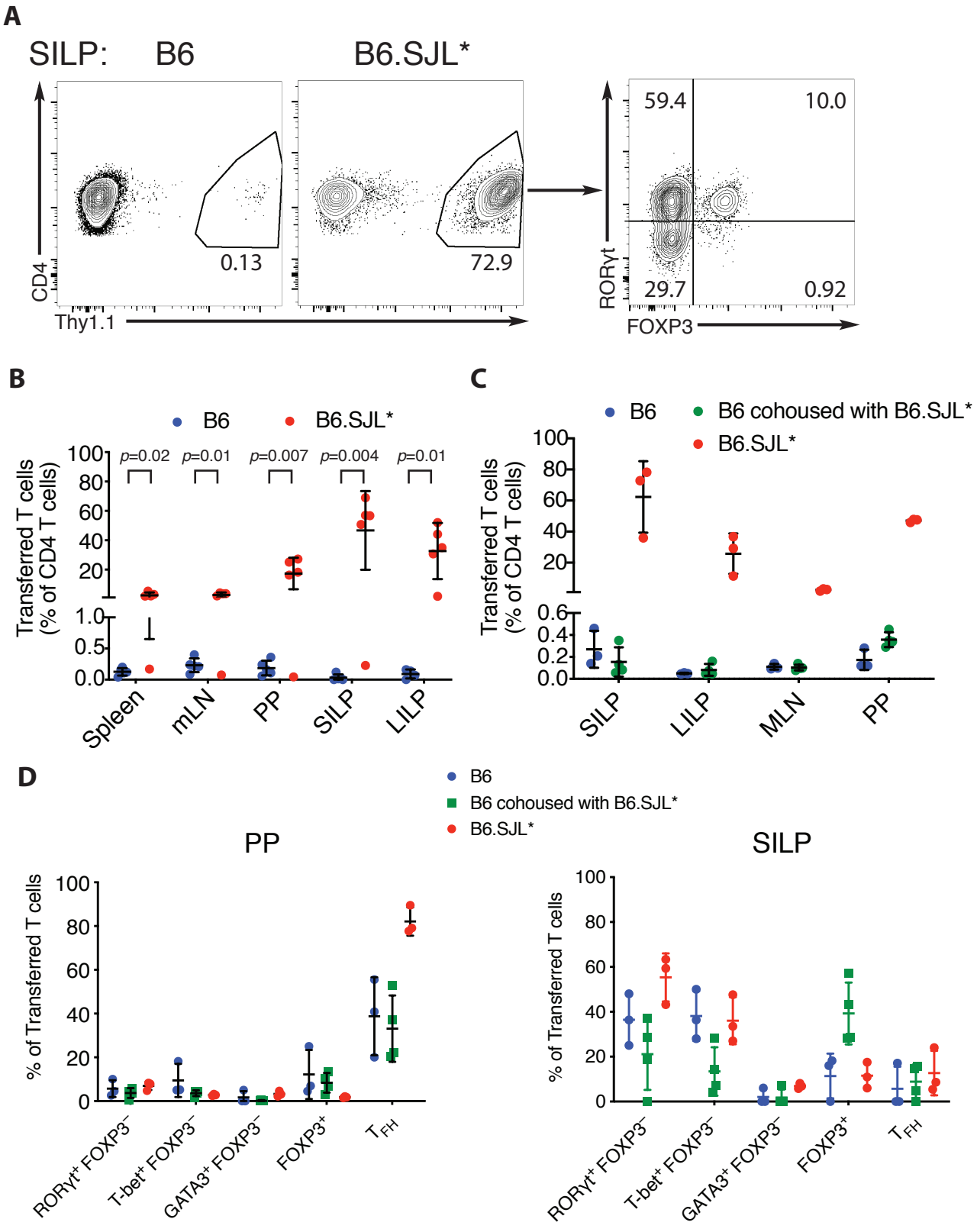
A
SILP: B6
B6.SJL*
CD4
Thy1.1
0.13
72.9
RORγt
FOXP3
59.4
10.0
29.7
0.92
B
B6
B6.SJL*
Transferred T cells (% of CD4 T cells)
p=0.02
p=0.01
p=0.007
p=0.004
p=0.01
Spleen
mLN
PP
SILP
LILP
C
B6
B6 cohoused with B6.SJL*
B6.SJL*
Transferred T cells (% of CD4 T cells)
SILP
LILP
MLN
PP
D
B6
B6 cohoused with B6.SJL*
B6.SJL*
PP
SILP
% of Transferred T cells
RORγt+ FOXP3−
T-bet+ FOXP3−
GATA3+ FOXP3−
FOXP3+
TFH

Figure 5.1: Exuberant activation and expansion of Amuc124 T cells in B6.SJL* mice

(**A**) Representative FACS plots depicting transferred Amuc124 T cells (Thy1.1$^+$) as a percentage of all CD4 T cells in B6 (Wild-Type) and B6.SJL* mice. (left) and transcription factor expression in B6.SJL* mice (right) in the SILP 12 days post adoptive transfer.

(**B**) Frequencies of transferred T cells as percentage of all CD4$^+$ T cells in intestinal tissues of B6 and B6.SJ* mice (n=5 mice per group) 12 days post adoptive transfer. Data are representative of three independent experiments.

(**C**) Frequencies of transferred T cells as percentage of all CD4$^+$ T cells in intestinal tissues of B6 mice, B6 mice cohoused with B6.SJ* mice, and B6.SJL* mice (Also cohoused with B6 mice) 12 days post adoptive transfer. n=3-4 mice per group.

(**D**) Expression of T_H1 (T-bet$^+$ FOXP3$^-$), T_H2 (GATA3$^+$ FOXP3$^-$), T_H17 (RORγt$^+$ FOXP3$^-$), T_{reg} (FOXP3$^+$) or T_{FH} (Bcl6$^+$ PD-1$^+$) markers by transferred T cells in intestinal tissues of B6, B6 cohoused with B6.SJL* or B6.SJL* mice (cohoused with B6)

Each symbol represents a mouse, error bars represent mean ± SD. *p*-values were calculated with unpaired Student's *t*-tests (D).

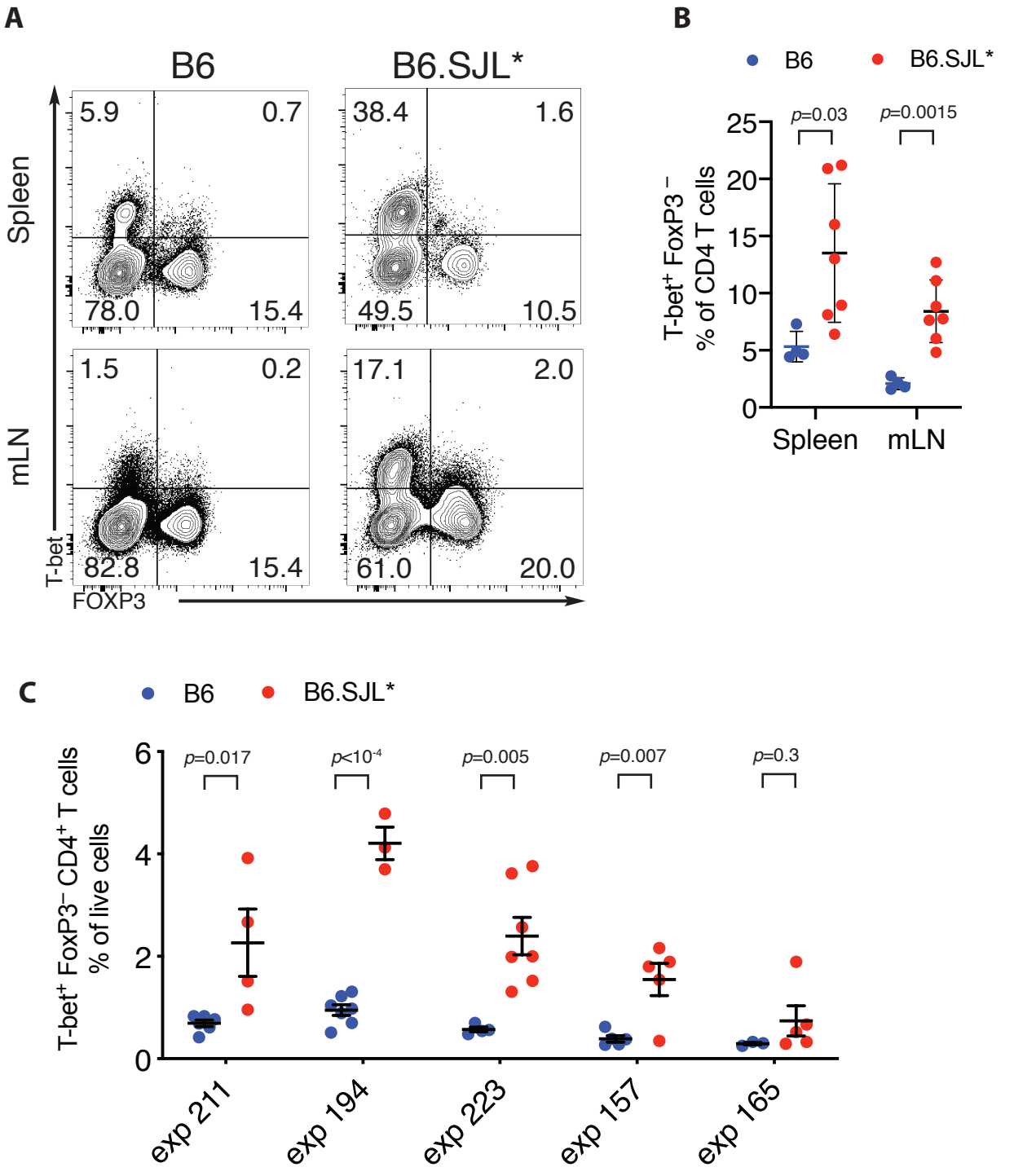

Figure 5.2: B6.SJL* mice induce aberrant Th1 responses
(**A**) Representative FACS plots depicting T_H1 (T-bet$^+$ FOXP3$^-$) CD4$^+$ T cells in the spleens and mLNs of B6 and B6.SJL* mice.
(**B**) Frequencies of T_H1 (T-bet$^+$ FOXP3$^-$) as percentage of all CD4$^+$ T cells in the spleens and mLNs of B6 and B6.SJL* mice. Data are representative of five independent experiments.

(**C**) Frequencies of T_H1 (T-bet$^+$ FOXP3$^-$) as percentage of all live cells in the mLNs of B6 and B6.SJL* mice. Data are shown for five independent experiments.
Each symbol represents a mouse, error bars represent mean ± SD. *p*-values were calculated with unpaired Student's *t*-tests.

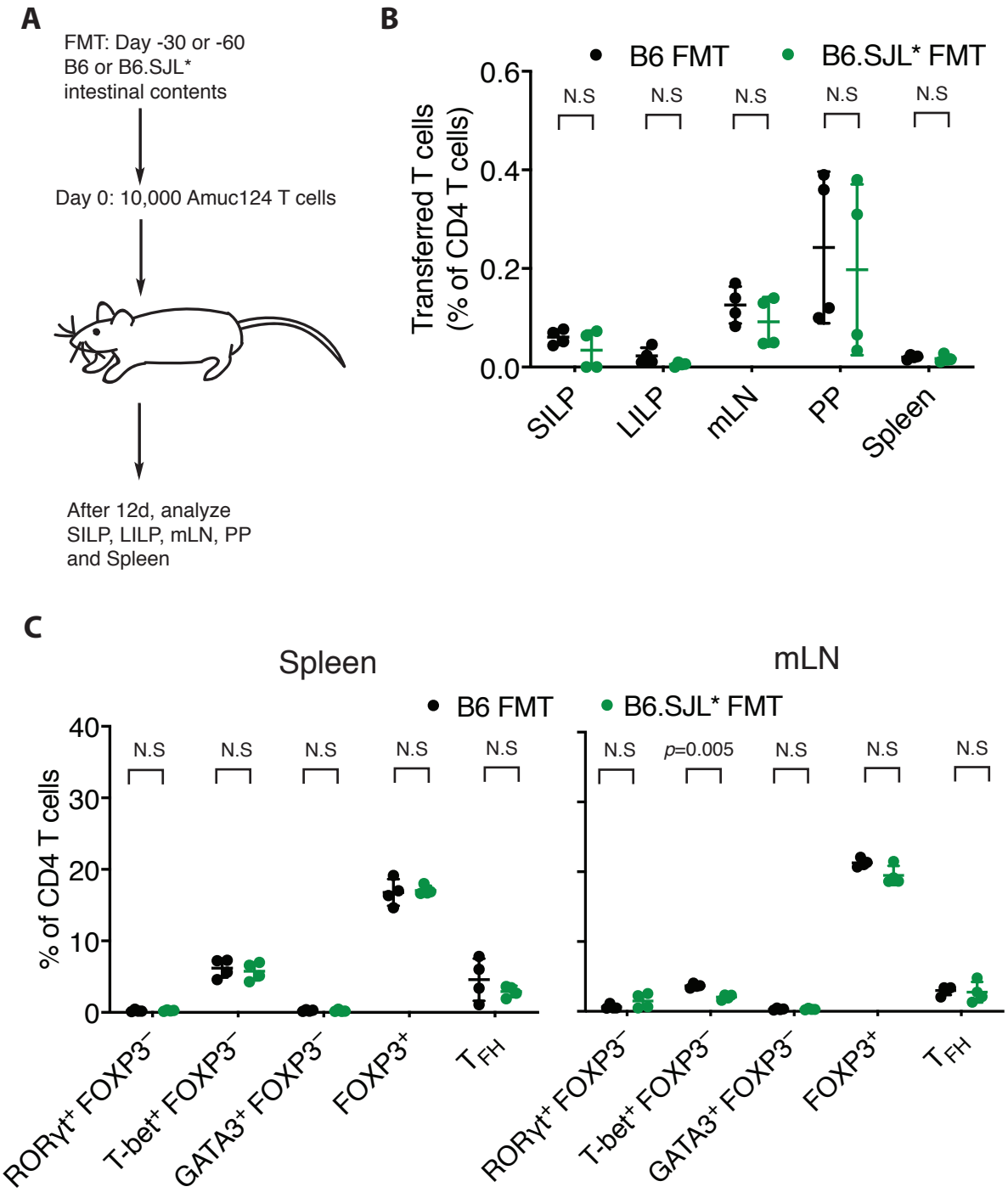

Figure 5.3: Fecal microbiota transplant into Germ-free mice fails to transfer the B6.SJL* phenotype

(**A**) Experimental design of fecal microbiota transplants into Germ-free (GF) mice. Intestinal contents from B6 or B6.SJL* mice were orally gavaged into GF mice. After 30 days (repeat 1) or 60 days (repeat 2), 10,000 naïve Amuc124 TCR transgenic T cells were transferred and analyzed 12 days later.

(**B**) Frequencies of transferred T cells as percentage of all $CD4^+$ T cells in intestinal tissues of B6 and B6.SJL* mice (n=4 mice per group) 12 days post adoptive transfer. Data are representative of two independent experiments.
(**C**) Frequencies of T_H1 ($T\text{-}bet^+$ $FOXP3^-$) as percentage of all live cells in the mLNs of B6 and B6.SJL* mice. n=4 mice per group, data are representative of two independent experiments.
Each symbol represents a mouse, error bars represent mean ± SD. *p*-values were calculated with unpaired Student's *t*-tests.

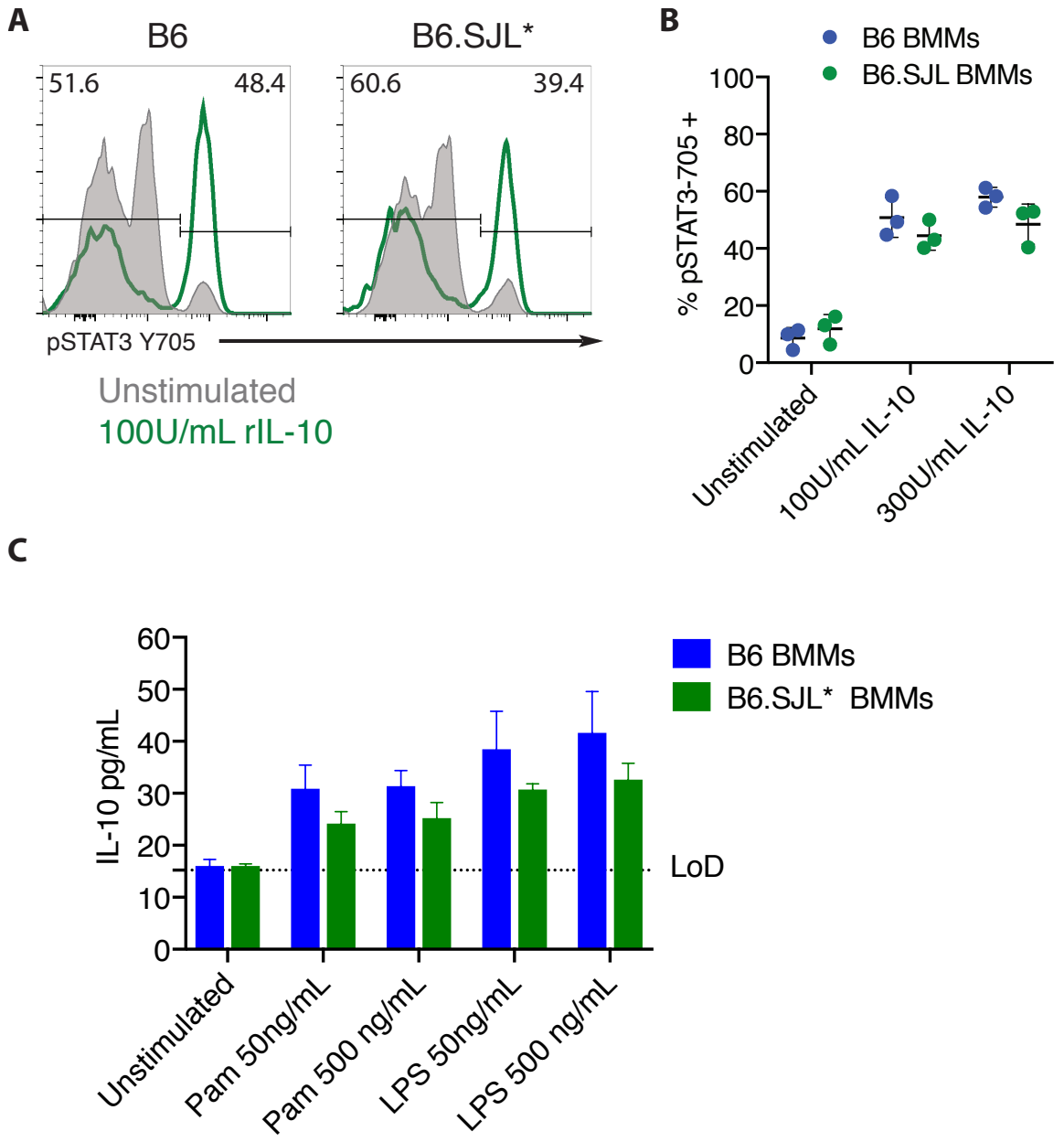

Figure 5.4: Cells derived from B6.SJL* mice are able to produce IL-10 and respond to IL-10 stimulation

(**A**) Representative FACS plots depicting STAT3 phosphorylation (Y705) upon stimulation of bone marrow-derived macrophages (BMMs) from B6 and B6.SJL* mice with recombinant mouse IL-10 (rIL-10)

(**B**) Frequencies of B6 and B6.SJL* BMMs with phosphorylated STAT3 (Y705) upon stimulation with mouse rIL-10. n=3 samples, each with BMMs from a different mouse.

(**C**) Production of IL-10 by B6 and B6.SJL* BMMs upon Pam3CSK4 or lipopolysaccharide (LPS) stimulation, as measured by CBA analysis. n=3 samples, each with BMMs from a different mouse.

Error bars represent mean ± SD.

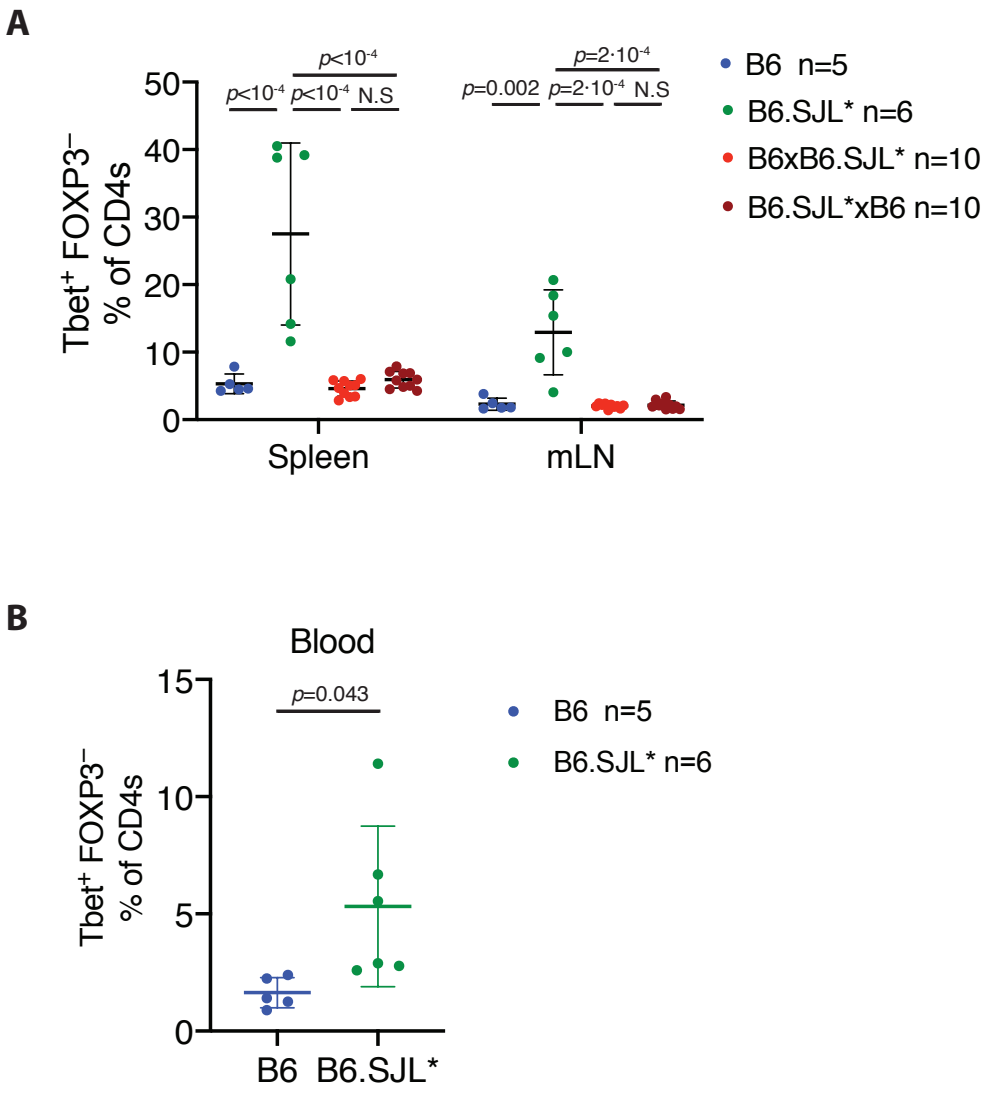

Figure 5.5: Genetic analysis of the B6.SJL* phenotype
(**A**) Percentage of CD4+ T cells expressing Th1 markers (T-bet+ FOXP3−) in 4 month old F1 mice derived from crossing B6.SJL* and C57BL/6J mice. F1 mice born to a B6 dam (red) or a B6.SJL* dam (brown) were kept separately.
(**B**) Percentage of CD4+ T cells expressing Th1 markers (T-bet+ FOXP3−) in the blood of B6 and B6.SJL* mice (same mice as in (A) a week earlier).
Error bars represent mean ± SD. *p*-values were calculated with one-way ANOVA with Sidak correction for multiple comparisons (A) or a Mann-Whitney test (B).

Chapter 6: Concluding remarks

Homeostatic adaptive immune responses to the microbiota are emerging as key players in the interaction between commensal microbes and the host (*12*). In the gut, select known commensal bacteria induce T-dependent antibodies and cognate T cell responses during homeostasis (*22*, *59*, *65*), while the majority of other commensal species are targeted by T-independent mechanisms (*36*). Dysregulation of antibody and T cell responses to the intestinal microbiota lead to inflammation and Inflammatory bowel diseases (*15*, *75*). Thus, understanding which commensal bacteria induce cognate adaptive responses and unveiling the signals and cell types involved in their induction and regulation remain key important questions. These questions, if answered, would shed light into basic mechanisms of host-microbiota symbiosis and the etiology of IBD.

Despite the large abundance of foreign antigens and frequencies of activated lymphocytes present in the intestine, very few commensal bacteria have been identified that induce cognate T cell and B cell responses during homeostasis. One possibility is that adaptive responses to commensals are limited to select immunostimulatory bacteria that exhibit certain functions, such as occupation of an epithelial-associated niche, interactions with epithelial cells, sampling through particular routes etc. If so, identifying these bacteria and characterizing cognate adaptive immune responses would be of utmost importance to the field. This first scenario is supported by the fact that existing examples of T cell-inducing intestinal bacteria are limited to a pathobiont, *Helicobacter* spp., and Segmented filamentous bacteria (SFB), an immunostimulatory commensal which burrows itself into epithelial cells and induces a robust Th17 response.

Another possibility is that a large fraction of commensal bacteria is targeted by cognate adaptive immune responses, but that only a few examples have been identified so far. This second scenario is not supported by the existing data comparing IgA-Seq in T cell-deficient and -sufficient mice (*35*), although this approach cannot identify bacteria that are highly bound by both TI and TD IgA. My IgG1-seq results identify only a few bacteria that induce T-dependent IgG1, which would not support this second scenario.

However, even if only select commensal bacteria are recognized by the adaptive immune system during homeostasis, it is unlikely that these responses are limited to SFB and *Helicobacter* spp. In fact, other intestinal bacteria from humans are sufficient to induce intestinal Th17 cells in the intestine in a gnotobiotic setting (*129*), although the antigen-specificity wasn't explored. Thus, identifying novel commensal bacteria that induce cognate adaptive immune responses during homeostasis remains an important task.

Here I have identified *A. muciniphila* as a commensal microbe that induces T-dependent IgG1 and IgA antibody responses as well as cognate intestinal T cell responses during homeostasis. The results from the IgG1-sequencing experiments

show that a few other commensal bacteria, such as a specific species within the *Muribaculaceae* family (also named Bacteroides S24-7), induce similar TD antibody responses. These high affinity local (IgA) and systemic (IgG1) antibody responses against *A. muciniphila* and *Muribaculaceae* spp. are likely to contribute to the important roles attributed to commensal-specific antibodies, such as protection from gut-derived septicemia (*42*, *74*) and education of the neonatal immune system (*41*, *72*). However, they may also contribute to disease pathogenesis in genetically susceptible people and mice through engagement of activating Fc receptors (*75*).

Interestingly, antibody and T cell responses to *A. muciniphila* were variable across SPF mice. These results suggest that there may be complex interactions with other commensal microbes present in the intestine, such as competition for a particular niche, alteration of the function of *A. muciniphila* based on the presence of other commensals, existence of bystander signals arising from other commensals etc. However, *A. muciniphila* was sufficient to induce cognate high affinity IgG1 and IgA antibodies in gnotobiotic mice colonized with the ASF microbiota. In this setting, T cell responses to *A. muciniphila* were also very reproducible and consisted of T follicular helper cells in the Peyer's patches. These results show that *A. muciniphila* engages the immune system directly, is sampled during homeostasis, and induces cognate adaptive immune responses.

T cell immunity to *A. muciniphila* was different than T cell responses to SFB or *Helicobacter* spp. *A. muciniphila* is the first example of a commensal bacterium that induces a response largely dominated by T_{FH} cells, with the absence of other T effector fates. Surprisingly, T cell immunity to *A. muciniphila* changed in the context of a conventional microbiota: adoptive transfers into SPF mice led to induction of *A. muciniphila*-specific Th1, Th17 and Treg responses that homed to the small intestine and large intestine lamina propria. Importantly, T cell skewing varied across mice and experiments. These results are consistent with the variable IgG1 and IgA antibody responses observed in SPF mice, and argue that responses to this commensal bacterium can be altered depending on contextual signals. Whether this is a general feature of commensal-specific T cell responses or a feature specific to *A. muciniphila* remains to be determined, since the other two examples of cognate T cell responses to a commensal do not exhibit this variability: T cell responses to SFB consist of Th17 both in monocolonized and SPF settings, and *Helicobacter* spp. induce $ROR\gamma t^{+}$ $FOXP3^{+}$ Treg cells in SPF mice.

Importantly, *A. muciniphila* is associated with protective effects in metabolic disease and in PD-1 cancer immunotherapy (*92*, *93*, *100*), among others. The mechanisms for these effects on host physiology remain elusive, but these effects involved $IFN\gamma$ and type-I immunity to *A. muciniphila,* respectively. In fact, protection from cancer immunotherapy in people correlated with peripheral Th1 cell responses to *A. muciniphila* antigens. My work provides a potential explanation for this correlation: if T cell immunity to *A. muciniphila* is similarly variable in humans, then perhaps only

patients with pre-existing Th1 immunity to this bacterium will benefit from the protective effects of this commensal upon PD-1 cancer immunotherapy.

While immune responses are likely to underlie many aspects of the interaction between these commensal bacteria and the host, other non-immune mechanisms should also be considered. Production of metabolites by commensal microbes is known to impact host physiology, such as induction of Treg cells (*8–10*) and colonization resistance (*130*), among others. T cell-inducing bacteria occupy niches that are in direct contact with host cells, and tend to be very abundant at these locations. Thus, metabolites derived from these commensal bacteria may preferentially impact host physiology locally but also at systemic sites. Indeed, *A. muciniphila*-derived nicotinamide has been shown to influence disease progression in mouse models of Amyotrophic Lateral Sclerosis (*97*).

Finally, T cell immunity to *A. muciniphila* changes dramatically in a specific mouse line identified in my laboratory (B6.SJL* mice). This mouse line likely carries a mutation in an immunoregulatory gene that impacts immunity to this bacterium in a T cell-extrinsic manner. While the nature of the mutation remains to be determined, the exuberant responses observed in this mouse line suggest that *A. muciniphila* becomes a major mucosal antigen in the context of inflammation, which could be mediated by its ability to colonize the healing epithelial mucosa. This would suggest that adaptive immunity to *A. muciniphila* may play critical roles during infection, inflammation and disease.

In summary, I have identified *A. muciniphila* as a novel commensal bacterium that induces antibody and T cell responses during homeostasis. Responses to *A. muciniphila* include TD IgG1 and IgA, as well as T_{FH} cells but also other T helper fates in conventional mice. Immunity to *A. muciniphila* can be shaped by contextual signals, and may underlie some of the systemic effects of this bacterium. Finally, *A. muciniphila* may become a major mucosal antigen during inflammation. Much work remains to understand the interactions between this bacterium and the host: How is this bacterium sensed? Which antigen-presenting cells are involved in this response? Why does it elicit adaptive immune responses? Are there other commensal bacteria with similar responses? How do antibody and T cell responses to *A. muciniphila* impact homeostasis and disease? Do T cell responses to *A. muciniphila* mediate protection against metabolic disease or influence cancer immunotherapy? If so, what are the mechanisms? What is the nature of B6.SJL* mice, and what is the fate and role of *A. muciniphila*-specific T cells induced in the context of inflammation? These questions will undoubtedly be explored in future scientific inquiry.

References:

1. S. H. E. Kaufmann, Immunology's foundation: The 100-year anniversary of the Nobel Prize to Paul Ehrlich and Elie Metchnikoff. *Nat. Immunol.* **9** (2008), pp. 705–712.
2. C. a Janeway, R. Medzhitov, Innate immune recognition. *Annu. Rev. Immunol.* **20**, 197–216 (2002).
3. Y. Belkaid, T. W. Hand, Role of the microbiota in immunity and inflammation. *Cell*. **157** (2014), pp. 121–141.
4. K. Endt, B. Stecher, S. Chaffron, E. Slack, N. Tchitchek, *et al.*, The microbiota mediates pathogen clearance from the gut lumen after non-typhoidal Salmonella diarrhea. *PLoS Pathog.* **6**, e1001097 (2010).
5. N. Kamada, G. Y. Chen, N. Inohara, G. Núñez, Control of pathogens and pathobionts by the gut microbiota. *Nat. Immunol.* **14**, 685–690 (2013).
6. A. J. Baümler, V. Sperandio, Interactions between the microbiota and pathogenic bacteria in the gut. *Nature*. **535** (2016), pp. 85–93.
7. S. Caballero, S. Kim, R. A. Carter, I. M. Leiner, B. Sušac, *et al.*, Cooperating Commensals Restore Colonization Resistance to Vancomycin-Resistant Enterococcus faecium. *Cell Host Microbe*. **21**, 592–602.e4 (2017).
8. Y. Furusawa, Y. Obata, S. Fukuda, T. a Endo, G. Nakato, *et al.*, Commensal microbe-derived butyrate induces the differentiation of colonic regulatory T cells. *Nature*. **504**, 446–50 (2013).
9. P. M. Smith, M. R. Howitt, N. Panikov, M. Michaud, C. A. Gallini, *et al.*, The microbial metabolites, short-chain fatty acids, regulate colonic Treg cell homeostasis. *Science*. **341**, 569–73 (2013).
10. N. Arpaia, C. Campbell, X. Fan, S. Dikiy, J. van der Veeken, *et al.*, Metabolites produced by commensal bacteria promote peripheral regulatory T-cell generation. *Nature*. **504**, 451–5 (2013).
11. L. V Hooper, D. R. Littman, A. J. Macpherson, M. P. Program, Interactions between the microbiota and the immune system. *Science (80-.).* **336**, 1268–1273 (2015).
12. Y. Belkaid, O. J. Harrison, Homeostatic Immunity and the Microbiota. *Immunity*. **46**, 562–576 (2017).
13. T. S. Stappenbeck, H. W. Virgin, Accounting for reciprocal host-microbiome interactions in experimental science. *Nature*. **534** (2016), pp. 191–199.
14. R. E. Vance, R. R. Isberg, D. A. Portnoy, Patterns of pathogenesis: discrimination of pathogenic and nonpathogenic microbes by the innate immune system. *Cell*

Host Microbe. **6**, 10–21 (2009).

15. R. B. Sartor, Mechanisms of disease: Pathogenesis of Crohn's disease and ulcerative colitis. *Nat. Clin. Pract. Gastroenterol. Hepatol.* **3** (2006), pp. 390–407.
16. R. Sender, S. Fuchs, R. Milo, Revised Estimates for the Number of Human and Bacteria Cells in the Body (2016), doi:10.1371/journal.pbio.1002533.
17. M. E. V Johansson, M. Phillipson, J. Petersson, A. Velcich, L. Holm, *et al.*, The inner of the two Muc2 mucin-dependent mucus layers in colon is devoid of bacteria. *Proc. Natl. Acad. Sci. U. S. A.* **105**, 15064–9 (2008).
18. A. J. MacPherson, E. Slack, M. B. Geuking, K. D. McCoy, The mucosal firewalls against commensal intestinal microbes. *Semin. Immunopathol.* **31**, 145–149 (2009).
19. L. R. Muniz, C. Knosp, G. Yeretssian, Intestinal antimicrobial peptides during homeostasis, infection, and disease. *Front. Immunol.* **3**, 310 (2012).
20. L. W. Peterson, D. Artis, Intestinal epithelial cells: regulators of barrier function and immune homeostasis. *Nat. Rev. Immunol.* **14**, 141–53 (2014).
21. S. Mukherjee, L. V Hooper, Review Antimicrobial Defense of the Intestine. **2** (2014).
22. J. J. Bunker, A. Bendelac, IgA Responses to Microbiota. *Immunity*. **49** (2018), pp. 211–224.
23. T. Cullender, B. Chassaing, A. Janzon, Innate and Adaptive Immunity Interact to Quench Microbiome Flagellar Motility in the Gut. *Cell host …*, 571–581 (2013).
24. G. P. Donaldson, M. S. Ladinsky, K. B. Yu, J. G. Sanders, B. B. Yoo, *et al.*, Gut microbiota utilize immunoglobulin A for mucosal colonization. *Science*. **360**, 795–800 (2018).
25. M. L. Balmer, E. Slack, A. de Gottardi, M. a E. Lawson, S. Hapfelmeier, *et al.*, *Sci. Transl. Med.*, in press, doi:10.1126/scitranslmed.3008618.
26. J. R. Grainger, E. a Wohlfert, I. J. Fuss, N. Bouladoux, M. H. Askenase, *et al.*, Inflammatory monocytes regulate pathologic responses to commensals during acute gastrointestinal infection. *Nat. Med.* **19**, 713–21 (2013).
27. M. J. Molloy, J. R. Grainger, N. Bouladoux, T. W. Hand, L. Y. Koo, *et al.*, Intraluminal containment of commensal outgrowth in the gut during infection-induced dysbiosis. *Cell Host Microbe*. **14**, 318–28 (2013).
28. N. Kamada, K. Sakamoto, S. U. Seo, M. Y. Zeng, Y. G. Kim, *et al.*, Humoral immunity in the gut selectively targets phenotypically virulent attaching-and-effacing bacteria for intraluminal elimination. *Cell Host Microbe*. **17**, 617–627 (2015).
29. R. Basu, D. B. O'Quinn, D. J. Silberger, T. R. Schoeb, L. Fouser, *et al.*, Th22 Cells Are an Important Source of IL-22 for Host Protection against

Enteropathogenic Bacteria. *Immunity*. **37**, 1061–1075 (2012).

30. J. M. Allaire, S. M. Crowley, H. T. Law, S.-Y. Chang, H.-J. Ko, *et al.*, The Intestinal Epithelium: Central Coordinator of Mucosal Immunity (2018), doi:10.1016/j.it.2018.04.002.

31. T. Joeris, K. Müller-Luda, W. W. Agace, A. M. I. Mowat, Diversity and functions of intestinal mononuclear phagocytes. *Mucosal Immunol.* **10** (2017), pp. 845–864.

32. G. Eberl, M. Colonna, J. P. Di Santo, A. N. J. McKenzie, Innate lymphoid cells. Innate lymphoid cells: a new paradigm in immunology. *Science*. **348**, aaa6566 (2015).

33. S. Rakoff-Nahoum, L. Hao, R. Medzhitov, Role of toll-like receptors in spontaneous commensal-dependent colitis. *Immunity*. **25**, 319–29 (2006).

34. L. Franchi, N. Kamada, Y. Nakamura, A. Burberry, P. Kuffa, *et al.*, NLRC4-driven production of IL-1β discriminates between pathogenic and commensal bacteria and promotes host intestinal defense. *Nat. Immunol.* **13**, 449–56 (2012).

35. J. J. Bunker, T. M. Flynn, J. C. Koval, D. G. Shaw, M. Meisel, *et al.*, Innate and Adaptive Humoral Responses Coat Distinct Commensal Bacteria with Immunoglobulin A. *Immunity*. **43**, 541–553 (2015).

36. J. J. Bunker, S. A. Erickson, T. M. Flynn, C. Henry, J. C. Koval, *et al.*, Natural polyreactive IgA antibodies coat the intestinal microbiota. *Science (80-.).* **358** (2017), doi:10.1126/science.aan6619.

37. C. Cunningham-Rundles, Physiology of IgA and IgA Deficiency. *J. Clin. Immunol.* **21**, 303–309 (2001).

38. N. W. Palm, M. R. De Zoete, T. W. Cullen, N. a Barry, J. Stefanowski, *et al.*, Immunoglobulin A coating identifies colitogenic bacteria in inflammatory bowel disease. *Cell*. **158**, 1000–1010 (2014).

39. E. Slack, S. Hapfelmeier, B. Stecher, Y. Velykoredko, M. Stoel, *et al.*, Innate and adaptive immunity cooperate flexibly to maintain host-microbiota mutualism. *Science (80-.).* **325**, 617–620 (2009).

40. A. J. Macpherson, K. D. McCoy, Stratification and compartmentalisation of immunoglobulin responses to commensal intestinal microbes. *Semin. Immunol.* **25**, 358–63 (2013).

41. M. A. Koch, G. L. Reiner, K. a Lugo, L. S. M. Kreuk, A. G. Stanbery, *et al.*, Maternal IgG and IgA Antibodies Dampen Mucosal T Helper Cell Responses in Early Life. *Cell*. **165**, 827–841 (2016).

42. M. Y. Zeng, D. Cisalpino, S. Varadarajan, J. Hellman, H. S. Warren, *et al.*, Gut Microbiota-Induced Immunoglobulin G Controls Systemic Infection by Symbiotic Bacteria and Pathogens. *Immunity*. **44**, 647–658 (2016).

43. G. Magri, L. Comerma, M. Pybus, J. Sintes, D. Lligé, *et al.*, Human Secretory IgM Emerges from Plasma Cells Clonally Related to Gut Memory B Cells and Targets

Highly Diverse Commensals. *Immunity*. **47**, 118–134.e8 (2017).

44. A. Iwasaki, R. Medzhitov, Regulation of adaptive immunity by the innate immune system. *Science*. **327**, 291–295 (2010).

45. K. S. Kim, S.-W. Hong, D. Han, J. Yi, J. Jung, *et al.*, Dietary antigens limit mucosal immunity by inducing regulatory T cells in the small intestine. *Science*. **351** (2016), doi:10.1126/science.aac5560.

46. M. B. Geuking, J. Cahenzli, M. a E. Lawson, D. C. K. Ng, E. Slack, *et al.*, Intestinal Bacterial Colonization Induces Mutualistic Regulatory T Cell Responses. *Immunity*. **34**, 794–806 (2011).

47. K. Gerlach, Y. Hwang, A. Nikolaev, R. Atreya, H. Dornhoff, *et al.*, TH9 cells that express the transcription factor PU.1 drive T cell–mediated colitis via IL-9 receptor signaling in intestinal epithelial cells. *Nat. Immunol.* **15** (2014), doi:10.1038/ni.2920.

48. M. G. Roncarolo, S. Gregori, R. Bacchetta, M. Battaglia, N. Gagliani, The Biology of T Regulatory Type 1 Cells and Their Therapeutic Application in Immune-Mediated Diseases. *Immunity*. **49** (2018), pp. 1004–1019.

49. N. Geva-Zatorsky, E. Sefik, L. Kua, L. Pasman, T. G. Tan, *et al.*, Mining the Human Gut Microbiota for Immunomodulatory Organisms. *Cell*. **168**, 928–943.e11 (2017).

50. E. Sefik, N. Geva-Zatorsky, S. Oh, L. Konnikova, D. Zemmour, *et al.*, MUCOSAL IMMUNOLOGY. Individual intestinal symbionts induce a distinct population of RORγ^{+} regulatory T cells. *Science*. **349**, 993–7 (2015).

51. K. Atarashi, T. Tanoue, T. Shima, A. Imaoka, T. Kuwahara, *et al.*, Induction of colonic regulatory T cells by indigenous Clostridium species. *Science*. **331**, 337–341 (2011).

52. K. Atarashi, T. Tanoue, K. Oshima, W. Suda, Y. Nagano, *et al.*, Treg induction by a rationally selected mixture of Clostridia strains from the human microbiota. *Nature*. **500**, 232–236 (2013).

53. T. G. Tan, E. Sefik, N. Geva-Zatorsky, L. Kua, D. Naskar, *et al.*, Identifying species of symbiont bacteria from the human gut that, alone, can induce intestinal Th17 cells in mice. *Proc. Natl. Acad. Sci. U. S. A.*, 201617460 (2016).

54. A. M. Farkas, C. Panea, Y. Goto, G. Nakato, M. Galan-Diez, *et al.*, Induction of Th17 cells by segmented filamentous bacteria in the murine intestine. *J. Immunol. Methods*. **421**, 104–111 (2015).

55. K. Atarashi, W. Suda, C. Luo, T. Kawaguchi, I. Motoo, *et al.*, Ectopic colonization of oral bacteria in the intestine drives T H 1 cell induction and inflammation. *Science (80-.).* **358**, 359–365 (2017).

56. T. Tanoue, S. Morita, D. R. Plichta, A. N. Skelly, W. Suda, *et al.*, A defined commensal consortium elicits CD8 T cells and anti-cancer immunity. *Nature*. **565**

(2019), doi:10.1038/s41586-019-0878-z.

57. I. I. Ivanov, R. D. L. Frutos, N. Manel, K. Yoshinaga, D. B. Rifkin, *et al.*, Specific microbiota direct the differentiation of IL-17-producing T-helper cells in the mucosa of the small intestine. *Cell Host Microbe*. **4**, 337–49 (2008).

58. I. I. Ivanov, K. Atarashi, N. Manel, E. L. Brodie, T. Shima, *et al.*, Induction of intestinal Th17 cells by segmented filamentous bacteria. *Cell*. **139**, 485–98 (2009).

59. Y. Yang, M. B. Torchinsky, M. Gobert, H. Xiong, M. Xu, *et al.*, Focused specificity of intestinal TH17 cells towards commensal bacterial antigens. *Nature*. **510**, 152–156 (2014).

60. Y. Goto, C. Panea, G. Nakato, A. Cebula, C. Lee, Segmented Filamentous Bacteria Antigens Presented by Intestinal Dendritic Cells Drive mucosal Th17 cell differentiation. *Immunity* (2014) (available at http://www.sciencedirect.com/science/article/pii/S1074761314000855).

61. C. Panea, A. M. Farkas, Y. Goto, S. Abdollahi-Roodsaz, C. Lee, *et al.*, Intestinal Monocyte-Derived Macrophages Control Commensal-Specific Th17 Responses. *Cell Rep.* **12**, 1314–1324 (2015).

62. S. K. Lathrop, S. M. Bloom, S. M. Rao, K. Nutsch, C.-W. Lio, *et al.*, Peripheral education of the immune system by colonic commensal microbiota. *Nature*. **478**, 250–4 (2011).

63. K. Nutsch, J. N. Chai, T. L. Ai, E. Russler-Germain, T. Feehley, *et al.*, Rapid and Efficient Generation of Regulatory T Cells to Commensal Antigens in the Periphery. *Cell Rep.* **17**, 206–220 (2016).

64. J. N. Chai, Y. Peng, S. Rengarajan, B. D. Solomon, T. L. Ai, *et al.*, *Helicobacter* species are potent drivers of colonic T cell responses in homeostasis and inflammation. *Sci. Immunol.* **2**, eaal5068 (2017).

65. M. Xu, M. Pokrovskii, Y. Ding, R. Yi, C. Au, *et al.*, C-MAF-dependent regulatory T cells mediate immunological tolerance to a gut pathobiont. *Nature*. **554**, 373–377 (2018).

66. M. C. Kullberg, J. M. Ward, P. L. Gorelick, P. Caspar, S. Hieny, *et al.*, Helicobacter hepaticus triggers colitis in specific-pathogen-free interleukin-10 (IL-10)-deficient mice through an IL-12- and gamma interferon-dependent mechanism. *Infect. Immun.* **66**, 5157–66 (1998).

67. S. R. Targan, C. J. Landers, H. Yang, M. J. Lodes, Y. Cong, *et al.*, Antibodies to CBir1 Flagellin Define a Unique Response That Is Associated Independently With Complicated Crohn's Disease (2005), doi:10.1053/j.gastro.2005.03.046.

68. Y. Cong, T. Feng, K. Fujihashi, T. R. Schoeb, C. O. Elson, A dominant, coordinated T regulatory cell-IgA response to the intestinal microbiota. *Proc. Natl. Acad. Sci. U. S. A.* **106**, 19256–61 (2009).

69. T. W. Hand, L. M. Dos Santos, N. Bouladoux, M. J. Molloy, A. J. Pagán, *et al.*, Acute gastrointestinal infection induces long-lived microbiota-specific T cell responses. *Science (80-.).* **337**, 1553–1556 (2012).

70. Y. Belkaid, N. Bouladoux, T. W. Hand, Effector and memory T cell responses to commensal bacteria. *Trends Immunol.* **34**, 299–306 (2013).

71. E. Ansaldo, L. C. Slayden, K. L. Ching, M. A. Koch, N. K. Wolf, *et al.*, Akkermansia muciniphila induces intestinal adaptive immune responses during homeostasis. *Science*. **364**, 1179–1184 (2019).

72. M. Gomez de Aguero, S. C. Ganal-Vonarburg, T. Fuhrer, S. Rupp, Y. Uchimura, *et al.*, The maternal microbiota drives early postnatal innate immune development. *Science (80-.).* **351**, 1296–1302 (2016).

73. D. Kirkland, A. Benson, J. Mirpuri, R. Pifer, B. Hou, *et al.*, B cell-intrinsic MyD88 signaling prevents the lethal dissemination of commensal bacteria during colonic damage. *Immunity*. **36**, 228–38 (2012).

74. J. R. Wilmore, B. T. Gaudette, D. Gomez Atria, T. Hashemi, D. D. Jones, *et al.*, Commensal Microbes Induce Serum IgA Responses that Protect against Polymicrobial Sepsis. *Cell Host Microbe*. **23**, 302–311.e3 (2018).

75. T. Castro-Dopico, T. W. Dennison, J. R. Ferdinand, R. J. Mathews, A. Fleming, *et al.*, Anti-commensal IgG Drives Intestinal Inflammation and Type 17 Immunity in Ulcerative Colitis. *Immunity*. **0** (2019), doi:10.1016/j.immuni.2019.02.006.

76. K. Suzuki, B. Meek, Y. Doi, M. Muramatsu, T. Chiba, *et al.*, Aberrant expansion of segmented filamentous bacteria in IgA-deficient gut. *Proc. Natl. Acad. Sci. U. S. A.* **101**, 1981–6 (2004).

77. A. J. Macpherson, D. Gatto, E. Sainsbury, G. R. Harriman, H. Hengartner, *et al.*, A primitive T cell-independent mechanism of intestinal mucosal IgA responses to commensal bacteria. *Science (80-.).* **288**, 2222–2226 (2000).

78. F. Fransen, E. Zagato, E. Mazzini, B. Fosso, C. Manzari, *et al.*, BALB/c and C57BL/6 Mice Differ in Polyreactive IgA Abundance, which Impacts the Generation of Antigen-Specific IgA and Microbiota Diversity. *Immunity*. **43**, 527–540 (2015).

79. C. Moon, M. T. Baldridge, M. a. Wallace, C. A. D. Burnham, H. W. Virgin, *et al.*, Vertically transmitted faecal IgA levels determine extra-chromosomal phenotypic variation. *Nature*. **521**, 90–93 (2015).

80. N. H. Salzman, H. De Jong, Y. Paterson, H. J. M. Harmsen, G. W. Welling, *et al.*, Analysis of 16S libraries of mouse gastrointestinal microflora reveals a large new group of mouse intestinal bacteria. *Microbiology*. **148**, 3651–3660 (2002).

81. K. L. Ormerod, D. L. A. Wood, N. Lachner, S. L. Gellatly, J. N. Daly, *et al.*, Genomic characterization of the uncultured Bacteroidales family S24-7 inhabiting the guts of homeothermic animals. *Microbiome*. **4**, 36 (2016).

82. M. Derrien, E. E. Vaughan, C. M. Plugge, W. M. de Vos, Akkermansia muciniphila gen. nov., sp. nov., a human intestinal mucin-degrading bacterium. *Int. J. Syst. Evol. Microbiol.* **54**, 1469–76 (2004).

83. J. P. Ouwerkerk, S. Aalvink, C. Belzer, W. M. de Vos, Akkermansia glycaniphila sp. nov., an anaerobic mucin-degrading bacterium isolated from reticulated python faeces. *Int. J. Syst. Evol. Microbiol.* **66**, 4614–4620 (2016).

84. S. S. Seregin, N. Golovchenko, B. Schaf, E. C. Martens, K. A. Eaton, *et al.*, NLRP6 Protects Il10 –/– Mice from Colitis by Limiting Colonization of Akkermansia muciniphila. *Cell Rep.* **19**, 733–745 (2017).

85. G. Caballero-Flores, K. Sakamoto, M. Y. Zeng, Y. Wang, J. Hakim, *et al.*, Maternal Immunization Confers Protection to the Offspring against an Attaching and Effacing Pathogen through Delivery of IgG in Breast Milk. *Cell Host Microbe*. **0** (2019), doi:10.1016/j.chom.2018.12.015.

86. J. J. Kozich, S. L. Westcott, N. T. Baxter, S. K. Highlander, P. D. Schloss, Development of a dual-index sequencing strategy and curation pipeline for analyzing amplicon sequence data on the miseq illumina sequencing platform. *Appl. Environ. Microbiol.* **79**, 5112–5120 (2013).

87. C. Quast, E. Pruesse, P. Yilmaz, J. Gerken, T. Schweer, *et al.*, The SILVA ribosomal RNA gene database project: improved data processing and web-based tools. *Nucleic Acids Res.* **41**, D590–D596 (2012).

88. I. Lagkouvardos, R. Pukall, B. Abt, B. U. Foesel, J. P. Meier-Kolthoff, *et al.*, The Mouse Intestinal Bacterial Collection (miBC) provides host-specific insight into cultured diversity and functional potential of the gut microbiota. *Nat. Microbiol.* **1**, 16131 (2016).

89. I. Lagkouvardos, T. R. Lesker, T. C. A. Hitch, E. J. C. Gálvez, N. Smit, *et al.*, Sequence and cultivation study of Muribaculaceae reveals novel species, host preference, and functional potential of this yet undescribed family. *Microbiome*. **7**, 28 (2019).

90. M. Derrien, M. C. Collado, K. Ben-Amor, S. Salminen, W. M. de Vos, The Mucin degrader Akkermansia muciniphila is an abundant resident of the human intestinal tract. *Appl. Environ. Microbiol.* **74**, 1646–8 (2008).

91. M. W. J. van Passel, R. Kant, E. G. Zoetendal, C. M. Plugge, M. Derrien, *et al.*, The genome of Akkermansia muciniphila, a dedicated intestinal mucin degrader, and its use in exploring intestinal metagenomes. *PLoS One*. **6**, e16876 (2011).

92. A. Everard, C. Belzer, L. Geurts, J. P. Ouwerkerk, C. Druart, *et al.*, Cross-talk between Akkermansia muciniphila and intestinal epithelium controls diet-induced obesity. *Proc. Natl. Acad. Sci.* **110**, 9066–9071 (2013).

93. R. L. Greer, X. Dong, A. C. F. Moraes, R. A. Zielke, G. R. Fernandes, *et al.*, Akkermansia muciniphila mediates negative effects of IFNγ on glucose metabolism. *Nat. Commun.* **7**, 13329 (2016).

94. N. Ottman, L. HuuskonenL., J. Reunanen, S. Boeren, J. Klievink, *et al.*, Characterization of outer membrane proteome of akkermansia muciniphila reveals sets of novel proteins exposed to the human intestine. *Front. Microbiol.* **7**, 1–13 (2016).

95. H. Plovier, A. Everard, C. Druart, C. Depommier, M. Van Hul, *et al.*, A purified membrane protein from Akkermansia muciniphila or the pasteurized bacterium improves metabolism in obese and diabetic mice. *Nat. Med.* (2016), doi:10.1038/nm.4236.

96. C. Depommier, A. Everard, C. Druart, H. Plovier, M. Van Hul, *et al.*, Supplementation with Akkermansia muciniphila in overweight and obese human volunteers: a proof-of-concept exploratory study. *Nat. Med.* **25**, 1096–1103 (2019).

97. E. Blacher, S. Bashiardes, H. Shapiro, D. Rothschild, U. Mor, *et al.*, Potential roles of gut microbiome and metabolites in modulating ALS in mice. *Nature* (2019), doi:10.1038/s41586-019-1443-5.

98. A. Alam, G. Leoni, M. Quiros, H. Wu, C. Desai, *et al.*, The microenvironment of injured murine gut elicits a local pro-restitutive microbiota. *Nat. Microbiol.* **1**, 1–8 (2016).

99. C. A. Olson, H. E. Vuong, J. M. Yano, Q. Y. Liang, D. J. Nusbaum, *et al.*, The Gut Microbiota Mediates the Anti-Seizure Effects of the Ketogenic Diet. *Cell*. **173**, 1728–1741.e13 (2018).

100. B. Routy, E. Le Chatelier, L. Derosa, C. P. M. Duong, M. T. Alou, *et al.*, Gut microbiome influences efficacy of PD-1-based immunotherapy against epithelial tumors. *Science (80-.).* **359**, 91–97 (2018).

101. J. J. Bunker, S. A. Erickson, T. M. Flynn, C. Henry, J. C. Koval, *et al.*, Natural polyreactive IgA antibodies coat the intestinal microbiota. *Science (80-.)*., eaan6619 (2017).

102. M. W. Brand, M. J. Wannemuehler, G. J. Phillips, A. Proctor, A. M. Overstreet, *et al.*, The altered schaedler flora: Continued applications of a defined murine microbial community. *ILAR J.* **56**, 169–178 (2015).

103. K. Zimmermann, A. Haas, A. Oxenius, Systemic antibody responses to gut microbes in health and disease. *Gut Microbes*, 37–41 (2012).

104. M. J. Lodes, Y. Cong, C. O. Elson, R. Mohamath, C. J. Landers, *et al.*, Bacterial flagellin is a dominant antigen in Crohn disease. *J. Clin. Invest.* **113**, 1296–1306 (2004).

105. D. J. Berg, N. Davidson, R. Kühn, W. Müller, S. Menon, *et al.*, Enterocolitis and colon cancer in interleukin-10-deficient mice are associated with aberrant cytokine production and CD4(+) TH1-like responses. *J. Clin. Invest.* **98**, 1010–1020 (1996).

106. P. Chiaranunt, J. T. Tometich, J. Ji, T. W. Hand, T Cell Proliferation and Colitis

Are Initiated by Defined Intestinal Microbes. *J. Immunol.* **201**, 243–250 (2018).

107. P. Kumar, L. Monin, P. Castillo, W. Elsegeiny, W. Horne, *et al.*, Intestinal Interleukin-17 Receptor Signaling Mediates Reciprocal Control of the Gut Microbiota and Autoimmune Inflammation. *Immunity*. **44**, 659–671 (2016).

108. V. Matson, J. Fessler, R. Bao, T. Chongsuwat, Y. Zha, *et al.*, The commensal microbiome is associated with anti-PD-1 efficacy in metastatic melanoma patients. *Science*. **359**, 104–108 (2018).

109. A. Sivan, L. Corrales, N. Hubert, J. B. Williams, K. Aquino-Michaels, *et al.*, Commensal Bifidobacterium promotes antitumor immunity and facilitates anti-PD-L1 efficacy. *Science (80-.).* **350**, 1084–1089 (2015).

110. S. Sanderson, N. Shastri, LacZ inducible, antigen/MHC-specific T cell hybrids. *Int. Immunol.* **6**, 369–376 (1994).

111. S. Sanderson, D. J. Campbell, N. Shastri, Identification of a CD4+ T cell-stimulating antigen of pathogenic bacteria by expression cloning. *J. Exp. Med.* **182**, 1751–7 (1995).

112. C. Li, J. R. Dispirito, D. Zemmour, R. G. Spallanzani, W. Kuswanto, *et al.*, TCR Transgenic Mice Reveal Stepwise, Multi-site Acquisition of the Distinctive Fat-Treg Phenotype. *Cell*. **174**, 285–299.e12 (2018).

113. M. Tsuji, N. Komatsu, S. Kawamoto, K. Suzuki, O. Kanagawa, *et al.*, Preferential generation of follicular B helper T cells from Foxp3 + T cells in gut Peyer's patches. *Science (80-.).* **323**, 1488–1492 (2009).

114. K. Hirota, J.-E. Turner, M. Villa, J. H. Duarte, J. Demengeot, *et al.*, Plasticity of Th17 cells in Peyer's patches is responsible for the induction of T cell-dependent IgA responses. *Nat. Immunol.* **14**, 372–9 (2013).

115. A. M. Kruisbeek, in *Current Protocols in Immunology* (John Wiley & Sons, Inc., Hoboken, NJ, USA, 2001; http://doi.wiley.com/10.1002/0471142735.im0314s24), vol. 24, p. 3.14.1-3.14.11.

116. S. J. Lee, J. B. McLachlan, J. R. Kurtz, D. Fan, S. E. Winter, *et al.*, Temporal expression of bacterial proteins instructs host CD4 T cell expansion and Th17 development. *PLoS Pathog.* **8**, e1002499 (2012).

117. P. Wang, J. Sidney, Y. Kim, A. Sette, O. Lund, *et al.*, Peptide binding predictions for HLA DR, DP and DQ molecules. *BMC Bioinformatics*. **11**, 568 (2010).

118. P. Dash, J. L. McClaren, T. H. Oguin III, W. Rothwell, B. Todd, *et al.*, Paired analysis of TCRalpha and TCRbeta chains at the single-cell level in mice. *J.Clin.Invest*. **121**, 288–295 (2011).

119. V. Kouskoff, K. Signorelli, C. Benoist, D. Mathis, Cassette vectors directing expression of T cell receptor genes in transgenic mice. *J. Immunol. Methods*. **180**, 273–280 (1995).

120. D. B. Graham, C. Luo, D. J. O'Connell, A. Lefkovith, E. M. Brown, *et al.*, Antigen

discovery and specification of immunodominance hierarchies for MHCII-restricted epitopes. *Nat. Med.* **24**, 1762–1772 (2018).

121. J. J. Moon, P. Dash, T. H. Oguin, J. L. McClaren, H. H. Chu, *et al.*, Quantitative impact of thymic selection on Foxp3+ and Foxp3- subsets of self-peptide/MHC class II-specific CD4+ T cells. *Proc. Natl. Acad. Sci.* **108**, 14602–14607 (2011).

122. J. Zimmermann, A. A. Kühl, M. Weber, J. R. Grün, J. Löffler, *et al.*, T-bet expression by Th cells promotes type 1 inflammation but is dispensable for colitis. *Mucosal Immunol.* **9**, 1–13 (2016).

123. F.-W. Shen, Y. Saga, G. Litman, G. Freemant, J.-S. Tung, *et al.*, "Cloning of Ly-5 cDNA (cell surface phenotypes/isoforms/hematopoiesis/congeneic mice)" (1985), (available at https://www-pnas-org.libproxy.berkeley.edu/content/pnas/82/21/7360.full.pdf).

124. D. A. Chisolm, W. Cheng, S. A. Colburn, A. Silva-Sanchez, S. Meza-Perez, *et al.*, Defining Genetic Variation in Widely Used Congenic and Backcrossed Mouse Models Reveals Varied Regulation of Genes Important for Immune Responses. *Immunity*. **51**, 155–168.e5 (2019).

125. S. Malarkannan, Y. Laouar, B. Choi, A. Podsiad, B. B. Moore, *et al.*, Mouse Susceptibility to Infection CD45.1 Congenic Mice with Consequences in Locus Identified in Ncr1 Mutation in the A Point –– Cutting Edge: Check Your Mice (2019), doi:10.4049/jimmunol.1701676.

126. P. Mombaerts, E. Mizoguchi, M. J. Grusby, L. H. Glimcher, A. K. Bhan, *et al.*, Spontaneous development of inflammatory bowel disease in T cell receptor mutant mice. *Cell*. **75**, 275–282 (1993).

127. R. Kühn, J. Löhler, D. Rennick, K. Rajewsky, W. Müller, Interleukin-10-deficient mice develop chronic enterocolitis. *Cell*. **75**, 263–274 (1993).

128. R. W. Michelmore, I. Paran, R. V Kesseli, Identification of markers linked to disease-resistance genes by bulked segregant analysis: a rapid method to detect markers in specific genomic regions by using segregating populations. *Proc. Natl. Acad. Sci. U. S. A.* **88**, 9828–32 (1991).

129. K. Atarashi, T. Tanoue, M. Ando, N. Kamada, Th17 cell induction by adhesion of microbes to intestinal epithelial cells. *Cell*. **163,** 1–14 (2015).

130. C. G. Buffie, V. Bucci, R. R. Stein, P. T. McKenney, L. Ling, *et al.*, Precision microbiome reconstitution restores bile acid mediated resistance to Clostridium difficile. *Nature*. **517**, 205–208 (2015).